THE ENDOMETRIAL-MYOMETRIAL INTERFACE (EMI) IN THE AETIOPATHOPHYSIOLOGY OF ADENOMYOSIS UTERI

Thesis submitted for the degree of

Doctor of Medicine

At the University of Leicester

By

Dr. Vijayakumar Kalathy MBBS

Reproductive Sciences Section

Department of Cancer Studies and Molecular Medicine

University of Leicester

October 2016

Acknowledgements

DEDICATION

To my Mother and Father,

For all they have done for me

To my wife Kavitha,

For her patience and support

To my daughter Keerthana,

Who gives a meaning to my life

& taught me to never give up…

Abstract

Adenomyosis is a uterine disease where ectopic, non-neoplastic endometrium is histologically observed within the myometrium. The research presented herein examines the hypothesis that uterine adenomyosis is caused by abnormal behaviour of the cells at the endometrial-myometrial interface (EMI) through the actions of nerve growth factors (NGF), their receptors, the caveolin proteins and wnt signalling pathways during estradiol (E2) or tamoxifen (TMX) stimulation. In a 3-dimensional co-culture model, the invasion depth of endometrial stromal cells from affected uteri was greater than that of unaffected uteri. Furthermore, invasion depth of unaffected and affected stromal cells increased by an average of 41.3% and 64.6%, respectively in the presence of E2 and 73.3% and 73.5%, respectively in the presence of TMX, indicating an inherent predisposition of the stromal cell for myometrial invasion and the enhancing effects of both E2 and TMX. Immunohistochemical analysis of NGF expression indicated a significant 2-4 fold increase in adenomyosis with the transcript level (measured by qRT-PCR) showing decreased expression in normal myocytes (0.72 fold) in response to E2 and increased expression in both normal (1.08 fold) and adenomyotic myocytes (1.20 fold) in response to TMX. Similarly, caveolin 1 protein expression was increased in the adenomyotic group, whilst transcripts for the caveolin 1a (0.70 fold) and caveolin 1b (0.82 fold) isoforms were reduced by E2 in normal myocytes. Conversely, TMX increased caveolin 1a (1.4 fold) and caveolin 1b (1.32 fold) expression in the adenomyotic myocytes. The data for the caveolin 2 data mirrored that of caveolin 1 in that caveolin 2a and 2b protein expression showed increased expression in the adenomyotic group, whilst the transcript levels of the caveolin isoforms 2a (0.65 fold) and 2b (0.79 fold) were reduced by E2 in normal myocytes, while upregulated by TMX in adenomyosis group (1.57 and 2.00 fold, respectively). Wnt5a expression at both the transcript and protein level was decreased in adenomyosis implicating the loss of wnt5a in adenomyosis progression. Furthermore, decidualisation experiments of isolated stromal cells from normal and adenomyotic uteri suggested no difference in the timing to decidualisation, with no significant difference in cell morphology, IGFBP-1 or prolactin expression, which strongly suggests that disordered stromal differentiation is not the main causal event in the pathogenesis of adenomyosis. Overall, the results from this research supported the key hypothesis of disordered cellular function and gene expression at the uterine endometrial-myometrial interface in adenomyosis.

Abbreviations

ABC	Avidin Biotin Complex
AMV-RT	Avian Myeloblastosis Virus Reverse Transcriptase
APC	Adenomatous Polyposis coli
APG	Advanced Post Graduate
BDNF	Brain Derived Neurotophic Factor
BSA	Bovine Serum Albumin
cAMP	Cyclic Adenosine Monophosphate
Cav 1 & 2	Caveolin 1 & 2
CCS	Charcoal Stripped Serum
cDNA	Complementary Deoxyribose Nucleic Acid
DEPC	Diethylpyrocarbonate
DMEM	Dulbecco's Modified Eagle's Medium
E2	Estradiol
E2+P	Estradiol + Progesterone
EMI	Endometrial-Myometrial Interphase
EtBr	Ethidium Bromide
EtOH	Ethanol
FBS	Fetal Bovine Serum
FCS	Fetal Calf Serum
FPLM	Four parametric logistic models
GAPDH	Glyceraldehyde-6-phosphate dehydrogenase
GERG	Gynaecology Endocrinology Research Group
H&E	Haematoxylin & Eosin
HBSS	Hanks Buffered Salt Solution
IGFBP-1	Insulin Like Growth Factor Binding Protein-1
IHC	Immunohistochemistry
ILK	Integrin-linked kinase
IM	Inner Myometrium
IMS	Industrial Methylated Spirits
JNK	c-jun N-terminal kinase
LEF	Lymphoid enhancing factor
LMP	Last Menstrual Period
MPA	Medroxy Progesterone Acetate
MRI	Magnetic Resonance Imaging
NaOH	Sodium Hydroxide
NGF	Nerve Growth Factor
NT-3	Neurotrophin 3
Oligo (dT)	Anchored Oligo (dT) $_{23}$
OM	Outer Myometrium
PBS	Phosphate Buffered Saline
PCR	Polymerase Chain Reaction
PI3K	Phosphotidylinositol 3-kinase
PIL	Patient information leaflet
PK	Protein kinase
Q-PCR	Quantitative -Polymerase Chain Reaction
RNA	Ribonucleic Acid
RT-PCR	Real Time-Polymerase Chain Reaction

siRNA	Silencing RNA
TAE	Tris-Acetate-Ethylenediamine tetra acetic acid
TBS	Tris Buffered Saline
TCF	T cell factor
Trk A	Tyrosine Kinase receptor A
Tmx	Tamoxifen
Wnt	Wingless MMTV integration site family members

Table of Contents

Chapter 1 Introduction

1.1 Adenomyosis - Clinical Definition

Adenomyosis uteri is defined as the presence of endometrial epithelium and stroma within the myometrium and histologically it is defined as the presence of ectopic, non-neoplastic endometrial epithelia and stroma within a myometrium that is surrounded by hypertrophic and hyperplastic myometrial smooth muscle cells (Hever et al., 2006, Bird et al., 1972).

1.2 Clinical Presentations

Adenomyosis is considered to be a benign disease of the uterus and is seen most commonly among multiparous women of between 40 to 50 years of age with a wide prevalence range of between 5 and 70% (Azziz, 1989). This wide range of prevalence may be due to dissimilarities in uterine size in different studies, differences in ages of subjects and also differences in the amounts of tissue sections examined (Emge, 1962, Fukamatsu et al., 1984). Another reason could be the presence of bias in that most studies have been based on selected groups of women who had hysterectomies, and not on the general female population (Fukamatsu et al., 1984).

1.3 Histological Diagnosis

Figure 1.1 shows several representative stained uterine sections demonstrating the relative positions of the endometrium (E), myometrium (M) and adenomyotic lesions (A) in the myometrium in normal and adenomyotic samples. Various histopathologic features have been evaluated to assess severity of disease and correlate it to symptoms, including depth and number of foci, number of glands, number of glands per focus, and ratio of depth of foci to muscle thickness (Nishida, 1991, Bird et al., 1972). The definitive diagnosis of adenomyosis can be made histologically; when glandular

invasion is >2.5mm from the endometrial-myometrial interface (EMI) (Ferenczy, 1998). The invasion may well extend through the entire myometrium and up to the serosa in some cases. If the lesion is <2mm from the EMI, it is called 'adenomyosis sub-basalis' but this is not accepted as being clinically relevant, but is often an indication of 'clinically relevant adenomyosis elsewhere in the uterus (Hever et al., 2006).

.
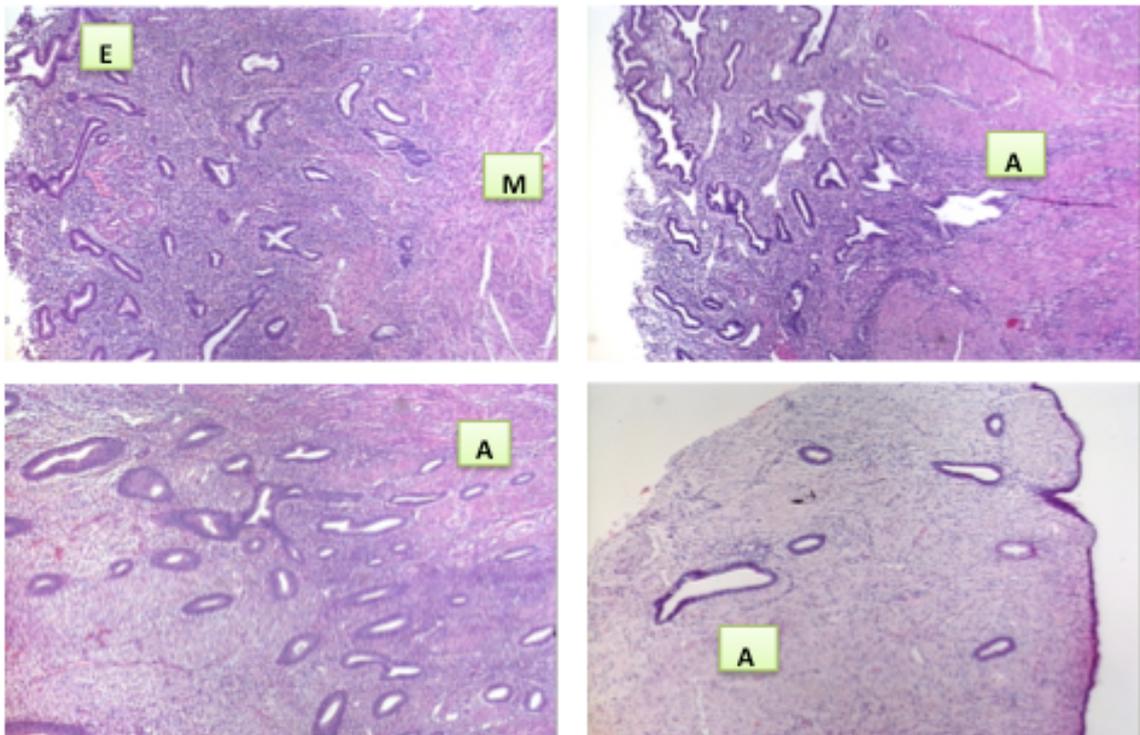
Figure 1.1: Histochemical staining showing adenomyotic lesion in the Myometrium (E: Endometrium; M: Myometrium; A: Adenomyotic lesion in myometrium)

1.3.1 Junctional Zone

An important component in regard to this disease is the endometrial-myometrial interface (EMI), which through MRI scans is also called the 'junctional zone'. The EMI components are the basal endometrium and sub-endometrial myometrium (inner myometrium: IM). These features are illustrated in Figure 1.2. These two tissues are thought to have arisen from a common embryological Müllerian origin that develops in the fetus during the second trimester of pregnancy (Ferenczy, 1998). By contrast, the outer myometrium is thought to originate from the mesenchyme and develops during the third trimester of the pregnancy, at which point these two tissue types fuse together (Ferenczy, 1998).
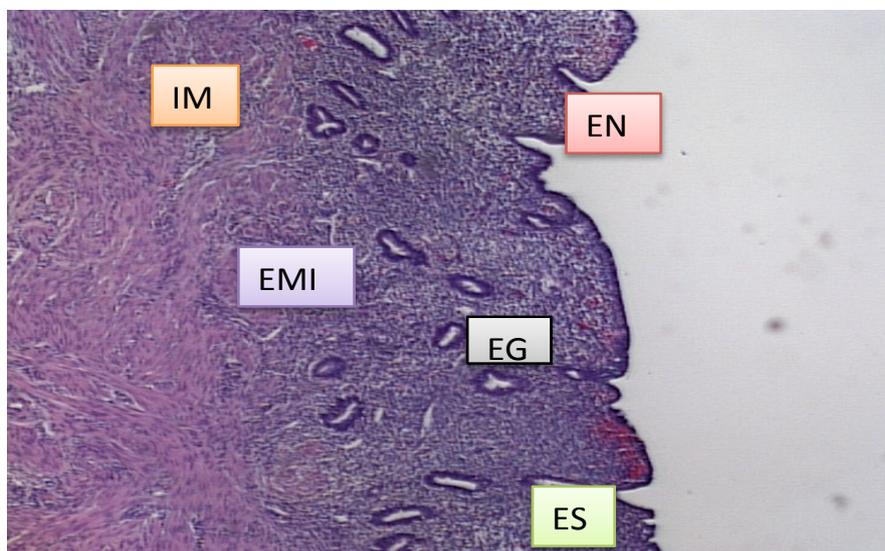
Figure 1.2: Histological cross section of a normal uterus showing: EN: Endometrium; EG: Endometrial Glands; ES: Stroma; EMI: Endometrial-Myometrial Interphase; IM: Inner Myometrium

1.3.2   Basal Endometrium

The basal endometrium that forms one side of EMI is approximately 1 mm thick and consists of branching lower segments and bases of glands (Figure 1.2: EG) and the associated stroma (Figure 1.2: ES). The characteristic features of this area are the presence of periglandular T cell aggregates within the periglandular basalis and the fact that this layer is not shed during menstruation, suggesting that it also differs from the endometrial functionalis, which is shed during menstruation (Ferenczy, 1998).

1.3.3   The Sub Endometrial Myometrium
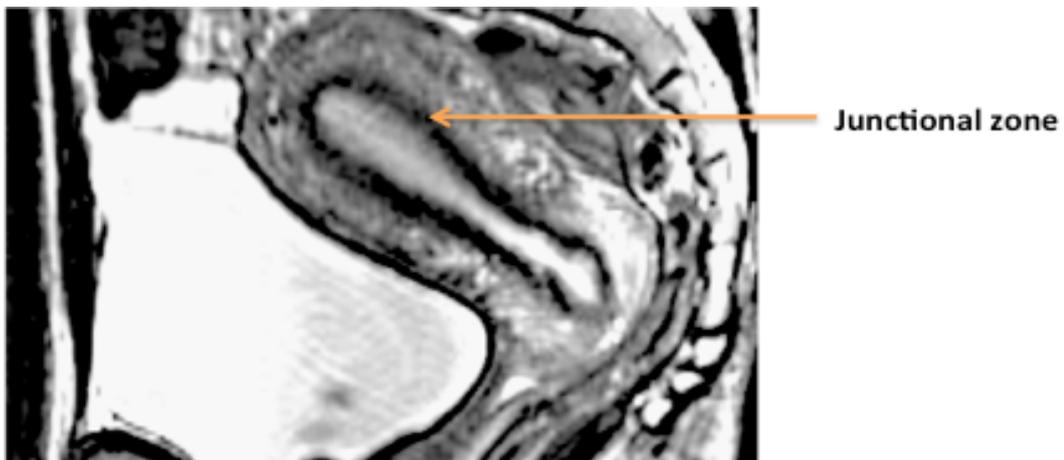
Figure 1.3: MRI at the level of the pelvis showing the 'Junctional zone' of the uterus

This forms the other side of the EMI, is approximately 5 mm thick and constitutes the inner third of the myometrium. It usually consists of longitudinal smooth muscle fibres running parallel to the endometrium in a fundus to isthmus direction. Even though the myometrium appears as a single homogenous tissue under light microscopy, imaging with MRI clearly shows the junctional zone as a hypo-intense area just beneath the endometrium (see Figure 1.3) (Brosens et al., 1998).

1.4   Functional Significance of the Sub-Endometrial Myometrium

There is a defined pattern of sub-endometrial myometrial contractility, which varies according to the phase of menstrual cycle. It is generally retrograde (from the cervix to fundus) throughout the cycle, and these actions may help sperm transport and conservation of the pre-implantation blastocyst in the upper part of the uterine cavity (Leyendecker et al., 1996).   During menstruation the sub-endometrial myometrial contraction is ante grade (from fundus to cervix), which may cause venous engorgement and thus help to reduce menstrual blood flow, but also help to shed fluid and debris from the uterine cavity (Tamaya et al., 1979).   In this function, the inner myometrium differs from the outer myometrium both structurally and functionally. The sub-endometrial myometrium exhibits a cyclical pattern of estrogen and progesterone receptor expression similar to that of the endometrium, whereas the outer myometrium, which forms the bulk of uterine muscle, does not, suggesting that the function of the EMI is controlled by gonadal sex steroid hormones (Sammour et al., 2002, Yamamoto et al., 1993). However, more recently, and using well characterised full thickness uterine biopsies from women with and without adenomyosis, our group was unable to confirm cyclical changes in steroid receptor expression in the inner myometrium (Mehasseb et al., 2011b) suggesting that more research in this area is required.

1.5   Clinical Symptoms

Adenomyosis is asymptomatic in 50% of women (Azziz, 1989) with the remaining 50% mostly presenting with menorrhagia (40-50%), dysmenorrhoea (10-30%) or metrorrhagia (10-12%). Patients sometimes also present with complaints of dyspareunia and dyschezia (Cohen et al., 1997), but there are no symptoms specific to adenomyosis (Kilkku et al., 1984). Reports in the literature propose a correlation between the severity

of symptoms and the depth of penetration of endometrial stroma and glands (Levgur et al., 2000) and also a positive relationship between dysmenorrhoea and pelvic pain (Sammour et al., 2002). In symptomatic women, the pain usually starts one week prior to the expected date of their menstrual period (Azziz, 1989) but in most cases, the precise cause of heavy bleeding is not known (McCausland, 1992) and in some cases the menorrhagia could be due to dysfunctional contractility of the myometrium (Brosens et al., 1995).

1.6   Clinical Associations

Adenomyosis is more commonly associated with other gynaecological conditions such as, leiomyoma (20-70%), pelvic endometriosis (6-24%), endometrial polyps (2-14%), endometrial hyperplasia (2-13%) and adenocarcinoma (2-5%) (Azziz, 1989). Sixty percent of women with endometrial carcinoma are reported to have adenomyosis. In another study, an association between adenomyosis with endometriosis was observed in 6-20% of cases (Hall et al., 1984).

1.7   Infertility

It has been reported that the Endometrial Myometrial Interphase (EMI) is altered in adenomyosis, and it is commonly believed that the altered structure of the EMI could interfere with the normal fertilization and implantation by altering uterine peristalsis. Uterine peristalsis plays an important role in reproduction by helping sperm transport towards the ipsilateral dominant follicle side and into the oviduct (Kunz et al., 1996, Leyendecker et al., 1996). Since adenomyosis has been reported to be the result of disordered stromal cell differentiation (Parrott et al., 2001), it is reasonable to say in such cases, that there will be some effect on decidualisation of stromal cells, which could result in disordered blastocyst reception, which is one of the main causes for

6

infertility. Decidualisation is a complex process in which the endometrial stromal cell undergoes morphological and biochemical changes that result in remodelling of the endometrial environment that ultimately aids the smooth implantation of embryo and proper trophoblast invasion (Salamonsen et al., 2003, Jones et al., 2006). During every menstrual cycle, the regular morphological changes that occur in the endometrial glands and stroma, and in endometrial vasculature, happen in anticipation of an embryo entering the uterus towards the end of that cycle (Salamonsen et al., 2003). Therefore, any abnormal or deficient decidualisation will result in early pregnancy loss or inadequate trophoblast invasion, possibly leading to pre-eclampsia in later pregnancy (Brosens et al., 2002). Decidualisation changes were noted in endometrial stromal cells in an *in vitro* study following treatment with progesterone (Tang and Gurpide, 1993, Frank et al., 1994) or a combination of 8-bromo-cAMP and medroxyprogesterone acetate (MPA) (Gellersen and Brosens, 2003).

Decidualised stromal cells are functionally different from non-decidualised cells and can be differentiated from the non-decidualised cell by measuring the production of secreted proteins such as insulin-like growth factor binding protein-1 (IGFBP-1) and prolactin, that are involved in embryo implantation and trophoblast invasion (Salamonsen et al., 2003). The decidualisation process starts during the late secretory phase of the menstrual cycle with functional differentiation in endometrial stromal cells. It then progresses further if conception results in that cycle (Ferenczy and Bergeron, 1991). Dysfunctional decidualisation may result in impaired placentation in early pregnancy, resulting in either miscarriage or preterm labour or fetal growth restriction (Brosens et al., 1972).

1.8 Clinical Diagnosis of Adenomyosis

So far no reliable non-invasive diagnostic test is available for adenomyosis. Hysterosalpingography was the first imaging modality used to diagnose adenomyosis but with very low sensitivity of 25% (Goldberger et al., 1949). In this test, the adenomyotic foci in the myometrium appears as multiple small spicules extending from endometrium into the myometrium with saccular endings (Wolf and Spataro, 1988). Trans-abdominal ultrasound is another mode of investigation used in the past but is not much emphasised nowadays because of it inconsistency in differentiating the adenomyosis from leiomyoma and also because it is difficult to evaluate the myometrium because of low resolution (Bulic et al., 1986, Bohlman et al., 1987). The invention of transvaginal ultrasound in 1985 helped to overcome those difficulties with trans-abnominal ultrasound. It uses high frequency transducers, which give better resolution and help to differentiate the different zones of the myometrium, and thus aids in the diagnosis of adenomyosis (Lyons et al., 1992).

In women of reproductive age, three different zones can be identified within the uterus using MRI. The normal endometrium and endometrial secretions appear as a high signal-intensity type stripe on T2-weighted sagittal image. Immediately subjacent to this is a band of low signal intensity that represents the innermost layer of the myometrium: the Junctional Zone (JZ) (Brown et al., 1991). The outer layer of the myometrium is of intermediate signal intensity. There is considerable variation in the normal JZ thickness ranging from 2 to 8 mm (Lee et al., 1985, Hauth et al., 2007). The appearance of diffuse or focal widening of the JZ on MRI is suggestive of adenomyosis.

There is growing evidence for the role of MRI in the diagnosis of adenomyosis. However, the high cost and limited availability hinder its routine use in the clinical setting. Several studies have compared the accuracy of TVS and MRI in the diagnosis of adenomyosis. Although the sensitivities and specificities of both techniques were comparable, MRI proved to be superior to TVS in women where associated leiomyomas or additional pathology was suspected (Bazot et al., 2001).

1.9   Aetiopathology of Adenomyosis

The deep invasion of the myometrium by endometrial tissue is thought to be brought about through stromal disruption of the endometrial-myometrial interface (EMI) or 'permissiveness' by the inner myometrium (Azziz, 1989). The sequence of events remains unknown, but in animal studies, the critical initial event appears to be involution of inner myometrial muscle fibres with concomitant reduction of up to one third of cell size, which, in turn, leads to distension of intercellular spaces. Once the arrangement of muscle fibres has been disturbed, glandular and stromal components appear to migrate and penetrate into the myometrium, resulting in adenomyosis (Brosens et al., 1998). However, from recent evidence from our laboratory, using the CD1 mouse model, neonatal administration of tamoxifen resulted in disruption of the inner myometrium together with the development of uterine adenomyosis in the mature mouse (Mehasseb et al., 2009). Similar administration of tamoxifen to the neonatal C57BL mice resulted in disruption of the inner myometrial layer, but the mice did not develop adenomyosis (Mehasseb et al., 2010a). These findings are significant as they demonstrate that disruption of the muscle layer is not sufficient for the development of the disease. Previous hypotheses on the aetiology of adenomyosis have focussed on the possible increased invasiveness of the stroma through intact or disrupted muscle

bundles, for example following sharp curettage (Levgur et al., 2000). Research in our laboratory has clearly demonstrated that the myocytes from adenomyosis affected uteri showed changes such as cellular hypertrophy, abnormal nuclear and mitochondria shapes, abundant myelin bodies and lengthening of sarcolemmal plaques with reduced caveolae. These findings are similar throughout the inner and outer myometrium and not localised just to the junctional zone (Mehasseb et al., 2011a). These features were not confined to the inner myometrium, suggesting a primary myometrial defect, and that the features observed are not the result of the presence of invading endometrium (Mehasseb et al., 2011a). Recent research from our laboratory has also shown that when stromal cells of either normal or adenomyotic uteri were placed on top of collagen containing myocytes obtained from uteri with adenomyosis, increased invasiveness of the stromal cells was observed in the cultures where either myometrial cells or stromal cells from women with adenomyosis were used compared to a matrix containing myocytes obtained from normal uteri (Mehasseb et al., 2010b). These data clearly showed that both the endometrium and the myometrium have important roles in the pathogenesis of adenomyosis.

1.10 Physiological and Iatrogenic Causes of Adenomyosis

There is a general hypothesis that suggests that any disturbance of the junctional zone (EMI), either directly by endometrial factors or indirectly by an altered immune response, may be the primary abnormality in the pathogenesis of adenomyosis. This hypothesis was supported by data showing that dysfunctional uterine hyper-peristalsis or contractility may cause mechanical damage to the EMI (Parrott et al., 2001, Kunz et al., 2000). Another important factor is mechanical damage by sharp curettage during pregnancy, which leads to dislocation of the endometrium into the myometrium

resulting in adenomyosis (Leyendecker et al., 2002). In multiparous patients, it is thought that trophoblast invasion may also cause disruption to the EMI predisposing these individuals to later adenomyosis (Lee et al., 1984). Although the triggering mechanism of endometrial invasion into the myometrium in women remains to be determined, some important clues have come from animal studies where oral dosing of CD1 mice with tamoxifen during a 5-day postnatal period resulted in severe adenomyosis at 90 days of age (Parrott et al., 2001). The histological findings, estrogen receptor status and gene expression data after tamoxifen treatment have suggested that adenomyosis might be due to alterations in stromal and myometrial differentiation during the neonatal period (the point of maximal uterine development in the mouse). In that study, the most affected gene was nerve growth factor (NGF) and the authors suggested that gonadal sex steroids might cause adenomyosis through disordered NGF signalling in the EMI (Parrott et al., 2001).

1.11 The Role of Neurotrophins

The role of nerve growth factor (NGF) in the uterus is unclear, although it has been suggested that NGF is considered as a regulator of uterine development and to be involved in uterine re-innervations after pregnancy (Haase et al., 1997, Varol et al., 2000). The effects of neurotrophins, including NGF, brain-derived neurotrophic factor (BDNF), neurotrophin-3 (NT-3), and NT-4/5 are mediated by their interactions with specific receptors that can occur in low- and high-affinity states (Seidl et al., 1998). All members of the neurotrophin gene family bind to the low-affinity receptor, named $p75^{NTR}$, and recent evidence strongly suggest that NGF and $p75^{NTR}$ might participate in the regulation of tissue morphogenesis, myogenesis and support non-neural cell systems on their way towards terminal differentiation (Seidl et al., 1998).

Thus, besides its role in the nervous system, NGF may be involved in functions other than neuronal survival and differentiation (Seidl et al., 1998). There are several observations in the literature noting the involvement of NGF in various type of cells, such as cells of the ovary (Dissen et al., 1991) and testis (Persson et al., 1990, Russo et al., 1994), myoblastic cells (Ueyama et al., 1993) and mast cells (Aloe, 1988). The development, maturation and regeneration of muscles involve different steps of proliferation, differentiation and morphogenesis that take place under the influence of signals from the cellular environment and also from paracrine and endocrine actions (Seidl et al., 1998).

After an injury or damage to a muscle, the growth and regeneration follows a pattern of its original embryonic myogenesis (Tajbakhsh, 2003) to some extent suggest this is possible from the resident myogenic stem cells which are normally present between the cell membrane and the basal lamina of muscle fibres (Tajbakhsh, 2003). Once the muscle injury happens, satellite cells get activated and undergo several rounds of proliferation before differentiating to form new fibres or repair the injured fibres (Schmalbruch and Lewis, 2000). This process of myogenesis is regulated by the signals from many growth factors, such as those of the insulin-like growth factor (IGF) and transforming growth factor (TGF)-β families (Deponti et al., 2009), fibroblast and hepatocyte growth factors (Balemans and Van Hul, 2002, Parker et al., 2003) and nerve growth factor (NGF) (Seidl et al., 1998, Erck et al., 1998). There is enough evidence in the literature supporting NGF as a major protein expressed in developing muscle (Ernfors et al., 1991, Wheeler and Bothwell, 1992, Ip et al., 2001) that normally is down-regulated in the neonatal period (Ernfors et al., 1991, Ip et al., 2001) and remains repressed is being re-expressed during adulthood and in a few pathological conditions

such as muscular dystrophy (Toti et al., 2003), amyotrophic lateral sclerosis (Kust et al., 2002) and in the regenerating fibres of damaged muscle (Toti et al., 2003, Chevrel et al., 2006), which suggests a proregenerative role of NGF (Menetrey et al., 2000). These observations also strongly suggest the possible role of NGF in myogenesis (Rende et al., 2000). The regeneration of muscle fibres begins with activation of resident myogenic stem cells which normally present between the cell membrane and the basal lamina of muscle fibres (Tajbakhsh, 2003). They proliferate and differentiate into multinucleated myotubes and eventually into myofibres (Menetrey et al., 2000) and during this process some of these myoblasts will fuse with the existing damaged myofibres to prevent them from degenerating completely (Huard et al., 1994).

Seidl *et al*., in 1998 demonstrated that NGF affects myogenic differentiation solely at the myoblast stage and that NGF is down regulated to almost undetectable levels during the phase of myogenic differentiation and fusion into myotubes, after the myoblast stage (Seidl et al., 1998). They also showed that the over-expression of NGF during that terminal differentiation stage caused repression of muscle cell development (Seidl et al., 1998). These data suggest that neurotrophins and their receptors are intimately involved in the function of myocytes during differentiation. Comparison of these data with the data from the experimental CD1 mouse model, where tamoxifen altered the differentiation of neonatal mouse myometrial development through the expression of NGF, suggests that a similar link between steroid action and NGF expression and action, in the inner myometrium of women might lead directly to adenomyosis (Parrott et al., 2001). However, this remains to be confirmed and the precise mechanism by which NGF might be responsible for adenomyosis is not yet fully clarified.

1.12 The Role of Wnt Family Growth Factors

The family of Wnt genes represent cysteine rich secreted glycoproteins that normally act through cell surface receptors (Nusse and Varmus, 1982) and their signalling plays crucial roles in cell proliferation, cell polarity, cell fate determination and overall tissue homeostasis (Logan and Nusse, 2004). Any defect in the Wnt pathway often leads to birth defects, cancer and other diseases in humans (Clevers, 2006). The Wnt gene (originally called int-1) was first discovered in 1982 and described as a proto-oncogene, which was activated by integration of mouse mammary tumour virus in mammary tumours (Nusse and Varmus, 1982).

So far, 100 Wnt genes have been isolated from species ranging from nematode worm (*Caenorhabditis elegans*) through to human and when any of these genes are mutated, a change in cell fate occurs because of inappropriate and abnormal target gene expression (Wodarz and Nusse, 1998). Within the Wnt family of growth factors, Wnt4, Wnt5a and Wnt7a have been shown to play crucial roles in the epithelial-mesenchymal interactions necessary for the correct patterning of the mammalian female reproductive tract (Mericskay et al., 2004, Miller et al., 1998, Miller and Sassoon, 1998, Franco et al.). Among these three factors, Wnt5a appears to play a very constructive role in the generation of uterine glands and is required for both cellular and molecular responses to exogenous estrogen in addition to mediation of developmental and estrogen-mediated changes in the uterine epithelium through the activation of Wnt5a (Mericskay et al., 2004).

This intracellular signalling has three possible pathways:

(1) The Wnt/β-catenin pathway or canonical pathway (Figure 1.5), which activates target genes in the nucleus (Huelsken and Behrens, 2002);

(2) The planar cell polarity pathway (Figure 1.6), which involves jun N-terminal kinase (JNK) and β-catenin involved cytoskeletal rearrangements (Huelsken and Behrens, 2002); and

(3) The Wnt/Ca^{2+} pathway (Figure 1.6) (Huelsken and Behrens, 2002).

The canonical pathway (Figure 1.5) plays a crucial role in maintaining various embryonic and adult stem cell functions (Grigoryan et al., 2008) than a dysfunction of this pathway often results in pathological conditions, such as cancer (Rask et al., 2003, Nishisho et al., 1991, Nakamura et al., 1991). In the planar cell polarity or non-canonical pathway, activation of JNK directs the asymmetric cytoskeletal organization and coordinated polarization of cells within the plane of epithelial sheets and this pathway involves the cadherin-related trans membrane molecule (Huelsken and Behrens, 2002). β-catenin acts as a dual function protein, both in the β-catenin/E-cadherin complex and as a transcriptional regulator in canonical Wnt signalling pathway (Daugherty and Gottardi, 2007). The structural integrity of tissues depends on the stability of epithelial cell-cell junctions organized by adhesion proteins and the underlying actin cytoskeleton (Drees et al., 2005).
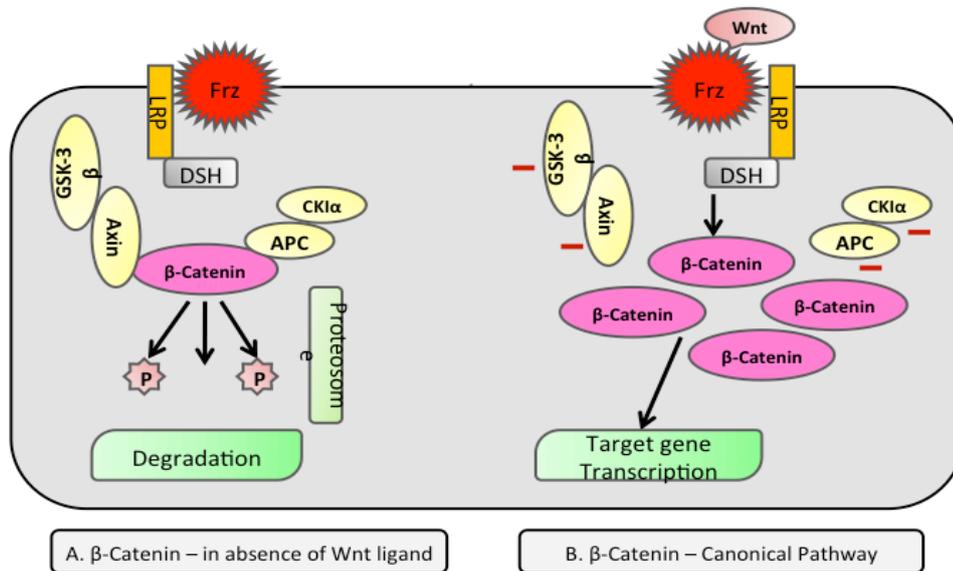
Figure 1.4: Canonical Pathway of Intracellular Wnt signalling mediated *via* Frizzled receptor (Frz) involving B-catenin for target gene transcription.
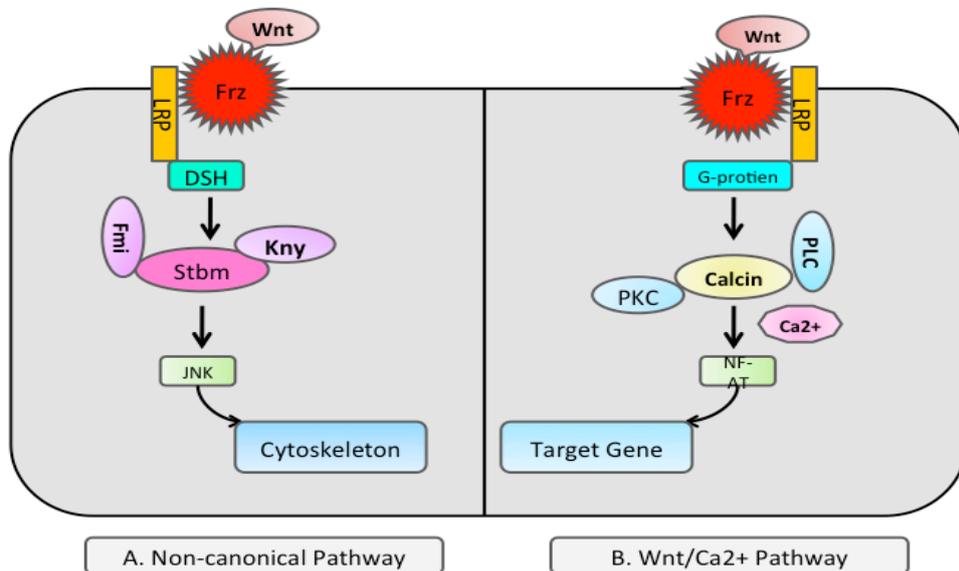
Figure 1-5: Non-Canonical pathway where JNK directs the asymmetric cytoskeletal organization and coordinated polarization of cells and Wnt/Ca^{2+} intracellular signalling pathway mainly mediated by calcium ions.

Based on experiments performed in C57MG mammary myoepithelial cells, Shimizu *et al.*, divided the most commonly encountered Wnt proteins into a transforming (Wnt-1, Wnt-2, Wnt-3, and Wnt-3a) group acting *via* the canonical pathway, and a non-transforming group (Wnt-4, Wnt-5a, Wnt-5b, and Wnt-7b) acting *via* non-canonical pathways (Figure 1.6) (Shimizu et al., 1997). This finding was supported by a later study, which demonstrated that Wnt-5a acts primarily *via* non-canonical pathways (Dejmek et al., 2006). These observations support the findings reported in the literature that Wnt5a is involved in cell adhesion, motility, and polarity *via* the β-catenin/E-cadherin complex (Moon et al., 1993, Pandur et al., 2002). The role of Wnt5a as a prognostic marker in various cancers has now been determined (Dejmek et al., 2005, Blanc et al., 2005, Kremenevskaja et al., 2005) and its low expression leads to decreased adherence of cells, resulting in increased invasion of the cancer cells (Jonsson and Andersson, 2001). Similar observations were noted in lung cancer where down regulation of Wnt7a resulted in decreased cadherin-catenin complex, decreased cell adhesion and increased invasion of cancer cells (Ohira et al., 2003).

1.13 The Role of Caveolin Family Members

Caveolins are components of caveolae, which are invaginations from the plasma membrane (Figure 1.7) (Couet et al., 2001). In 1955, Yamada named these flask-shaped invaginations of the plasma membrane, caveolae (Yamada, 1955). Caveolae are present in large numbers in adipocytes, endothelial cells, fibroblasts and smooth muscle cells (Scherer et al., 1996). They are found to play important roles in intracellular transport (Parton and Simons, 2007) as scaffolding proteins for signal transduction (Patel et al., 2008), and as buffers regulating plasma membrane lipid composition and fatty acid incorporation (Ortegren et al., 2007). There are three members of the caveolin family

(Cav-1, -2, and -3), which are essential for the formation of caveolae (Razani et al., 2002). Two isoforms of caveolin 1 have been identified, namely cav-1α (172 amino acid residue) and cav-1β (144 amino acid residue) (Scherer et al., 1995) and similarly three isoforms for caveolin 2 (α, β & γ) have been identified (Scherer et al., 1996).
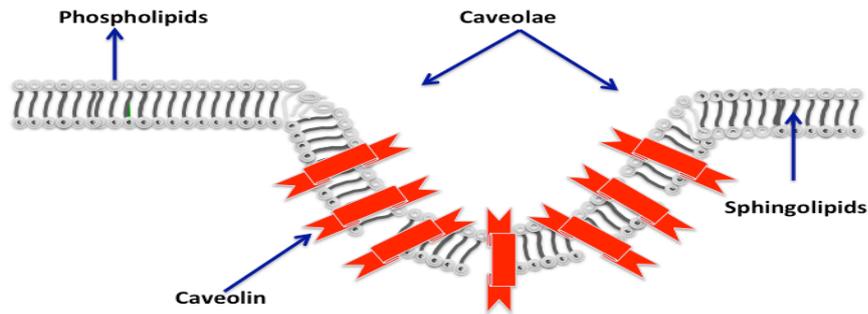
Figure 1.6: Structure of Caveolae and its Caveolin components

Caveolin-2α encodes a 162 amino acid residue protein with sequence similar to caveolin-1 and the remaining two caveolin 2 isoforms are uncharacterised (Scherer et al., 1996). Caveolin-3 is a single 151-residue protein found mostly in cardiac and skeletal muscles (Tang et al., 1996). Caveolin-1 and 2 proteins are also cell-specific and appear to co-localize with each other (Tang et al., 1996, Das et al., 1999). These three caveolin family members (Cav-1, 2, and 3) function as scaffolding proteins to concentrate and organize specific lipids and lipid-modified signalling molecules within caveolae membranes (Lisanti et al., 1994). The actin cross-linking proteins filament and myosin sub-fragment-I were identified as ligands for Cav-1 and the caveolae are aligned along these actin filaments (Lisanti et al., 1994, Izumi et al., 1988). The binding of Cav-1 to cell cytoskeleton acts as organisational framework for the distribution of caveolae and also as an anchorage point for caveolae formation at the

plasma membrane (Mundy et al., 2002). Microtubules and their associated motor proteins may be involved in the intracellular movement of Cav-1–bearing vesicles (Mundy et al., 2002). During growth and development, most cells do not attach each other to form tissues (Gumbiner, 1996), but instead each cell needs to be assembled and organised into a very diverse and distinctive pattern (Gumbiner, 1996), which is possible only through the use of a variety of cell adhesion mechanisms, which their connection to internal cytoskeleton helps to determine the overall architecture (Gumbiner, 1996) and three dimensional patterns within tissue (Gumbiner, 1996). Perl *et al*., in 1998, demonstrated the loss of E-cadherin was a causal factor for tumour progression in a transgenic mouse model of pancreatic β-cell carcinoma (Perl et al., 1998) and later studies also showed that restoring E-cadherin expression increased cell-cell adhesion and limited tumorigenecity by suppressing the invasiveness of the tumour cells (Frixen et al., 1991, Vleminckx et al., 1991).

Although cadherins and catenin constitute the major structural components of adherens junctions, they are all need to be properly arranged in the ultrastructure of the plasma membrane (Lu et al., 2003), such that caveolae and caveolins come into play to target, traffic and anchor these proteins in their respective subcellular sites (Lu et al., 2003). The evidence in the scientific literature also shows a role of caveolin in the regulation of cellular proliferation, invasiveness and the metastatic potential of cancer cells (Bagnoli et al., 2000, Bender et al., 2000). As a general rule, during transformation of normal epithelium into invasive or metastatic cancer cells there should be accumulation of a combination of various defects such as increased mutational activity, suppression of tumour suppressor gene expression (Bishop, 1991), loss of adhesion (Vogelstein et al., 1988), increased cellular proliferation (King and Cidlowski, 1998) and insensitivity

to apoptosis (Vogelstein et al., 1988, King and Cidlowski, 1998). So any reduction in the number of caveolae through reduced caveolin expression would be expected to directly affect the expression level of the cadherin-catenin complex, which in turn, would affect the stability of intercellular contacts and cell adhesion resulting in increased permeability.

1.14 Hypothesis

It is thus hypothesised that the pathogenesis of adenomyosis entails steroid-mediated myometrial penetration by the overlying endometrium involving differential expression of neurotrophins, caveolins and Wnt signalling pathway proteins.

1.15 Plan of Investigation

The aims of this study were therefore:

1. To examine the effect of estradiol and tamoxifen on stromal cell invasion in a co-culture model to assess whether the addition of steroids changes the invasion characteristics of stromal cells.

2. To study the steroid mediated differential expressions of NGF and the proteins Wnt5a, Wnt4, Wnt7a, caveolin 1 and 2 in the inner and outer myometrium of normal and adenomyotic uteri.

3. To study stromal cell differentiation (the decidualisation process) in adenomyosis by using *in vitro* cultures of stromal cells obtained from women with or without adenomyosis and examining for the expression of the decidualisation markers, IGFBP-1 and prolactin to see if decidualisation is altered in adenomyosis.

Chapter 2   Methodology

2.1 Patient Recruitment

Recruitment was from women scheduled for hysterectomy for benign conditions. Participation did not influence their treatment in any way, as research was only conducted on the removed specimens. The study was performed under local Research Ethics Committee approval (LREC number 09/H0406/99; Appendix 2). Patients were given the approved PIL (patient information leaflet) and consent form to sign (Appendix 3). The only data collected at the time was the date of the last menstrual period, their age, and drug history, to confirm that they had not been taking hormonal medication, such as the oral contraceptive pill.

Inclusion Criteria

Inclusion was any women undergoing hysterectomy for benign conditions, such as heavy periods, uterine prolapse or benign lesions, such as polyps.

Exclusion Criteria

- Women currently taking steroid therapy (estrogen, progestagen, and/or androgen).
- Women with gynaecological cancer or precancerous conditions.
- Pregnancy within the last 6 months.
- Women with large fibroids.
- Women with endometritis (infection of womb inner lining)
- Women unable to give informed consent

2.2 Tissue Collection

The specimens, obtained from the women undergoing hysterectomy, consisted of full thickness biopsies of about 2 cm x 1 cm x 3 cm including the entire uterus from the

endometrium to the serosal edge and were taken from the midline of the uterus on the uppermost (anterior) surface of the uterus and near to the fundus. This was done to be consistent with previous work (Mehasseb et al., 2011a) and because previous debates on where best to take the biopsy are yet to be resolved (Marwan Habiba, 2016). Such small biopsies do not interfere with the requirements for clinical diagnosis and I established links with the histopathology department to ensure clinical priority. Any uteri with suspicious lesions were excluded. The biopsy was fixed in neutral-buffered saline for 24 hours before being embedded in paraffin wax. Haematoxylin and eosin (H&E) staining for all samples was performed to confirm the phase of the menstrual cycle and the presence or absence of adenomyosis. Histological dating of the biopsy was characterised as either early, mid or late proliferative or early, mid or late secretory according to Noyes criteria (Noyes et al., 1975).

Another part of the specimen was also separated into outer and inner myometrium. Each piece measuring approximately 2 mm x 2 mm x 5 mm was flash frozen in liquid nitrogen for the production of RNA. Additionally, similar sized pieces of inner and outer myometrial were cut into small pieces, treated with collagenase I using techniques used in the gynaecology endocrinology research group (GERG) to create individual primary myometrial cell cultures. Small pieces of endometrium were also treated in the same way to generate stromal cell cultures.

2.3   Initial preparation of cell cultures

After the uterus had been removed by hysterectomy and before adding to formalin, a full thickness myometrium including the endometrium was cut at the fundus of the uterus. The endometrium was 'scooped out' and the myometrium alone cut into small

pieces with sterile scalpels, transferred to a small pot of phosphate-buffered saline (PBS) and transported to the tissue culture lab on ice, where the perimetrium was dissected off the myometrium. The myometrial tissue were minced into small pieces (1 mm x 1 mm x 1 mm) in a Petri dish using a scalpel blade and added to collagenase (50 mg in 25 ml of growth medium) warmed to 37°C. The digested tissue was placed into a shaking water bath for 3 hours, then removed and allowed to stand for two minutes so that the undigested material settled to the bottom of the Falcon tube under gravity. The digested material above any tissue lumps were transferred to a fresh 50 ml tube with a serological pipette and the volume increased to 50 ml with ice-cold growth medium (10% Charcoal-stripped FBS/DMEM F12 media) and centrifuged at 1400 rpm for 5 min at 4°C. Supernatant was aspirated and the pellet resuspended in 50 ml of growth medium and centrifuged again. This washing step was repeated three times. After the final wash, the supernatant was discarded and the cells resuspended in 10 ml of growth medium, transferred into a culture flask and an extra 10-15 ml extra growth medium was added and incubated for 24 hours. Media was changed on the day 1 (24 hrs), day 3 (72 hrs) then on day 5 (120 hrs) (Arnold et al., 2001).

Once the culture reached 70-80% confluence, the cells were subcultured. For subculture, medium was removed, and the cells washed with 5-10 ml of sterile PBS, 2 ml of trypsin-EDTA added and incubated with the cells for 3-5 min at 37°C. Cells were then 'squirted' from the plastic surface with the aid of 10 ml of growth medium and transferred into 3 flasks with more growth medium added to bring the cell volume to 20 ml and the cells regrown to 70-80% confluence (Arnold et al., 2001). At this point, one flask was kept in the incubator for further subculture and storage purposes, whilst the remaining two flasks were used to set up experiments. For storage, the collected cell

pellets were resuspended in 500 µl of growth medium and 500 µl of cell freezing solution (20% DMSO: 10% FCS: 70% medium) added, carefully mixed, placed into cryovials and frozen at -80°C for later experiments. The same culture method been used to culture the endometrial stromal cells. The scooped endometrium was treated with collagenase and subjected to the above process to separate the stromal cells. Separated cells were cultured, harvested and stored in cryovials at -80°C. Each specimen was given unique code to identify them without difficulty. Once the histopathology confirmed the presence or absence of adenomyosis from the uterine specimen sent to the lab earlier, the cell cultured obtained from that particular uterine specimen is labelled as normal or adenomyotic sample and stored separately and used for the project experiments.

2.4   Immunohistochemical Studies

2.4.1   Materials

The types and sources of the antibodies used are shown in Table 2-1. The optimal dilutions were determined on control sections.

Table 2.1: Details of antibodies used for immunohistochemical studies

Species	Antigen	Catalogue Number	Supplier	Optimal Dilution
Rabbit	NGF	sc-584	(Santa Cruz)	1 in 100
Rabbit	Cav-1	ab-18199	(Abcam)	1 in 400
Rabbit	Cav-2	ab-79397	(Abcam)	1 in 100
Rabbit	Wnt 4	hpa-011397	(Atlas)	1 in 100
Rabbit	Wnt 5	ab-72583	(Abcam)	1 in 100
Rabbit	Wnt 7a	hpa-015719	(Atlas)	8 in 250

Reagents:

Citrate Buffer (10x)	19.21g citric acid, made up to 500ml with water, pH adjusted to 6.0 with NaOH and made up to 1L.
6% H_2O_2	30% H_2O_2 (Fisher Scientific) + dH_2O
PBS (10x)	2g KCl, 2g KH_2PO_4, 80g NaCl, 11.5g Na_2HPO_4, pH to 7.4 with HCl and made up to 1 Litre
PBS/Tween $_{20}$ (1x)	200ml x10 PBS, 1.8L dH_2O, 1ml Tween$_{20}$
BSA Blocking Solution	0.75g Bovine Serum Albumin, 50 ml 1xPBS
Goat Anti Rabbit antibody	Polyclonal Goat anti rabbit (Dakocytomation)
Rabbit Anti Mouse antibody	Polyclonal Rabbit Anti Mouse Antibody
Xylene	(Genta Medical, Tockwith, York)
Industrial Methylated Spirit (IMS 99%)	(Genta Medical, Tockwith, York)

2.4.1.1 *Immunohistochemistry Protocol for NGF*

The biopsy specimens obtained from the women undergoing hysterectomy were fixed in neutral-buffered saline for 24 hours before being embedded in paraffin wax and cut at 4 μm thickness and dried onto silane-coated glass histology slides.

All slides were then de-waxed and rehydrated with the following protocol:

- Xylene   for 3 minutes, three times
- 99% IMS   for 3 minutes, twice

- 95% IMS   for 3 minutes, once

- dH$_2$O   for 3 minutes, once

The specimen slides were then placed in 10 mM citric acid buffer and heated in a microwave at 800 Watts for 15 min followed by a 20 min cool down period to facilitate antigen retrieval. Once cooled the slides were subject to a 5 min wash in tap water to remove the citric acid buffer. Following the wash, slides were incubated in 6% H$_2$O$_2$ for 10 min to suppress endogenous peroxidase activity, followed by a further wash in tap water to remove traces of hydrogen peroxide. Slides were then washed in phosphate-buffered saline (1xPBS) for 5 min then in 0.05% Tween 20 diluted in 1xPBS, for a further 5 min. The tissue sections on the slides were then wiped around using tissue paper to create a surface tension barrier that prevents solutions from running off the tissue sections. To each slide, 100 µl of blocking solution comprising of a BSA and serum mix (1.8 ml of 1.5% BSA + 200 µl normal goat serum) was added. More than 100 µl was added to certain tissue sections, if the original aliquot was insufficient to completely coat the tissue section. Primary blocking incubation was performed for 1 hr to prevent non-specific binding of antibodies to mis-shaped antigens produced during tissue preparation and antigen retrieval. After this, incubated sections were drained and excess-blocking solutions wiped off the slides. To each of the sections, 100-200 µl of primary antibody was introduced at the dilutions listed in table 2.1 and incubated at 4°C overnight in a humidified chamber to prevent antibody evaporation.

After the overnight incubation, slides were washed in PBS/Tween$_{20}$ solution for 30 min to prevent unwanted cross-reactivity between the primary and secondary antibodies. Next, 100-200 µl of secondary antibody (goat anti-rabbit antibodies, 1:400) conjugated to biotin were added and incubated at room temperature for 30 min. Slides were then

washed again in PBS/Tween$_{20}$ for 30 min before being exposed to avidin-biotin complexes conjugated to horseradish peroxidase for 30 min to introduce the avidin-biotin-HRP complex to the surface of the secondary antibodies. A final wash in PBS/Tween$_{20}$ was performed for 30 min to remove excess unbound ABC reagent before being exposed to 100-200µl of 3, 3'-diaminobenzidine for 5 min. Samples were then washed in running tap water, dehydrated through 95% IMS, 99% IMS twice for 3 minutes each, clearing twice in xylene for 3 min, before being mounted in DPX and left to dry for 24 hr.

2.4.1.2   Immunohistochemistry Protocol for Caveolin 1 & 2, Wnt 4, 5a & 7a:

All slides were de-waxed and rehydrated with the following protocol:

Xylene for 3 min, three times

99% IMS for 3 min, twice

95% IMS for 3 min, once

70% IMS for 3 min, once

50% IMS for 3 min, once

dH$_2$O for 3 min, once

The biopsy specimens obtained from the women undergoing hysterectomy was fixed in neutral-buffered saline for 24 hours before being embedded in paraffin wax. The specimen slides were then heated in a microwave at 800 watts for 20 min in tri-sodium citrate buffer to facilitate antigen retrieval followed by a 20 min cool down period to allow proteins to refold. Once cooled, the slides were subject to a 5 min wash in tap water to remove the citric acid buffer. The slides were washed twice for 5 min in tris-buffered saline (TBS) plus 0.025% Triton X-100 with gentle agitation. Tissues were

then wiped around using tissue paper to create a surface tension barrier. To each slide, 100 µl of blocking solution comprising 1% BSA in TBS and serum mix (1.8 ml of 1% BSA in TBS + 200 µl normal goat serum) was added. More than 100 µl was added to certain tissue sections if the original aliquot was insufficient to completely coat the tissue. Primary blocking incubation was performed for 2 hr to prevent non-specific binding of antibodies to mis-shaped antigens produced during tissue preparation and antigen. After this, incubated sections were drained and excess-blocking solutions wiped off the slides. To each of the sections, 100-200 µl of primary antibody was introduced at the dilutions listed in table 2.1 and incubated at 4°C overnight in a humidified chamber.

After the overnight incubation, slides were removed and washed in TBS/0.025% Triton X-100 twice for 5 min, with stirring. Following the second wash, slides were incubated in 6% H_2O_2 for 10 min to suppress endogenous peroxidase activity. Then, 100-200 µl of secondary antibody (goat anti-rabbit conjugated to biotin diluted in TBS; 1:400) was added to each slide and incubated at room temperature for 1 hr. Slides were then twice washed again in TBS/Triton X-100 for 5 min each before being exposed to avidin-biotin complexes conjugated to horseradish peroxidase for 30 min. The slides were subjected to a final wash in TBS for 20 min to remove excess unbound ABC reagent. The slides were then exposed to 100-200 µl of 3, 3'-diaminobenzidine for 5 min and then washed in running tap water, dehydrated through 95% IMS, 99% IMS twice, 70% IMS, 50% IMS for 3 min each, cleared twice in xylene for 3 min before being mounted in DPX and allowed to dry for 24 hr.

2.4.1.3   Immunohistomorphometric Analysis

Slides were examined under light microscopy and the staining patterns for each of the antigens observed and recorded. For the histomorphometric analyses, 10 random fields of the inner and outer myometrium for each antigen were taken on an Axioplan microscope equipped with a Sony DXC-151P analogue camera, with the light levels set at 6400K in the presence of neutral density and daylight filters. The images were captured using Axiovision version-4.5 software and saved as individual Tiff files. Images were then processed through Aperio ImageScope software to determine a histoscore for each field, using the Positive Pixel Count Version 9.0 module, with a low staining threshold of 205, a staining threshold of 175 and an intense staining threshold of 105. The number of negative pixels was also recorded and the histoscore calculated using the follow formula:

$$\frac{(100 \ x \ the \ low \ staining \ count) + (200 \ x \ the \ stained \ count) + (300 \ x \ the \ intense \ staining \ count)}{Total \ count \ (all \ negative \ and \ positive \ pixels)}$$

The mean and standard deviation for each slide and antigen was then calculated.

2.5   Myometrial Cell Culture Experiment

These cultures were set up from cells frozen following histological diagnosis using the protocols in section 2.2. Myometrial cells from both normal and adenomyotic uteri were taken from the freezer and thawed rapidly at 37°C, placed in growth medium (10% Charcoal-stripped FBS/DMEM F12) and grown to 80-90% confluence in 75-cm^2 flasks, before being sub-cultured at 2 x 10^5 cells/well into 6-well plates (in triplicate) and allowed to attach and grow for 48 hr. At this point, the cells were treated with 10^{-6} M estradiol or 10^{-6} M tamoxifen for 48 hr (see Figure 2.2). RNA was then extracted using

the TRIzol method, treated with DNase I to remove contaminating genomic DNA, reverse transcribed and subjected to RT-PCR as explained in the following sections.

2.5.1 Materials

2 x 6 well plates	BD Biosciences
17β-estradiol	Sigma Aldrich
Tamoxifen	Sigma Aldrich
Ethanol	Sigma Aldrich
DMEM F12/1:1	GIBCO
Trypsin-EDTA	GIBCO

2.6 RNA Extraction

2.6.1 Materials

TRIzol	Invitrogen
Chloroform HPLC Grade (99.5%)	Sigma Aldrich
Isopropanol	Sigma-Aldrich
DNase I Reaction Buffer 10x	Promega
RNase-Free DNase 1, 1U/µl obtained from bovine pancreas. 10mM HEPES (pH 7.5), 50% glycerol, 10mM CaCl$_2$	Promega
RNase inhibitor (RNasin)	Promega
DEPC Treated Water	One litre of water, plus 1ml DEPC
75% Ethanol	75ml Ethanol, 25ml DEPC treated water
Agarose	ICN Biolabs

Chloroform: isoamyalcohol (24:1)	Sigma Aldrich
Phenol: chloroform: isoamylalcohol (25:24:1)	Sigma Aldrich
TAE buffer	37.2g EDTA, 242g Tris Base, 57.1ml glacial acetic acid

2.6.2 Method

Cells were exposed to TRIzol reagent (1 ml/well), scraped off the plastic with a cell scraper and the resultant mixture transferred to a microfuge tube. After incubation at room temperature for 5 min, 200 µl of chloroform was added, the mixture shaken vigorously for 15 sec and allowed to stand at room temperature for 3 min. After centrifugation at 13000 rpm for 15 min at $4^{o}C$, the upper aqueous layer was transferred to a fresh microfuge tube, where RNA was precipitated by incubation of 0.5 ml of isopropyl alcohol at room temperature for 10 min and the RNA collected by centrifugation for 10 min at 13000 rpm at $4^{o}C$. The RNA pellet was washed with 1ml of 75% ethanol in DEPC-dH_2O, and the RNA collected again by centrifugation for 5 min at 13000 rpm at $4^{o}C$. The RNA was allowed to air dry for 7 min before being dissolved in DEPC-dH_2O at $55^{o}C$ for 5 min. The RNA was briefly centrifuged to collect the solution at the bottom of the tube and stored at $-80^{o}C$ for DNase I treatment and RT-PCR analysis.

2.7 qRT-PCR

2.7.1 Materials

SYBR Green PCR Kit (Roche)	Light Cycler FastStart DNA Master SYBR Green 1
DNA ladders	Ready Load 100bp DNA ladder, 0.1µg/µl (Invitrogen)

	1000bp ladder (New England Biolabs)
AMV-RT	Avian Myeloblastosis Virus Reverse Transcriptase (Promega) 10U/µl
AMV-RT Buffer 5X	comprised of: 50mM DTT, 2.5mM Spermidine, 250mM Tris-HCL (at pH 8.3), 50mM $MgCl_2$ and 250mM KCl (Promega)
Taq DNA Polymerase	Crimson Taq Polymerase®, 100mM KCl, 10mM Tris-HCl (pH 7.4 at 25°C), 0.1 mM EDTA, 1mM dithiothreitol, 0.5% Tween 20, 0.5% NP-40 and 50% glycerol. (New England Biolabs)
Oligo (DT):	Anchored Oligo (dT) $_{23}$ Primers, 0.5µg/µl in sterile water (Sigma Aldrich)
10mM dNTP mix	diluted dGTP, dTTP, dCTP, dATP in sterile water (Roche)
Primer Sequences:	(Sigma Aldrich) for full sequences see appendix 2

2.7.2   DNase Treatment

2.7.2.1 Materials

Table 2.2: Materials used for DNase treatment

Materials	Volume for each sample
10x DNase Reaction Buffer	15 µl
RNase-Free DNase 1	10 µl
RNasin	3.15 µl
DEPC treated water	21.85 µl
Total Volume	50 µl

2.7.2.2 Method

DNase I treatment was applied to all RNA samples to remove contaminating genomic DNA. This required the incubation of the RNA samples with a master mix solution (table 2.2). After ensuring that the initial volume of total cellular RNA was adjusted to 100 μl in DEPC-treated dH_2O, 50 μl of master mix was added to the samples and the mixture incubated at 37^oC for 1 hr. After this, an equal amount (150 μl) of acid phenol: chloroform: iso-amyl alcohol (25:24:1) was added and vortexed for 1 min at high speed. The solution was then centrifuged for 2 min at 4^oC, at 11,000-x g. The resulting supernatant was transferred to a RNA-free microfuge tube, where an equivalent amount (~160μl) of chloroform: isoamylalcohol (24:1) was added.

The samples were vortexed for 10 sec and then centrifuged at 11,000-x g at 4^oC. Again, the supernatant was transferred to a fresh microfuge tube and 0.6x the equivalent volume of isopropanol (~100 μl) added. The samples were vortexed for 10 sec and then incubated for 1 hr at -20^oC. The RNA was pelleted by centrifugation at 11,000-x g for 5 min at 4^oC, washed and re-suspended in 1 ml of ice-cold 75% ethanol in DEPC-treated dH_2O, and centrifuged at 7500-x g for 5 min. RNA pellets were allowed to air dry in inverted microfuge tubes for no longer than 7 min, with excess ethanol removed by wiping inside the inverted microfuge tube with a paper tissue. RNA was then re-suspended in DEPC-treated dH_2O in a volume ranging from 20-100 μl depending on the original amount of sample.

2.7.3 AMV-RT Reverse Transcriptase

2.7.3.1 Materials

Table 2.3: Materials used for Reverse Transcriptase reaction

Material	RT+	RT-
5X AMV Buffer	5.00 µl	5.00 µl
RNasin	0.62 µl	0.62 µl
Anchored Oligo (dT)$_{23}$	1.00 µl	1.00 µl
10mM dNTPs	2.50 µl	2.50 µl
AMV RT	0.50 µl	-
DEPC-Treated water	-	0.50 µl
Total Volume	9.62 µl	9.62 µl

2.7.3.2 Method

Samples of RNA were thawed on ice and samples prepared as follows, with an extra microfuge tube prepared as a negative control (this is indicated as RT-) with the mastermix composition indicated in table 2.3. To each mastermix, approximately 1 µg of RNA was added and made up to the final volume of 25µl with DEPC-treated dH$_2$O. The samples were then vortexed to mix thoroughly, centrifuged briefly to collect the sample at the bottom of the tube and then incubated at 42°C for one hr. At the end of the incubation period the temperature was raised to 95°C for one min to denature all of the enzymes. The resulting cDNA was either used immediately for downstream PCR amplifications or stored at 4°C until needed.

2.7.4 RNA/DNA Quantification

Both DNA and RNA levels were quantified using NANODrop analysis to produce accurate concentrations for later RT-PCR and standard PCR.

2.7.5 Quantitative polymerase chain reaction (qPCR)

2.7.5.1 Materials

Table 2.4: Materials used for qPCR reactions

Material	Volume
SYBR® green mix	64.0 µl
Forward Primer	32.0 µl
Reverse Primer	32.0 µl
10mM dNTPs	32.0 µl
NaCl Buffer	51.2 µl
PCR grade Water	364.8 µl
Total Volume	576 µl (32x Reactions)

2.7.5.2 Method

To obtain quantitative measurements the relative gene expression, qPCR was used. A standard reagent master mix (table 2.4) was used. Materials and solutions were obtained directly from Roche Diagnostics™ (Lewes, Sussex, UK) and prepared/used in accordance with the manufacturer's instructions. The composition of the mastermix was created so that it resulted in a reaction volume of 18 µl per capillary tube. To each capillary tube containing 18 µl of master mix, 1 µl of template DNA was introduced. The capillary caps were inserted, and the capillaries were loaded into the carousel in order, with position, sample and capillary number all being recorded. The carousel was centrifuged a minimum of 2 times at 3000rpm for 15 seconds to ensure that samples mixed thoroughly and collected at the base of each capillary tube. The conditions required for qPCR analysis was directly comparable to standard PCR analysis, except for time used for the denaturation, annealing and extension steps, which were reduced and cycle numbers increased to 40, which was due to lower sample volume and higher

efficiency of both solutions and equipment. The qPCR conditions for the genes quantified are as shown in table 2.5. All the qRT-PCR experiments were performed as described in the MIQE guidelines (Bustin et al., 2010). In my real time PCR assay a positive reaction is detected by accumulation of a fluorescent signal. The Ct (cycle threshold) is defined as the number of cycles required for the fluorescent signal to cross the threshold (exceeds background level). Ct levels are inversely proportional to the amount of target nucleic acid in the sample (the lower the Ct level the greater the amount of target nucleic acid in the sample).

Table 2.5: Temperature and cycle conditions used for qPCR

Gene	Initial Denaturation		Denaturation		Annealing		Extension	
GAPDH	95˚C	600 sec	94˚C	10 sec	60˚C	5 sec	72˚C	13 sec
NGF	94˚C	600 sec	94˚C	10 sec	62˚C	5 sec	72˚C	13 sec
Wnt5a	95˚C	600 sec	95˚C	12 sec	60˚C	12 sec	72˚C	24 sec
Caveolin	95˚C	600 sec	95˚C	12 sec	60˚C	12 sec	72˚C	24 sec

2.7.6 GAPDH as reference Gene

In real-time RT-qPCR, one of major step is the normalization of gene quantification by including an endogenous control (reference gene) to improve the reliability of the result, to correct for sample-to-sample variation and errors in sample quantification. A biologically meaningful reporting of target mRNA copy numbers requires accurate and relevant normalization to some standard and as such, is strongly recommended in quantitative RT-PCR. Data normalization can be carried out against an endogenous unregulated reference gene transcript and GAPDH (glyceraldehyde 3-phosphate dehydrogenase) was the reference gene I used in the experiments presented herein. GAPDH was used as the housekeeping gene because it has already been proven to be

unaffected in the endometrium and myometrium through the menstrual cycle. It is also unaffected in the transition from reproductive age to non-reproductive age, in benign versus cancerous tissue and in endometriotic or adenomyotic tissue or the presence polyps or cystic glands or any other uterine pathology (von Wolff et al., 2000). Also, it is unaltered in the decidua, placenta or fetal membranes (Arenas-Hernandez and Vega-Sanchez, 2013) and so a valid normalization gene for transcript levels in the uterus.

2.8   Myometrial – Endometrial Co-culture

2.8.1   Materials

Rat-tail collagen 1	Becton Dickinson, BD Biosciences, Oxford (3.11 mg/ml solution containing 0.02M acetic acid)
10 x Hank's Balanced Salt Solution (HBSS)	GIBCO
2M NaOH	diluted from 6M stock and then sterilise by filtration through 0.2μm filters
Fetal Calf Serum (sterile)	GIBCO
12-well culture plates	BD Biosciences, Oxford
Cell culture inserts of 3.0 μm pore size	Becton Dickinson, Oxford
Cell culture growth media	(DMEM-Glutamax^{+TM} with 10% FCS, and 5% Antibiotic/ Antimycotic solution (Penicillin/ Streptomycin/Amphotericin)

3% Agarose in Hank's Buffered Salt solution	prepared freshly on the final experimental day
10% Neutral-buffered formalin	10% formaldehyde in PBS (pH 7.4)

2.8.2   Method

In this procedure, it is extremely important that all reagents and equipment remain cold otherwise the collagen sets. Briefly, eight parts of rat-tail collagen type I were mixed with 2 parts of cell culture medium and gently mixed using a cell culture pipette (kept in fridge) to avoid introducing air bubbles, and then 11.5 μl of 2M NaOH per one ml of collagen was added to neutralise the acidic gel mixture. The colour change (red to light pink) of the solution was used as an additional guide to indicate that neutrality had been achieved.

The first two plates consisting of plain collagen onto which stromal cells were placed on top were prepared as follows: after neutralisation of the collagen, 22.5 ml of collagen was transferred to a separate tube and 2.5 ml of DMEM medium added, mixed thoroughly without introducing air bubbles. One ml of the collagen/medium mixture was transferred to each insert, sitting in the 12-well plates, and the gel polymerised by incubation at 37°C for 1 hr. For the remaining four plates, consisting of myometrial cells embedded in collagen, another two tubes were taken and 22.5 ml of neutralised collagen was transferred into each tube with one labelled 'normal' and the other 'adenomyosis'.

The biopsy specimens obtained from the women undergoing hysterectomy were cut into small pieces, treated with collagenase I using techniques used in the gynaecology

endocrinology research group (GERG) to create individual primary myometrial cell cultures. Small pieces of endometrium were also treated in the same way to generate stromal cell cultures. Cells from the cultures are labelled as normal or adenomyotic, based on the histopathology diagnosis on the original uterine tissue sent to the lab. Normal and adenomyotic myometrial cells were collected from the cultures by trypsinisation, washed with medium and the cell pellet suspended in 2 ml of DMEM. The cells were then counted on a haemocytometer and the volumes adjusted to ensure that the cell density was ~1,000,000 cells/ml. Then, 2.5 ml of suspended cells was mixed with the neutralised collagen in the corresponding tube and thoroughly mixed. One ml of collagen containing myometrial cells was transferred to the inserts of respective plates (normal myometrial cells in plates 3 & 5 and adenomyotic cells in plates 4 & 6). The plates and cells were incubated at 37°C for 1 hr. Once the collagen had polymerised, the gel was covered with medium for about 15 min before inoculating with the stromal cell suspension. In the meantime, stromal cells were harvested from culture with trypsin-EDTA, the pellets collected and re-suspended in 20 ml of medium. Cells were counted and 100,000 cells were added to each insert on top of the collagen (normal stromal cells in plates 1, 2, & 4 and adenomyotic cells in plates 3, 5, & 6).

One ml of normal media was placed in the bottom well under the insert and 0.5 ml in the inserts. The plates were all then incubated at 37°C. After 10 days of culture, 1 ml of melted 3% agarose gel in HBSS (boiled and allowed to cool to room temperature) was added on top of the inserts and allowed to set fully in the incubator. The collagen matrix-agarose blocks were removed carefully, using forceps, and placed in 10% neutral-buffered formalin for 24 hr and then embedded in paraffin wax for histology and immunohistochemistry.

2.8.3   Immunohistochemistry for α-smooth muscle actin

The paraffin-embedded sections were dewaxed in xylene, and rehydrated in graded alcohols and water. Endogenous peroxidase activity was blocked with 6% (v/v) hydrogen peroxide (H_2O_2) in water for 10 min. Specific mouse-on-mouse blocking reagent (Vector labs, Peterborough, UK) was applied for one hr. Sections were incubated overnight at 4^oC with the primary antibodies against α-SMA (clone SMM1, Vector labs, Peterborough, UK). Biotinylated rabbit anti-mouse was applied at a concentration of 1:400 (v/v) for 30 minutes at room temperature. Immunoreactivity was demonstrated with 3,3'-diaminobenzidine/H_2O_2 (DAB solution) (Vector labs, Peterborough, UK). Sections were lightly counterstained with haematoxylin, then dehydrated and cleared in graded alcohol and xylene, and finally covered with glass slips. Image capture and analysis was performed using Axioplan® 2 light microscopy (Carl Zeiss, Germany) and an image capture system. The system was based on a single chip colour video camera (Sony DXC-151P, Sony Inc., Japan) connected to a camera adapter (Sony CMA-151P, Sony Inc., Japan) that transmits the image to a Windows® based computer *via* a Meteor 2 MMC graphics display interface and the Axiovision image analysis software (version 4.5, Carl Zeiss, Germany).

2.9   Decidualisation experiment

2.9.1   Materials

12 well plates	BD Biosciences, Oxford
17β-estradiol	Sigma Aldrich (Cat No: E2257)
8-Bromo Cyclic Adenosine Monophosphate	Sigma Aldrich (Cat No: B5386)

| Ethanol | Sigma Aldrich (Cat No: 459844) |
| MedroxyProgesterone Acetate | Sigma Aldrich (Cat No: P1649) |

2.9.2   Method

Normal and adenomyotic stromal cells were taken from the freezer, thawed rapidly at 37°C and transferred into culture flasks. The cells were grown in DMEM/F12 media supplemented with 10% charcoal-stripped fetal bovine serum (FBS) and 1% antibiotics (penicillin/streptomycin) until they reached confluence. Cells were harvested by trypsinisation and centrifugation at 300-x g for 5 min, counted on a haemocytometer and 2×10^5 cells transferred into six wells of a 12-well plate. One ml of media with 10% charcoal stripped serum and antibiotics were added and the cells incubated at 37°C in a humidified atmosphere with 5% CO_2.

2.9.3   Decidualisation

To initiate stromal cell decidualisation, cells were treated with 1 μM medroxyprogesterone acetate (MPA), 0.5 mM of 8-br-cAMP and 10^{-8} M of 17β-estradiol or an equivalent amount of ethanol in the controls for 21 days, with the media changed every 2-3 days. At the end of the treatment, RNA was extracted, DNase 1 treated, quantified by Nanodrop and stored at -80°C

2.9.4   RT-PCR

2.9.4.1   Materials

Table 2.6: Materials used for the standard PCR reaction

Material	Volume
Red Taq Polymerase (5U/µl)	0.125 µl
10X Buffer IV	2.5 µl
dNTP Mix (10mM)	2.0 µl
MgCl$_2$	1.5 µl
Forward Primers	1.25 µl
Reverse Primers	1.25 µl
cDNA	1.0 µl
DNase Free Water	15.375 µl
Total Volume/tube	**25.0 µl**

2.9.4.2   Method

cDNA samples and reagents were thawed on ice and PCR primers prepared fresh each time an experiment was performed. A mastermix sufficient for 26 tubes was prepared (table 2.6), thoroughly mixed and 24 µl aliquoted to a thin walled PCR tube. Representative cDNA (1 µl) from decidualised and non-decidualised cultures were added to respective tubes. The samples were mixed, briefly centrifuged to collect the reagents to the bottom of the tube and transferred to thermal cycler. The PCR ran using the following cycle conditions.

Table 2.7: Temperature and cycle conditions used for standard PCR

Gene	Initial Denaturation		Denaturation		Annealing		Extension		Cycle Number
GAPDH	95˚C	600 sec	94˚C	10 sec	60˚C	5 sec	72˚C	13 sec	40
IGFBP-1	95˚C	120 sec	94˚C	30 sec	57˚C	60 sec	72˚C	90 sec	35
Prolactin	95˚C	120 sec	94˚C	30 sec	60˚C	60 sec	72˚C	13 sec	40
Wnt5a	95˚C	600 sec	95˚C	12 sec	60˚C	12 sec	72˚C	24 sec	40

After the PCR, the samples were centrifuged briefly, 20 µl of PCR product was loaded onto a 3% TAE agarose gel and the samples separated by electrophoresis at 120 Volts for 70 min. The bands were visualised using a Syngene UV System (Syngene UK) and analysed using Scion Image software (http://scion-image.software.informer.com). Data were corrected for the levels of GAPDH transcript.

Chapter 3   Myometrial-Stromal Cell Culture Model

3.1 Introduction

As stated in Chapter 1, an important component in the aetiopathology of adenomyosis is the endometrial-myometrial interface (EMI), which is also called the 'junctional zone' through MRI scans. Abnormal stromal cell invasion has been proposed in the aetiology of adenomyosis (Ferenczy, 1998), but the features in the microenvironment that limit myometrial penetration by the overlying endometrium and the changes that precede or trigger the development of uterine adenomyosis remain unknown. Steroids affect adenomyosis, and its pathogenesis may be linked to local hyperestrogenism (Benagiano et al., 2012, Urabe et al., 1989), which may be mediated through the action of aromatase on androgen precursors or by the activity of estrone sulphatase or dehydrogenases (Ezaki et al., 2001). A range of ultrastructural abnormalities in the inner and outer myometrial layers of women with uterine adenomyosis (Mehasseb et al., 2011a) have recently been described by our research group and we also demonstrated that the development of adenomyosis in the CD1 mouse after neonatal exposure to tamoxifen is associated with thinning, lack of continuity, and disorganization of the inner myometrium (Mehasseb et al., 2009).

Our research group recently established a primary stromal cell/myometrial cell co-culture model (Mehasseb et al., 2010b) in which myometrial cells are dispersed through a rat-tail collagen matrix in a Boyden chamber and stromal cells plated on top (Figure 3.1). When the stromal cells of either normal or adenomyotic uteri were placed on top of the collagen containing myocytes obtained from uteri with adenomyosis, increased invasiveness of stromal cells was observed compared to a collagen containing myocytes obtained from normal uteri (Mehasseb et al., 2010b). As explained in Chapter 1, the problem with those studies was that the effect of sex steroid hormones, particularly

estradiol and tamoxifen were not assessed with regard to stromal cell invasion. Therefore, in this Chapter, I will describe what effect (if any) that estradiol and tamoxifen has on stromal cell invasion in the co-culture model to assess whether the addition of steroids changes the invasion characteristics of the two types of stromal cells.

3.2 Co-culture model

Figure 3-1 shows a schematic representation of a cross-section through the 3D co-culture model after setting up. It shows how the stromal cells are plated above a rat-tail collagen matrix in which 10^5 myometrial cells were imbedded.
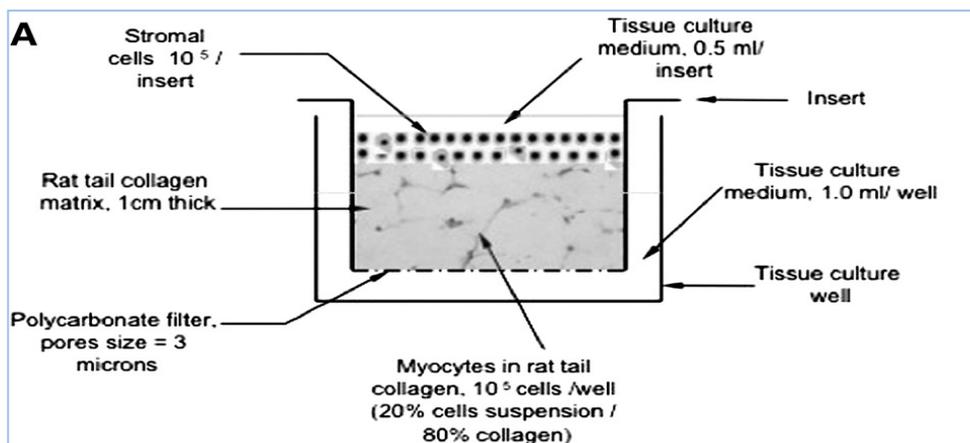
Figure 3.1: Schematic representation of the co-culture model showing its different compartments and cell components taken from reference (Mehasseb et al., 2010b)

3.3 Results

Figure 3.2 shows representative images of stromal cells from normal and adenomyotic uteri grown on top of either rat-tail collagen alone or gels impregnated with myometrial cells from normal or adenomyotic uteri. The red arrow in each case shows the depth of

penetration of the blue (haematoxylin-stained) stromal cells within the collagen-impregnated layer. The brown α-sma stained myocytes can be seen dispersed throughout the collagen layer (where they have been added).

3.4   α-SMA immunostained section
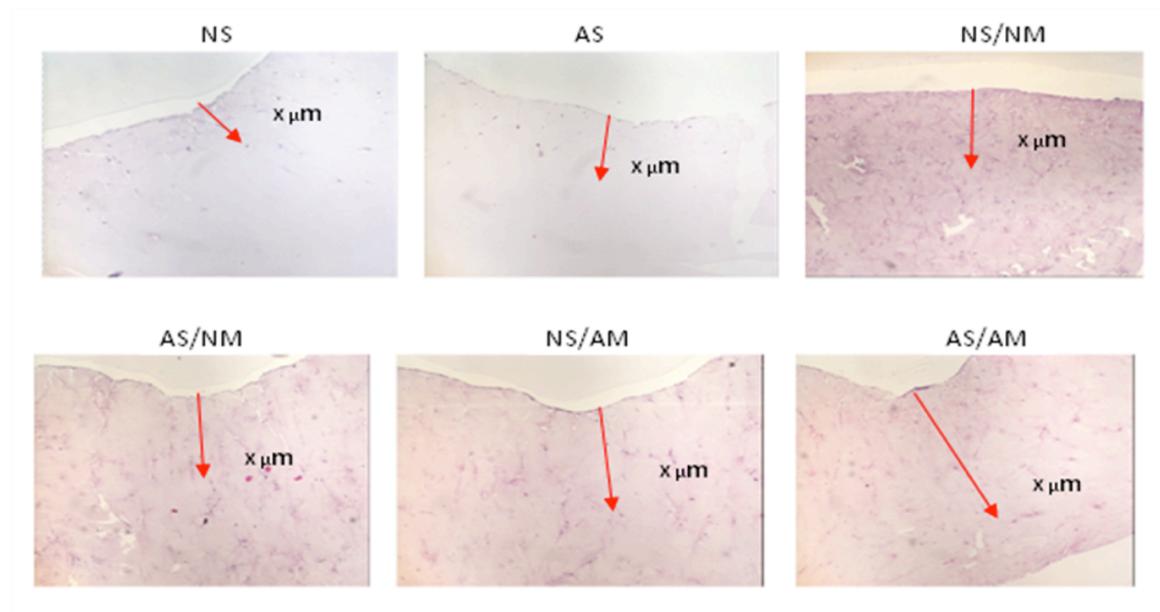
Figure 3.2: Represents the α-smooth muscle actin (a-SMA) immunostained paraffin section showing the migration of stromal cells under different co-culture condition. NS: Normal Stromal cells on Collagen alone; AS: Adenomyotic Stromal cells on Collagen alone; NS/AM: Normal Stromal cells on Normal Myometrial cells; AS/NM: Adenomyotic Stromal cells on Normal Myometrial cells; NS/AM: Normal Stromal cells on Adenomyotic Adeno Myometrial cells; AS/AM: Adenomyotic stroma cells on Adenomyotic Myometrial cells.

3.4.1   Cell migration in the absence of treatments

Normal stromal cells grown on collagen alone migrated 125.0 ± 4.2 μm into the collagen gel whilst adenomyotic stromal cells migrated slightly further through the collagen gel than their normal counterparts, with a mean migration of 185.8 ± 26.5 μm. However, that migratory distance was not significantly different to the distance travelled by the normal stromal cells (Figure 3.3). The movement of both normal and

adenomyotic stromal cells grown on collagen containing myometrial cells from normal uteri was greater than that of either cell type grown on collagen alone, such that normal stromal cells grown on normal myometrial cells showed a mean migration of: 253.6 ± 22.4 μm (p<0.05 when compared to NS alone), whilst there was a 3-fold increase in migration noted in adenomyotic stromal cells grown on collagen with normal myometrial cells (AS/NM: mean migration 647.4 ± 37.7 μm; p<0.05 when compared to AS alone).

Normal stromal cells grown on collagen mixed with adenomyotic myometrial cells showed an increased migration (NS/AM: mean migration = 666.1± 37.9 μm) when compared to the normal stromal cell migration on normal myometrial cells (NS/NM mean migration = 253.6 ± 22.4 μm; p<0.01). The maximum stromal cell migration occurred when adenomyotic stromal cells were grown on collagen mixed with adenomyotic myometrial cells (AS/AM). These cells showed a mean migration of 863.9 ± 61.9 μm), which was significantly longer than normal stromal cells on adenomyotic myometrial cells (NS/NM p<0.01) or adenomyotic stromal cells on normal myometrial cells (AS/NM p<0.05). Adenomyotic stromal cell (AS) grown on collagen alone shows significant increase in migration when compared to normal stromal cells (NS) grown on collagen. Highest migration noted when adenomyotic stroma cells grown on collagen mixed with adenomyotic myometrial cells (AS/AM). Adenomyotic stromal cell (Pink bars) layered onto collagen alone showed significant increased migration through the collagen layer when compared to normal stromal cells (brown bars). Stromal cell migration was enhanced in the presence of myocytes in the collagen layer with the greatest migration noted when adenomyotic stroma cells were placed on top of collagen

containing adenomyotic myometrial cells (far right). Data are the mean ± SEM of 12

independent measurements made on duplicate cultures performed 3 times.
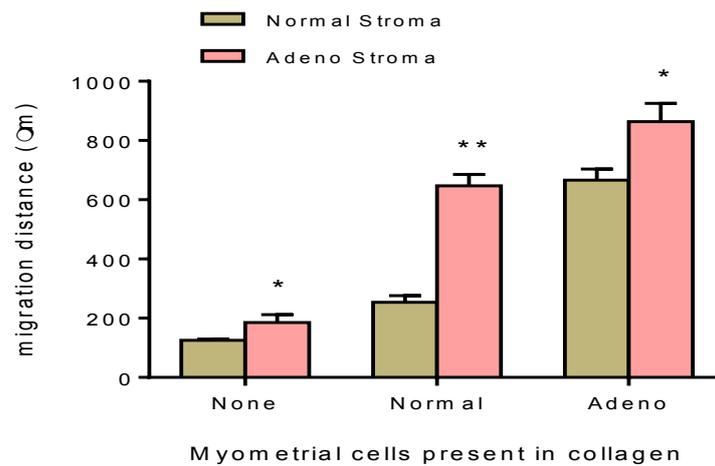
Figure 3.3: Shows differences in distance migrated by stromal cells in different combination of cultures. (*p<0.05; **p<0.01 Student's unpaired *t*-test; for adenomyotic stromal cells compared with normal stromal cells; n=6, Error bar: SEM)

3.4.2 Cell migration in the presence of estradiol & Tamoxifen

Both estradiol and tamoxifen significantly increased the migration of both normal and

adenomyotic stromal cells through a collagen matrix in the absence of myocytes (Figure

3.4), in the presence of normal myocytes (Figure 3.5) and in the presence of

adenomyotic myocytes (Figure 3.6). The depth of invasion of stromal cells from

unaffected and affected uteri increased by an average of 41.3% and by 64.6%,

respectively in the presence of E2 and 73.3% and 73.5% respectively in the presence of

TMX from unaffected uteri. Both estrogen and tamoxifen enhanced stromal cell invasion (diseased and control), and the greater depth of invasion of adenomyotic stromal cells was maintained under all experimental conditions.
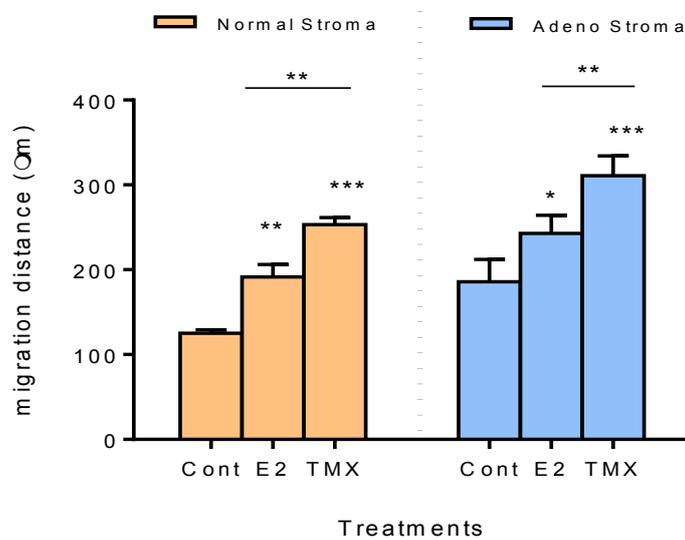
Figure 3.4: Migration of stromal cells in the presence of 10^{-6}M estradiol (E2) or 10^{-6}M tamoxifen (TMX) through a collagen matrix in the absence of myocytes. (*p<0.05; **p<0.001; **p<0.001; one-way ANOVA with Bonferroni's *ad hoc* post-test; n=6).
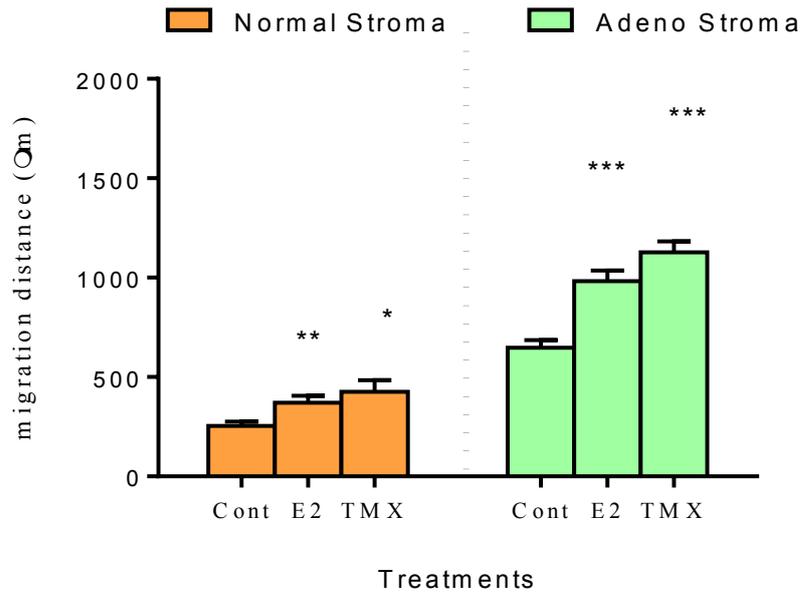
Figure 3.5: Migration of stromal cells in the presence of 10^{-6}M estradiol (E2) or 10^{-6}M tamoxifen (TMX) through a collagen matrix in the presence of normal myocytes. (*p<0.05; **p<0.001; **p<0.001; n.s. = non-significant compared to relative control or E2 treatment; one-way ANOVA with Bonferroni's *ad hoc* post-test; n=6).
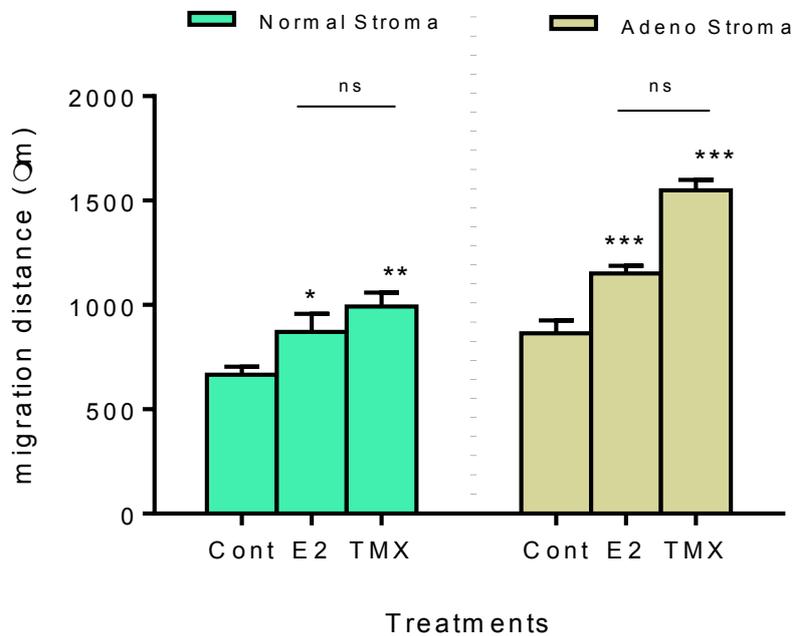

Figure 3.6: Migration of stromal cells in the presence of 10^{-6}M estradiol (E2) or 10^{-6}M tamoxifen (TMX) through a collagen matrix in the presence of adenomyotic myocytes. (*p<0.05; **p<0.001; **p<0.001; n.s. = non-significant compared to relative control or E2 treatment; one-way ANOVA with Bonferroni's *ad hoc* post-test; n=6)

3.5 Discussion

Three-dimensional (3D) co-culture models have been previously used to study cancer invasion (Jones et al., 1997, Jones et al., 2003), where tumour cell invasion has been shown to be modulated by the presence of normal myoepithelial cells (Jones et al., 2003). Co-culture has also been used to examine the invasive properties of trophoblast (Cohen and Bischof, 2009). Recently, our research group reported on the use of a modified 3D co-culture model to examine interactions between endometrial stromal cells and myometrial cells derived from uteri with or without adenomyosis (Mehasseb et al., 2010b), where it was demonstrated that endometrial stromal cells from women with uterine adenomyosis exhibited greater invasion into the collagen matrix than stromal cells from women without adenomyosis (Mehasseb et al., 2010b). This observation is consistent with the hypothesis that adenomyosis results from invasion of the endometrial stroma into the myometrium, but it also suggests that increased invasiveness is an innate property of the adenomyotic stroma. The addition of myocytes from women with adenomyosis to the collagen matrix also increased the depth of invasion of stromal cells from both control and adenomyosis affected uteri, which suggests that adenomyotic muscle might produce soluble factors that enhance stromal cell migration. Previous research suggested a role for estrogen in the pathogenesis of adenomyosis and also linked adenomyosis to tamoxifen use in women with breast cancer (Cohen et al., 1995). The CD1 neonatal model showed a role for tamoxifen but not estradiol in the pathogenesis of adenomyosis (Mehasseb et al., 2009) suggesting a difference between the actions of these two molecules in the rat and human uteri. Considering the nature of this disease and the influence of estrogen and tamoxifen in its

pathogenesis, I have used this novel three-dimensional co-culture model to assess the role of these two molecules on stromal cell invasion and expanded the study to examine the influence of adenomyosis on the outcomes.

The untreated culture that resulted in the most migrant stromal cell was the culture of adenomyotic stromal cells grown on adenomyotic myometrial cells (Figure 3.6) supporting the idea that an inherent property of the stromal cell and the myocytes from adenomyotic uteri is maintained in culture. Additionally, both normal stromal cell and adenomyotic stromal cell showed significant migration on adenomyotic myometrial cells in common with the previous data (Mehasseb et al., 2010b). Both E2 and TMX significantly increased the migration of both normal and adenomyotic stromal cells through a collagen matrix in the absence of myocytes (Figure 3.4), in the presence of normal myocytes (Figure 3.5) and in the presence of adenomyotic myocytes (Figure 3.6). The depth of invasion of stromal cells from unaffected and affected uteri increased by an average of 41.3% and by 64.6%, respectively in the presence of E2 and 73.3% and 73.5% respectively in the presence of TMX from unaffected uteri. Both estrogen and tamoxifen enhanced stromal cell invasion (diseased and control), and the greater depth of invasion of adenomyotic stromal cells was maintained under all experimental conditions.

In this study, I have shown that both estradiol and particularly tamoxifen enhance cell migration in single stromal cell culture and when co-cultured with myocytes, with the migration of stromal cells taken from the uteri of women with adenomyosis always being greater than that of stromal cells obtained from the uteri of women without adenomyosis. These observations suggest that although estrogen potentiates the effect,

the observed difference in invasiveness is innate rather than specifically induced by the steroid. A similar conclusion could be drawn about the effect on myocytes in this culture, suggesting that the role of estrogenic steroids may be to potentiate rather than to induce the disease. The effect of tamoxifen in this model was interesting as it promoted stromal cell invasion to a greater degree compared with estradiol. The observation is interesting because tamoxifen is often considered to be a 'weak' estrogen when compared to estradiol. This is in line with observations from the neonatal CD1 mouse that develops adenomyosis when exposed to tamoxifen or toremifene but no other selective estrogen receptor modulators (Parrott et al., 2001) or estradiol. This probably signifies that there are tissue- and species-specific differences in the actions of estradiol and tamoxifen. For example, when similar studies were performed on the Balb/c mouse, tamoxifen had no effect on the development of adenomyosis. This signifies that genetic predisposition to the development of adenomyosis probably applies, but such studies need to be performed in the future. However, I acknowledge that the *in vitro* model has its limitations. It lacks the complexity of a complete endometrium, which contains other 3D structures including complete glandular tissue and extracellular matrix components, blood vessels; immune cells and at different stages of development. The influence of these (if any) or their secretions cannot be adequately assessed in this model. Equally, the extracellular matrix of the myometrium consists of a variety of different collagen fibres and other embedded structural glycoproteins (such as the caveolins) that mediate interactions between adjacent cells, and some of these extracellular factors may be involved in adenomyosis.

Another possible limitation is the relatively short-term survival of embedded myocytes, which does not allow for longer incubation periods. The number of myocytes that could

be embedded in the collagen matrix was also limited. It would have been theoretically advantageous to have a higher myocytes concentration, but this was hampered by cell clumping at higher cell densities (Mehasseb et al., 2010b). Nevertheless, the data presented in this Chapter suggest that the interaction between stromal cell and myocytes in the uterus is affected by the presence of either estradiol or tamoxifen and that effect is exacerbated by adenomyosis. The suggestion that factors released by either the stromal cell or the myocyte, such as nerve growth factor (Greaves and White, 2006), the caveolins (Mehasseb, 2010) or the wnt5a protein (Mehasseb, 2010) may be affected by the presence of the estradiol or tamoxifen and thus affect the migratory potential of the stromal cell. Each of these factors will now be examined in turn.

Chapter 4   Nerve Growth Factor

4.1 Nerve Growth Factor

Although it has been suggested that NGF is considered as a regulator of uterine development and has been involved in uterine re-innervations after pregnancy, the precise role of nerve growth factor (NGF) expression in the uterus remains unclear (Haase et al., 1997, Varol et al., 2000). What is known is that the effects of NGF in other tissues are mediated by interactions with specific receptors, such as the low affinity p75^{NTR} receptor and the high affinity TrkA, TrkB, TrKC and NT3/NT4 receptors. Recent evidence strongly suggests that NGF and p75^{NTR} might participate in the regulation of tissue morphogenesis, myogenesis and support non-neural cell systems on their way towards terminal differentiation (Seidl et al., 1998). So, besides its role in the nervous system, NGF may be involved in functions other than neuronal survival and differentiation (Seidl et al., 1998). There are several observations in the literature that noted the involvement of NGF in various type of cells, such as those of the ovary (Dissen et al., 1991) and testis (Persson et al., 1990, Russo et al., 1994), myoblastic cells (Ueyama et al., 1993) and mast cells (Aloe, 1988).

Other studies have demonstrated an active role for NGF in endometriosis, where the authors have attributed the generation of pain related symptoms to the expression of NGF (Evans et al., 2007, Tokushige et al., 2006). Data from the experimental newborn CD1 mouse models of adenomyosis, where tamoxifen altered the differentiation of neonatal mouse myometrial development resulting in adenomyosis, has demonstrated an increased expression of NGF, inflammation and neo-vascularisation (Parrott et al., 2001). By extension of those studies, a similar link between tamoxifen/steroid action and NGF expression and action, in the inner myometrium of women might lead directly to adenomyosis (Parrott et al., 2001). However, this hypothesis remains to be

confirmed. Additionally, the precise mechanism by which NGF might be responsible for adenomyosis in the CD1 mouse model has not yet been fully clarified. Therefore, this chapter presents results of experiments studying the expression of NGF in normal and adenomyotic myometrium using immunohistochemistry. The data are supported by primary myometrial cell culture work, where transcript levels of NGF were measured in response to treatment with estradiol or tamoxifen.

4.2   NGF Immunohistochemistry:

For immunohistochemistry, a total of 24 samples (12 normal, 12 adenomyosis) were used for this experiment, with 6 samples from each phase of the menstrual cycle: two samples each from the early-, mid- and late-proliferative phases and similarly two samples each from the early-, mid- and late-secretory phases. The expression of NGF was measured in the form of a histoscore using ImageScope (as described in Chapter 2, page 29). NGF immunoreactivity was visible at a low intensity but present in both the normal and the adenomyotic tissue (Figures 4.1 and 4.2). NGF staining was present in the cytoplasm and the nucleus of most cells.   The expression of NGF was predominantly observed in the smooth muscle cells surrounding blood vessels (Figure 4.2), luminal epithelial cells, glandular cells, and stromal cells of the endometrium (Figure 4.3).

NGF immunohistochemical positive signals were scarce in myometrial cells, but staining appeared to increase in the adenomyotic myometrium (Figure 4.1). To perform more accurate histomorphometric analysis of the data in the various types of tissue, the number of cells present in the observed field was used to correct the amount of NGF immunostaining. This was an important consideration, because the cellularity (number of cells per μm^2) differs between the inner and outer myometrium Table 4.1 shows

NGF expression per cell (number of pixels x pixel intensity/number of cells) in inner and outer myometrium, respectively. In adenomyosis, there was significant increase in expression of NGF/cell noted (Table 4.1 and Figure 4.4) in both the secretory and proliferative phases of the menstrual cycle when compared to controls, both in inner and outer myometrium (IM: $p<0.01$; OM: $p<0.001$). With regards to menstrual phase, there was a trend for increased NGF expression from the proliferative to secretory phase in both normal and adenomyosis samples but those differences were statistically significant only in the outer myometrium of adenomyotic samples.
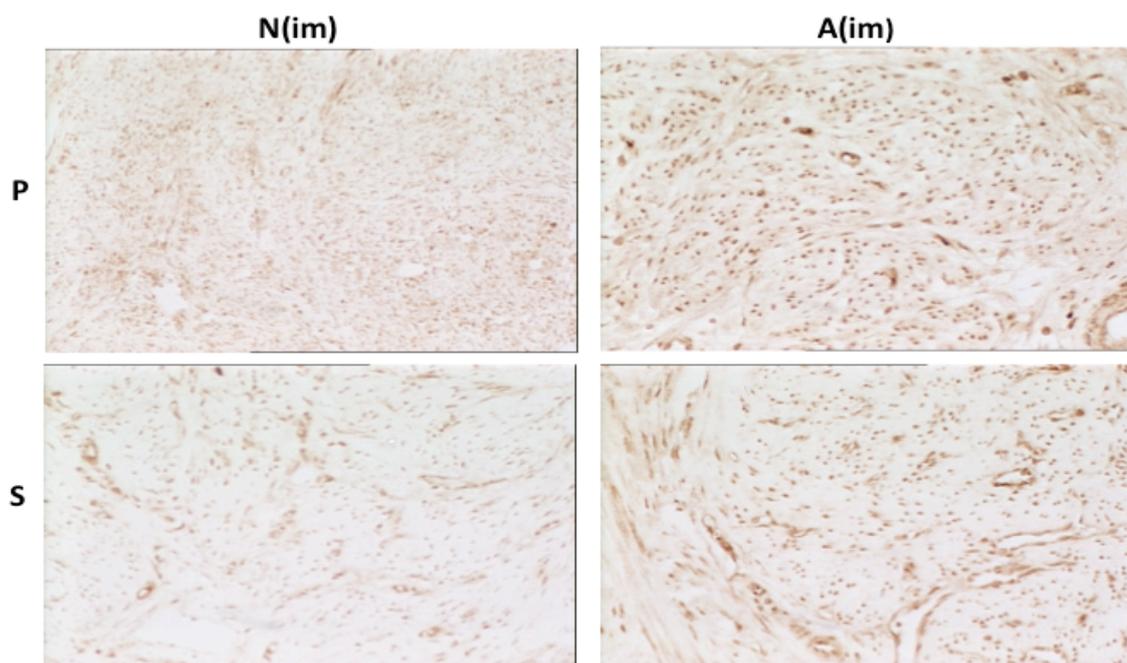
Figure 4.1: IHC showing Caveolin 1 expression in inner myometrium (im) in Proliferative phase (P) and Secretory phase (N (im): normal myometrium), A (im): adenomyotic myometrium) 20x Magnification.
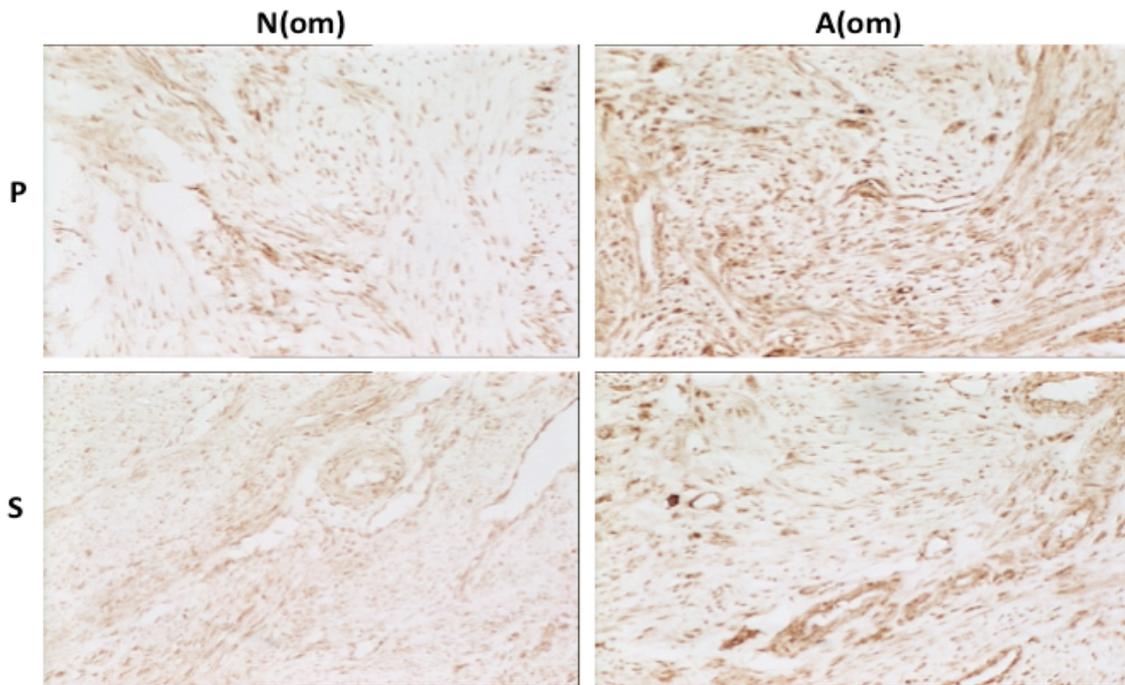
Figure 4.2: IHC showing Caveolin 1 expression in outer myometrium (om) in Proliferative phase (P) and Secretory phase (N (om): normal myometrium), A (om): adenomyotic myometrium) 20x magnification
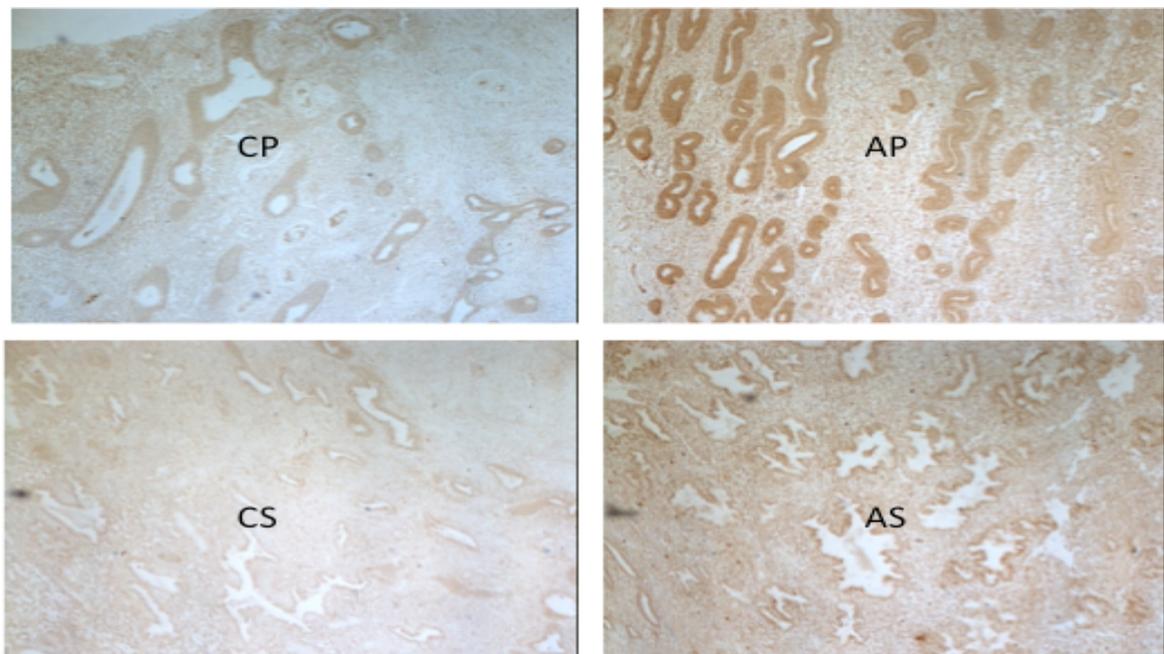
Figure 4.3: Shows NGF expression in proliferative (P) and secretory (S) phases of the menstrual cycle in both control (C) and adenomyotic (A) endometrium. Control proliferative (CP); Adenomyotic proliferative (AP); Control secretory (CS); Adenomyotic secretory (AS) 20x magnification.

Table 4.1: ImageScope histoscore data corrected to amount of NGF/cell for inner (IM) and outer myometrium (OM) for normal (N) and adenomyotic (A) myometrium subdivided into the proliferative (P) and secretory (S) phases of the menstrual cycle. Data are presented as the mean scores for all the six slides (10 fields/slide) examined.

NGF/cell	NP(im)	AP(im)	NS(im)	AS(im)	NP(om)	AP(om)	NS(om)	AS(om)
Mean (n=6)	0.035	0.097	0.060	0.108	0.068	0.172	0.118	0.170
SEM	0.013	0.005	0.005	0.004	0.016	0.007	0.007	0.006
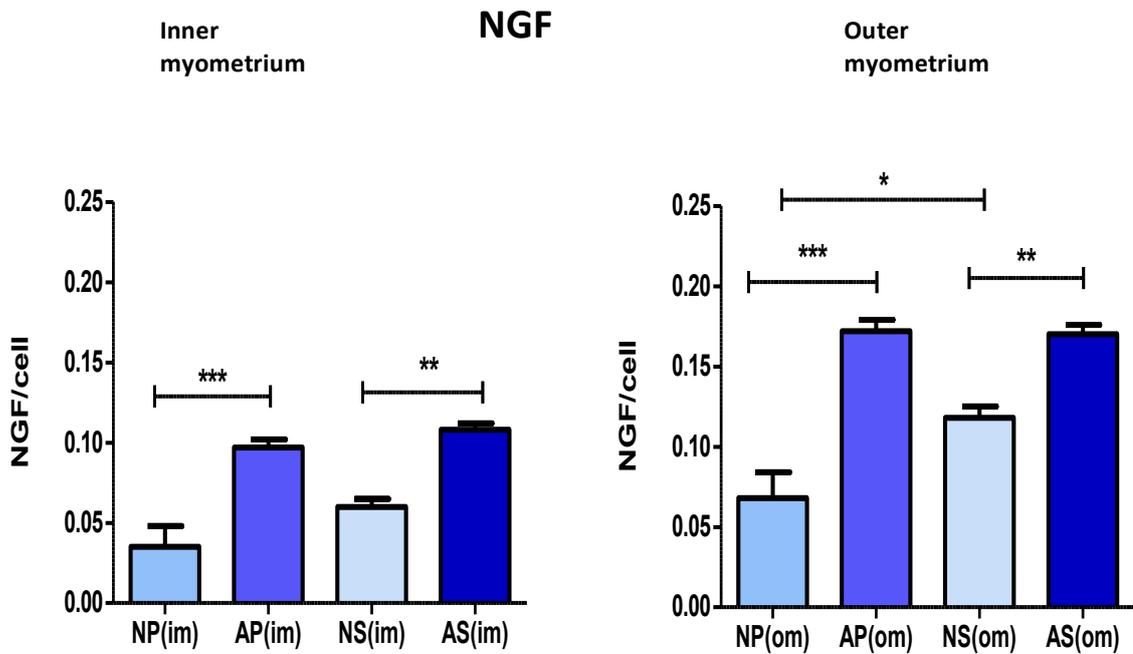
Figure 4.4: NGF expression/cell in inner (im) & outer myometrium (om). Np: normal proliferative; Ap: adenomyotic proliferative; Ns: normal secretory; As: adenomyotic secretory (Error bar: SEM; One way ANOVA with Bonferroni's Multiple comparison test, *p<0.05, **p<0.01, ***p<0.001)

4.3 NGF Q-PCR Experiment

To assess the transcript levels of NGF in normal and the diseased condition, quantitative real-time RT-PCR was used. To this, the response of cells obtained from both normal and adenomyotic uteri subjected to treatment with estradiol or tamoxifen for 48 hours was examined. In the normal myometrial cell cultures, estradiol down regulated the expression of NGF but tamoxifen up regulated it (Figure 4.5). In myocytes obtained from uteri of women with adenomyosis, estradiol showed no effect but tamoxifen increased the NGF transcript levels (Figure 4.5). Using the untreated normal myometrial cells as the control for the experiment, NGF transcript levels in both normal and disease were calculated (Table 4.2) and normalised to the level of untreated normal by using Paffl's method (Pfaffl, 2001). NGF level is higher in adenomyosis group.

Table 4.2: Summary of NGF Q-PCR data Paffl's method(Pfaffl, 2001) used for PCR calculation

N=12	Control GAPDH (Ct)	Control NGF (Ct)	Treated GAPDH (Ct)	Treated NGF (Ct)	Fold Change NGF	Fold Change GAPDH	RATIO NGF/GAPDH (Mean)	SEM
Normal								
E2	26.44	32.96	25.45	32.53	1.41	2.05	0.72	0.12
TMX	26.44	32.96	26.29	32.85	1.56	1.44	1.08	0.26
Adenomyosis								
E2	26.21	32.65	26.45	33.21	0.71	1.00	1.00	0.50
TMX	26.21	32.65	26.27	33.16	0.71	1.22	1.20	0.60
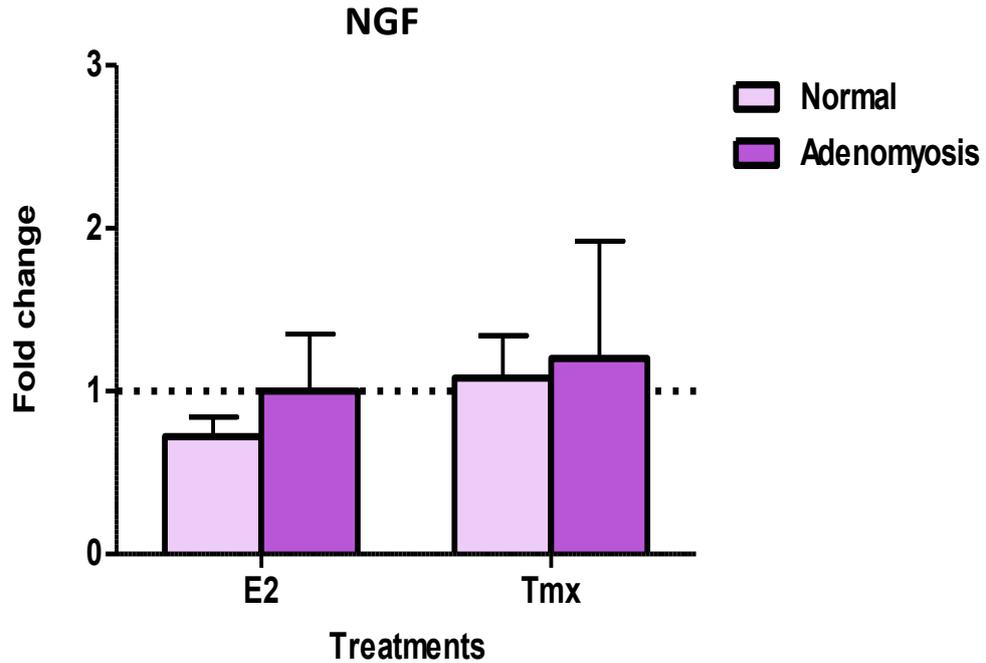
Figure 4.5: NGF transcript levels in primary myometrial cells derived from normal and adenomyotic uteri and treated with either 10^{-6}M E2 or 10^{-6}M TMX for 48hr. Data are presented as the mean ± SEM; NGF transcript levels in both cell types were compared to 'Control' untreated cultures (Mean: 1.00). One-way ANOVA with Bonferroni's Multiple Comparison *ad hoc* post-test; n=12.

4.4   Discussion

NGF was the first neurotropic factor discovered to play a crucial role in the release of inflammatory factors and aggregation of immunocytes resulting in production and transmission of pain (Snider, 1994). The transmission of pain occurs in different pathways involving inflammatory mediators such as interleukins, cytokines and nerve growth factors (Snider, 1994, Evans et al., 2007, Levi-Montalcini, 1987). There is an increased density of nerve fibres in the uterus of adenomyotic women (Zhang et al.), so NGF might provide a major contribution towards the generation of pain in this disease by increasing the density of the nerve fibres in symptomatic women (Watson et al., 2008, Mendell et al., 1999). NGF could mediate immunoreactions by acting as a chemo attractant for mast cells and granulocytes (Lewin et al., 1994) and could increase the

excitability of afferent neurons by altering ion channels (Mamet et al., 2002) and neurotransmitter production (Bielefeldt et al., 2003). So it is reasonable to speculate that the observed increased NGF expression in adenomyosis might contribute to the release of pain-producing substances (Lewin et al., 1994), resulting in the aggressive pain associated with adenomyosis (Lewin et al., 1994).

In my immunohistochemical studies, I observed a statistically significant increase in myometrial NGF expression in adenomyosis in both phases of the menstrual cycle. To obtain further evidence to support my IHC findings, I set up myometrial cell cultures to assess the transcript level of NGF in both normal myocytes and in adenomyotic myocytes in response to treatment with E2 or TMX for 48 hours. On comparing the untreated controls in both normal and disease group, I observed increased NGF transcript levels (Table 4.2 and Figure 4.5) in the adenomyotic myocyte cultures when compared to normal myocytes, thus supporting the similar observations obtained in the immunohistochemical study. Yan Li *et al*. studied the expression of NGF and its receptors in uteri and dorsal root ganglia in an adenomyosis mouse model, as well as their relationship with the severity of adenomyosis (Li Y, 2010). In their study, tamoxifen treated newborn ICR mice developed adenomyosis and the NGF and its receptors levels were proportionately increased with the severity of the disease when compared to untreated mice, where levels were unchanged. Evidence in the literature demonstrates the ability of estrogen to alter the peripheral neural and CNS architecture through its effects on synaptogenesis, dendritic and axonal growth (Kadish and Van Groen, 2002, McEwen, 2002). It is unclear how estrogen mediates changes in density of sympathetic innervations in the uterus but there is evidence to show that nerve growth factor activates the high affinity tyrosine kinase A receptor (trkA) to promote axonal

outgrowth (Belliveau et al., 1997). Adenomyosis has been shown to be an estrogen-dependent disease that has abnormal local estrogen production in the uterus ((Urabe et al., 1989, Yamamoto et al., 1993, Kitawaki, 2006). Therefore, abnormal local estrogen levels might be responsible for the observed increase in NGF expression. But, in my immunohistochemical study, I observed a significant increase in NGF expression in both the estrogen and progesterone dominated menstrual phases, suggesting that there might be some other factors, which could increase the NGF level in adenomyosis in addition to estrogen.

NGF has been reported to be involved in many autoimmune and inflammatory diseases, such as allergies and asthma (Bonini et al., 2002, Abram et al., 2009), intestinal mucosa inflammation (Agro and Stanisz, 1993), in which elevated NGF levels correlate well with the severity of the diseases. In women, adenomyosis is also associated with various autoimmune reactions where there is an increased number of macrophages, gamma- and delta-T cells in ectopic and eutopic endometrium (Ota et al., 1998) and elevated pre-inflammatory factors and cytokines, such as TNF-α, IL-10 and IL-18 in the uterus and peritoneal fluid (Huang et al., Wang et al., 2009, Huang et al., 2010), in which case the augmentation of NGF might be the result of inflammatory status, which then mediates and/or regulates a later immune response (Snider, 1994, Evans et al., 2007). Therefore, with the infiltration and growth of ectopic endometrium, uterine inflammation and local estrogen synthesis are increased, which could then promote NGF synthesis. This increase in NGF might then participate in neural plasticity, local inflammation and production of pain. This suggests that the presented IHC findings of increased myometrial NGF expression in adenomyosis in both phases of the menstrual cycle might be due to the above-mentioned factor(s) and this statistically significant

increase in the proliferative phase might be due to an additional estrogenic effect. These observations are supported by the myocyte cell culture findings where a significant increase in NGF transcript level was noted in cells derived from the disease group when compared to normal, which actually showed a drop in NGF transcript levels.

Therefore, on the basis of my findings from both immunohistochemical and cell culture studies and also based on the available information from the literature, it is reasonable to conclude that the abnormal expression of NGF is only an associated factor and may not be causative factor for adenomyosis.

Chapter 5   Caveolins

5.1   Introduction

There are three members of the caveolin family (Cav-1, -2, and -3), which are essential for the formation of caveolae (Razani et al., 2002). Two isoforms of caveolin 1 have been identified namely cav-1α (172 amino acid residues) and cav-1β (144 amino acid residues) (Scherer et al., 1995). Similarly, three isoforms for caveolin 2 (α, β & γ) have been identified (Scherer et al., 1996). Caveolin-2α encodes a 162 amino acid residue protein with a sequence that is 38% identical and 58% similar to caveolin-1 (Scherer et al., 1996) and the remaining two isoforms are currently uncharacterised (Scherer et al., 1996).

5.2   Caveolin 1 Immunohistochemistry

Experiments for caveolin-1 and 2 were performed separately using commercially available antibodies. The amount of immunoreactive proteins was measured in the form of a histoscore using ImageScope (as described in Chapter 2, page 29). Caveolin 1 immunoreactivity was at a moderate intensity and present in both the normal and the adenomyotic tissue (Figures 5.1 and 5.2). Caveolin 1 staining was present in the cytoplasm and the nucleus of most cells. The expression of caveolin 1 was predominantly observed in the smooth muscle cells surrounding blood vessels (Figures 5.1 and 5.2). Caveolin 1 immunohistochemical positive signals were also present in myometrial cells, with the staining intensity being slightly more intense in the adenomyotic myometrium (Figures 5.1 and 5.2). Interestingly, caveolin 1 immunoreactivity also appeared to be more intense in the secretory phase of the menstrual cycle.

Histomorphometric analysis confirmed that there was a higher level of caveolin-1 immunoreactivity present in the secretory phase (1.5 to 2-fold higher when compared to proliferative phase) both in inner and outer myometrium in both normal and adenomyosis, but that only the expression of caveolin-1 in the normal myometrium was significantly increased by 2-fold in the inner myometrium, whereas only caveolin-1 immunoreactivity was significantly increased in the outer myometrium of the adenomyotic tissue (Table 5.1 & Figure 5.1). When the adenomyotic myometrium was compared to normal myometrium, there was a significant increase in caveolin-1 expression, but only in the proliferative phase adenomyotic myometrium (Table 5.1 & Figure 5.1). A similar pattern of increase was noted in the outer myometrium but did not reach statistical significance (Table 5.1 & Figure 5.3).
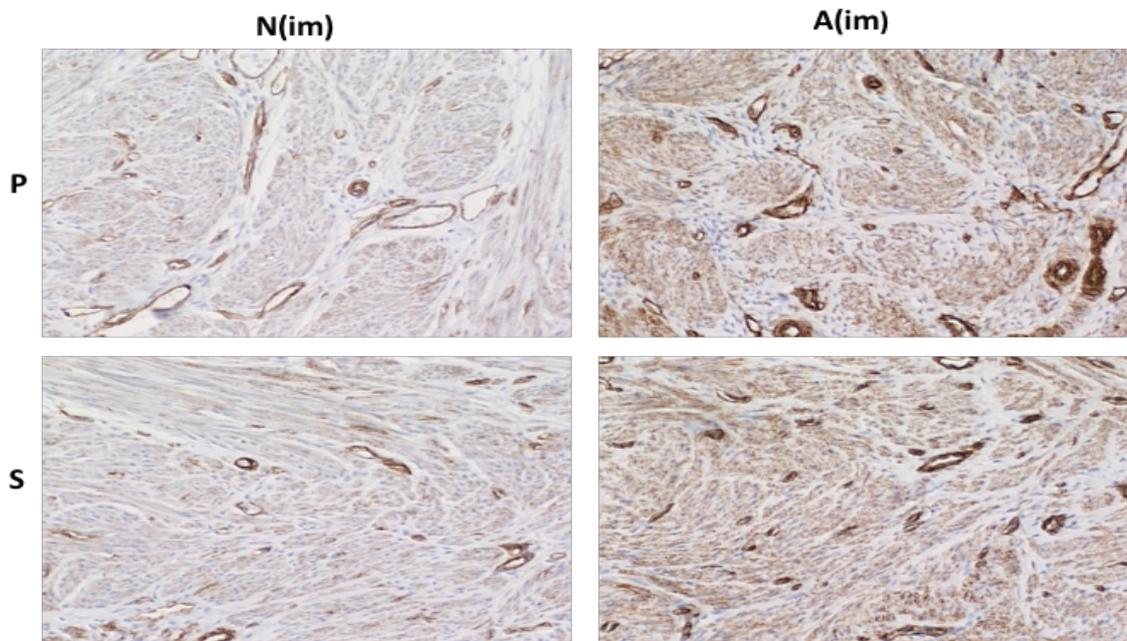
Figure 5.1: IHC showing Caveolin 1 expression in inner myometrium (im) in Proliferative phase (P) and Secretory phase (N (im): normal myometrium), A (im): adenomyotic myometrium) 20x magnification
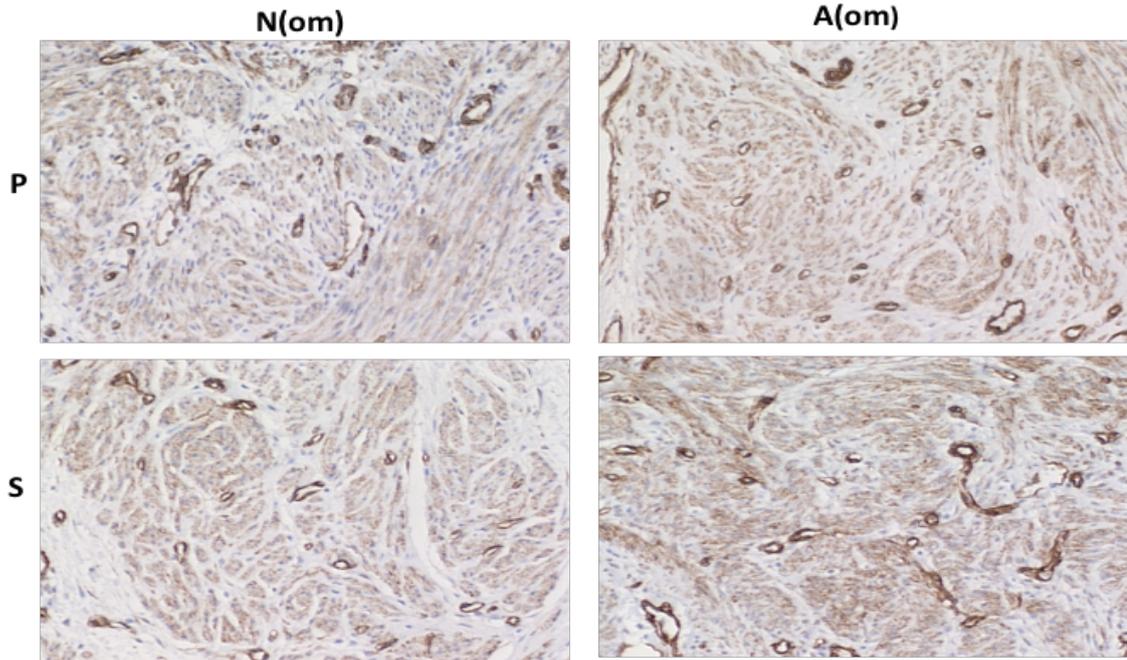
Figure 5.2: IHC showing Caveolin 1 expression in outer myometrium (om) in Proliferative phase (P) and Secretory phase (N (om): normal myometrium), A(om): adenomyotic myometrium) 20x magnification

Table 5.1: ImageScope histoscore data corrected to amount of caveolin-1/cell for inner (IM) and outer (OM) myometrium for normal (N) and adenomyotic (A) myometrium subdivided into the proliferative (P) and secretory (S) phases of the menstrual cycle. Data are presented as the mean scores for all six slides (10 fields/slide) examined.

Caveolin 1/cell	NP(im)	AP(im)	NS(im)	AS(im)	NP(om)	AP(om)	NS(om)	AS(om)
Mean (n=6)	0.046	0.081	0.096	0.087	0.076	0.086	0.103	0.131
SEM	0.003	0.011	0.005	0.007	0.011	0.008	0.010	0.013
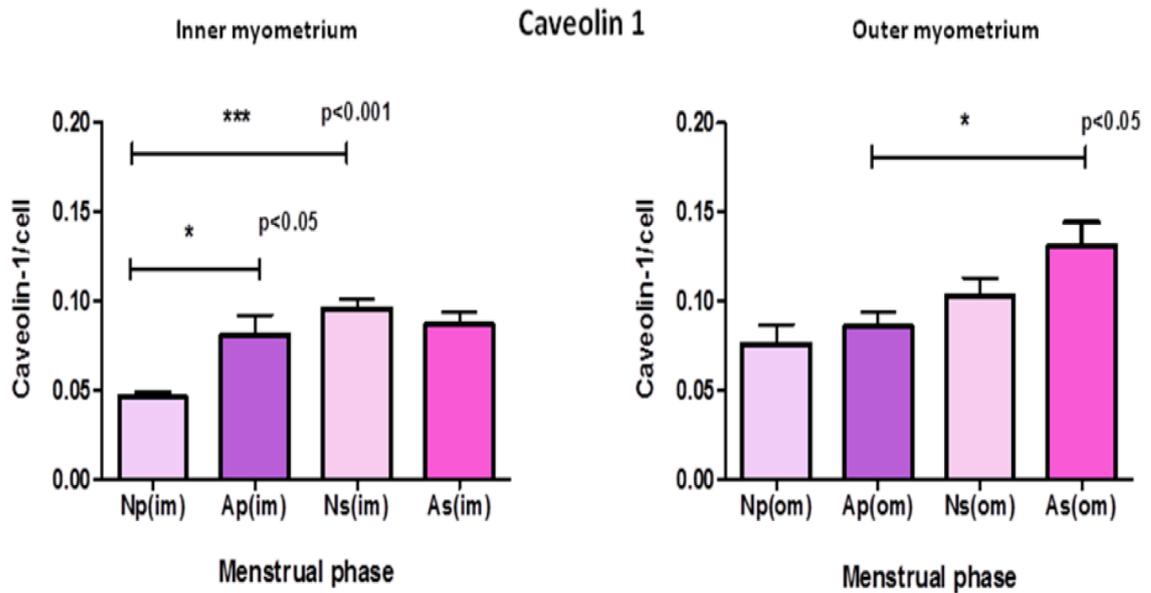
Figure 5.3: Effect of menstrual cycle phase on immunoreactive caveolin-1 levels in the inner (im) & outer myometrium (om) of normal proliferative (Np) and adenomyotic proliferative (Ap) normal secretory (Ns) and adenomyotic secretory (As) tissue. The data are presented as mean ± SEM Histoscore; *p<0.05, ***p<0.001; one-way ANOVA with Bonferroni's multiple comparison test (n=6).

5.3 qRT-PCR Experiments: Caveolin 1a & 1b

In cultures of primary myometrial cells derived from normal and adenomyotic uteri treated with either 10^{-6}M E2 or 10^{-6}M TMX for 48 hours, transcript levels of both caveolins 1 isoforms when measured and compared to untreated control showed that E2 decreases the expression caveolin isoforms 1a (Table 5.2 & Figure 5.4) & 1b (Table 5.3 & Figure 5.5) in the normal myocytes, but had variable effects on the isoform expression of adenomyotic myocytes. By contrast, TMX had variable effects on normal myocytes but consistently up-regulated the expression of all caveolin isoforms for myocyte cultures obtained from adenomyotic tissue These data suggest that a consistent but opposite effect of E2 and TMX on caveolin expression in normal and adenomyotic myocytes placed in culture.

5.3.1 Caveolin 1a

Table 5.2: Summary of caveolin-1a Q-PCR data using Paffl's method(Pfaffl, 2001). The data are from n=9 independent primary myometrial cell cultures and corrected for the levels detected in untreated cultures.

N=9	Control GAPDH (Ct)	Control Cav-1a (Ct)	Treated GAPDH (Ct)	Treated Cav-1a (Ct)	Fold Change Cav-1a	Fold Change GAPDH	RATIO Cav-1a/GAPDH (Mean)	SEM
Normal								
E2	26.67	27.48	25.79	27.16	1.28	1.89	0.70	0.11
TMX	26.67	27.48	26.43	27.51	0.99	1.53	1.00	0.29
Adenomyosis								
E2	26.33	27.27	26.18	27.40	0.96	1.24	0.84	0.10
TMX	26.33	27.27	26.78	27.46	0.89	0.95	1.47	0.52
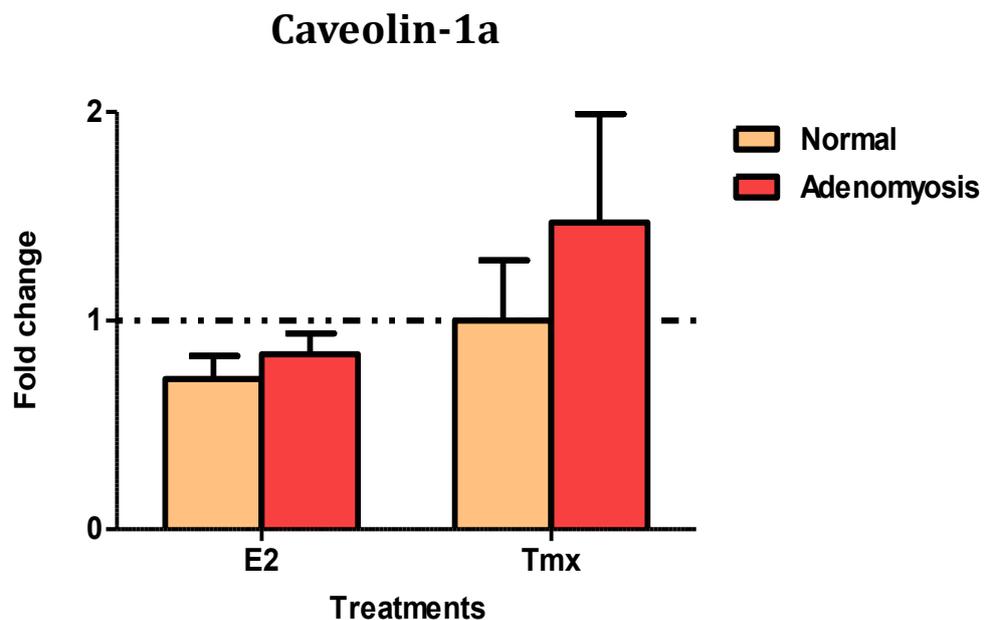
Figure 5.4: Caveolin-1a transcript levels in primary myometrial cells derived from normal and adenomyotic uteri and treated with either 10^{-6}M E2 or 10^{-6}M TMX for 48hr. Data are presented as the mean ± SEM; Caveolin-1a transcript levels in both cell types were compared to Control untreated cultures (Mean: 1.00). One-way ANOVA with Bonferroni's Multiple Comparison *ad hoc* post-test; n=9.

5.3.2 Caveolin 1b

Table 5.3: Summary of caveolin-1b Q-PCR data using Pfaffl's method(Pfaffl, 2001). The data are from n=9 independent primary myometrial cell cultures and corrected for the levels detected in untreated cultures.

N=9	Control GAPDH (Ct)	Control Cav-1b (Ct)	Treated GAPDH (Ct)	Treated Cav-1b (Ct)	Fold Change Cav-1b	Fold Change GAPDH	RATIO Cav-1b/GAPDH (Mean)	SEM
Normal								
E2	26.67	25.96	25.79	25.47	1.48	1.89	0.82	0.19
TMX	26.67	25.96	26.43	26.09	0.96	1.53	0.85	0.19
Adenomyosis								
E2	26.33	25.70	26.18	25.31	1.92	1.24	1.31	0.37
TMX	26.33	25.70	26.78	25.77	1.20	0.95	1.32	0.12
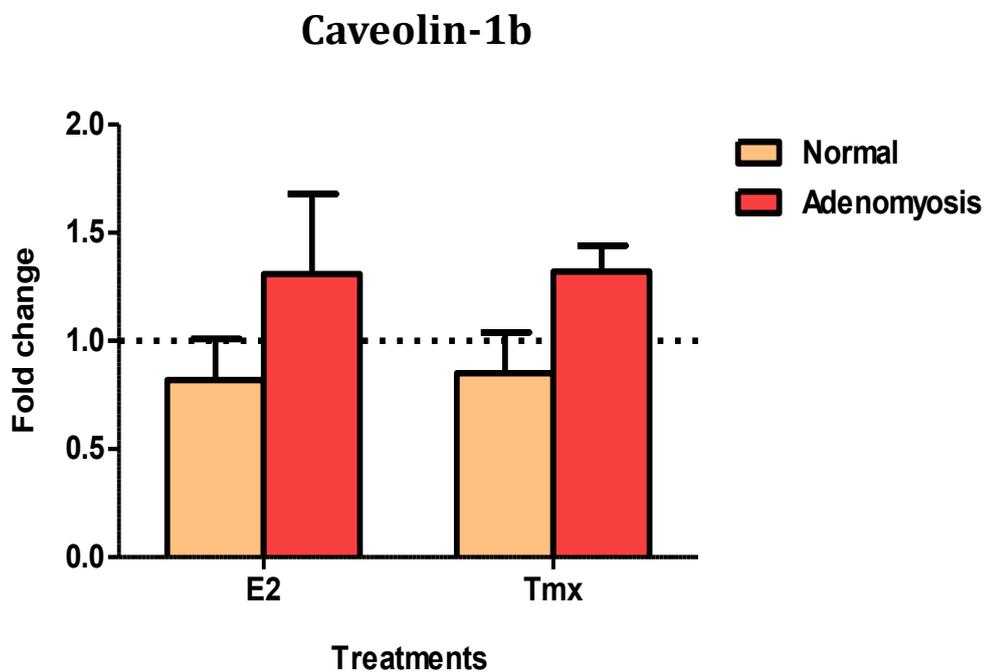
**Figure 5.5: Caveolin-1b transcript levels in primary myometrial cells derived from normal and adenomyotic uteri and treated with either 10^{-6}M E2 or 10^{-6}M TMX for 48hr. Data are presented as the mean ± SEM; Caveolin-1b transcript levels in both cell types were compared to Control untreated cultures (Mean: 1.00). One-way ANOVA with Bonferroni's Multiple Comparison *ad hoc* post-test; n=9.**

5.4   Caveolin 2 Immunohistochemistry

Caveolin-2 immunoreactivity was present in both the normal and the adenomyotic tissue (Figures 5.6 and 5.7). Caveolin-2 staining was present in the cytoplasm and the nucleus of most cells including the myometrium and the smooth muscle cells surrounding blood vessels (Figures 5.6 and 5.7). Histomorphometric analysis of the staining data revealed that there was a higher level of caveolin-2 present in the secretory phase of both inner and outer myometrium in both normal and adenomyotic tissue. In normal tissue, caveolin-2 immunoreactivity significantly increased in both the inner and outer myometrium during the transition to the secretory phase, whereas in adenomyotic tissue, it only increased in the outer myometrium (Figure 5.8). Additionally, caveolin-2 expression was only significantly increased in the inner myometrium of adenomyotic myometrium when compared to normal myometrium and only in the proliferative phase of the menstrual cycle. Although caveolin-2 expression was higher in comparable groups, the data were not significantly different (Figure 5.8).
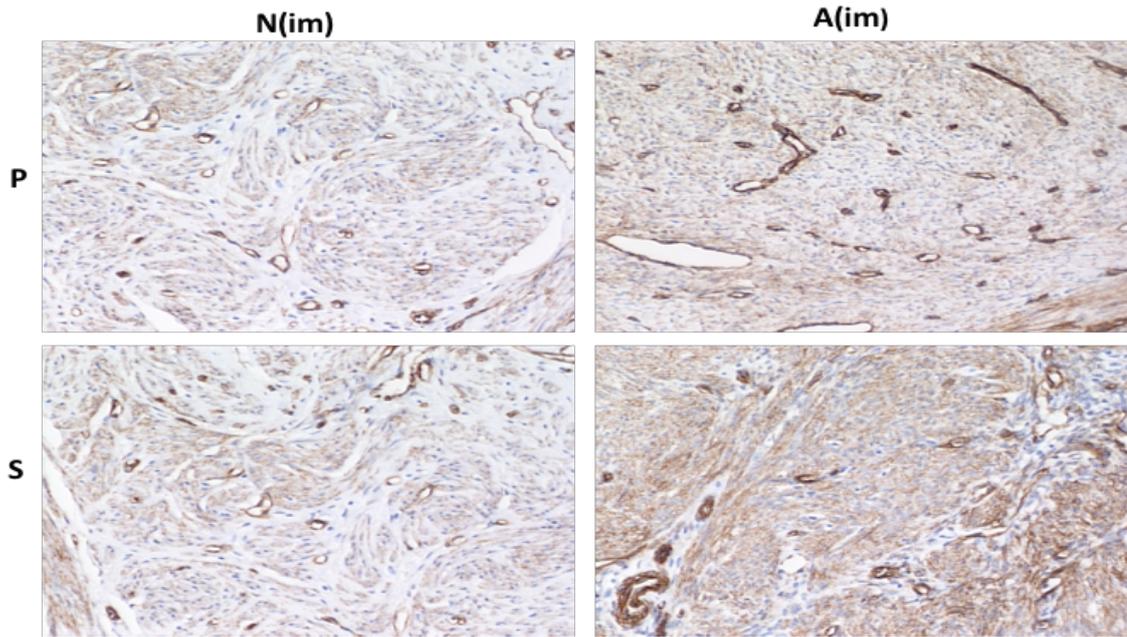
Figure 5.6: IHC images of caveolin 2 immunoreactivity in inner myometrium (im) in the proliferative (P) and secretory phase (S) of the menstrual cycle of normal myometrium (N) and adenomyotic myometrium (A). 20x magnification
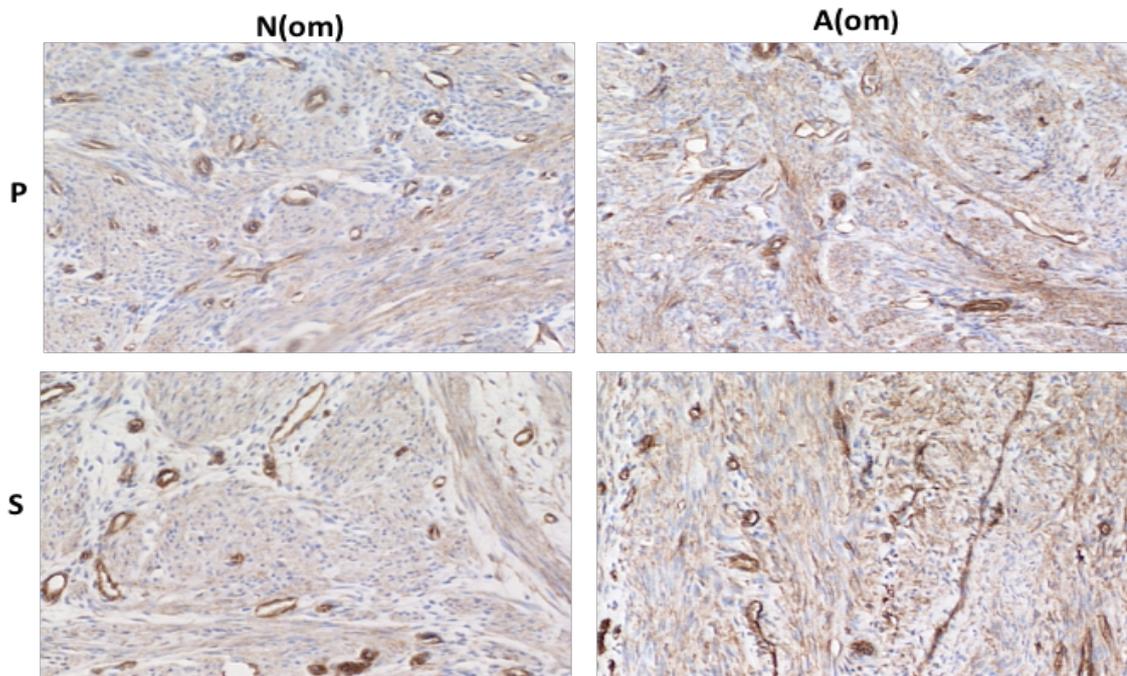
Figure 5.7: IHC images of caveolin 2 immunoreactivity in the outer myometrium (om) of proliferative phase (P) and secretory phase (S) normal myometrium (N) and adenomyotic myometrium (A). 20x magnification

Table 5.4: ImageScope histoscore data corrected to amount of caveolin-2/cell for inner (IM) and outer myometrium (OM) for normal (N) and adenomyotic (A) myometrium subdivided into the proliferative (P) and secretory (S) phases of the menstrual cycle. Data are presented as the mean scores for all the six slides (10 fields/slide) examined

Caveolin 2/cell	NP(im)	AP(im)	NS(im)	AS(im)	NP(om)	AP(om)	NS(om)	AS(om)
Mean (n=6)	0.027	0.057	0.059	0.078	0.064	0.069	0.090	0.101
SEM	0.004	0.011	0.008	0.014	0.006	0.006	0.009	0.011
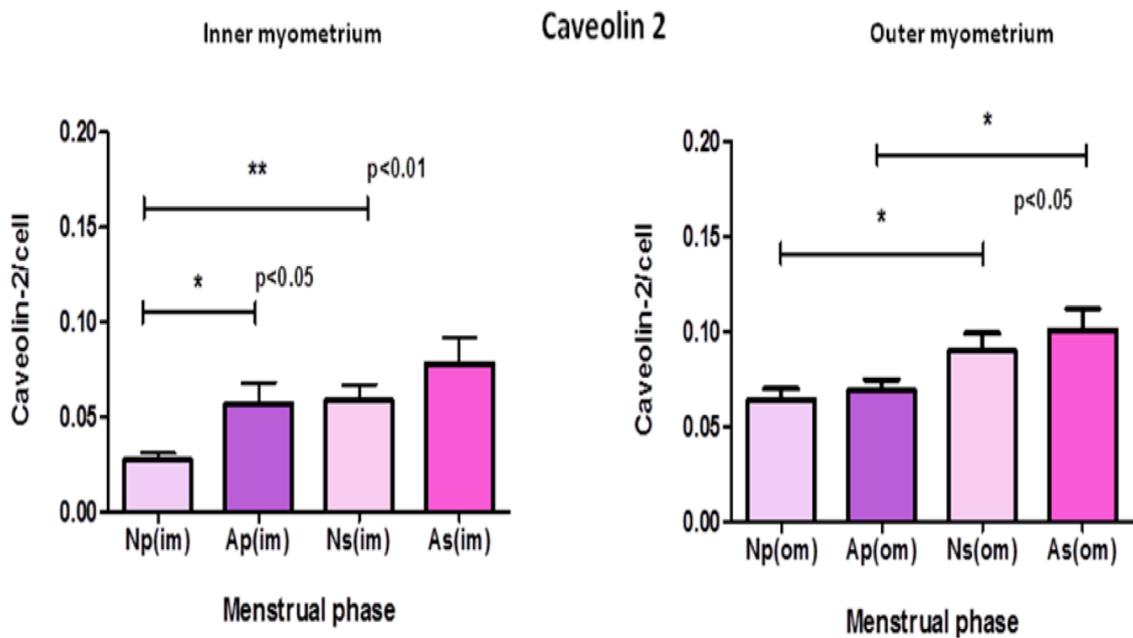
Figure 5.8: Caveolin-2 expression/cell in inner (im) & outer myometrium (om). Np: normal proliferative; Ap: adeno proliferative; Ns: normal secretory; As: adeno secretory (Error bar: SEM; One way ANOVA with Bonferroni's Multiple comparison test, *p<0.05, **p<0.01)

5.5 qRT-PCR Experiments

Similar to caveolin isoforms 1a and 1b, cultures of primary myometrial cells derived from normal and adenomyotic uteri treated with either 10^{-6}M E2 or 10^{-6}M TMX for 48 hours, transcript levels of caveolins 2a and 2b when measured and compared to untreated control showed that E2 decreases the expression of all caveolin isoforms in the normal myocytes, but had variable effects on the isoform expression of adenomyotic myocytes. By contrast, TMX had variable effects on normal myocytes but consistently up-regulated the expression of all caveolin isoforms for myocyte cultures obtained from adenomyotic tissue. These data suggest that a consistent but opposite effect of E2 and TMX on caveolin expression in normal and adenomyotic myocytes placed in culture.

5.5.1 Caveolin 2a

Table 5.5: Summary of Caveolin-2a Q-PCR data using Paffl's method(Pfaffl, 2001). The data are from n=9 independent primary myometrial cell cultures and corrected for the levels detected in untreated cultures.

N=9	Control GAPDH (Ct)	Control Cav-2a (Ct)	Treated GAPDH (Ct)	Treated Cav-2a (Ct)	Fold Change Cav-2a	Fold Change GAPDH	RATIO Cav-2a/GABDH (Mean)	SEM
Normal								
E2	26.67	27.41	25.79	27.17	1.22	1.89	0.65	0.06
TMX	26.67	27.41	26.43	27.33	1.22	1.53	0.93	0.14
Adenomyosis								
E2	26.33	27.12	26.18	26.84	1.28	1.24	1.11	0.12
TMX	26.33	27.12	26.78	27.15	1.00	0.95	1.57	0.51
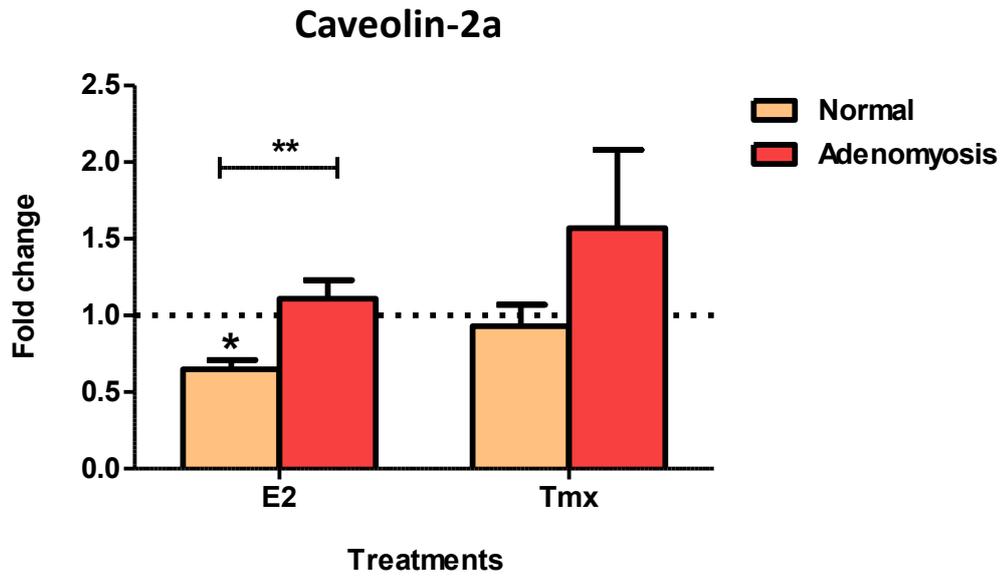
Figure 5.9: Caveolin-2a transcript levels in primary myometrial cells derived from normal and adenomyotic uteri and treated with either 10^{-6}M E2 or 10^{-6}M TMX for 48hr. Data are presented as the mean ± SEM; Caveolin-2a transcript levels in both cell types were compared to Control untreated cultures (Mean: 1.00). One-way ANOVA with Bonferroni's Multiple Comparison *ad hoc* post-test; n=9.

5.5.2 Caveolin 2b

Table 5.6: Summary of Caveolin-2b Q-PCR data using Paffl's method(Pfaffl, 2001)**. The data are from n=9 independent primary myometrial cell cultures and corrected for the levels detected in untreated cultures.**

| N=9	Control GAPDH (Ct)	Control Cav-2b (Ct)	Treated GAPDH (Ct)	Treated Cav-2b (Ct)	Fold Change Cav-2b	Fold Change GAPDH	RATIO Cav-2b/GABDH (Mean)	SEM
Normal								
E2	26.67	29.09	25.79	28.61	1.42	1.89	0.79	0.13
TMX	26.67	29.09	26.43	29.16	0.98	1.53	0.90	0.22
Adenomyosis								
E2	26.33	28.80	26.18	28.41	1.39	1.24	1.19	0.11
TMX	26.33	28.80	26.78	28.63	1.19	0.95	2.00	0.91
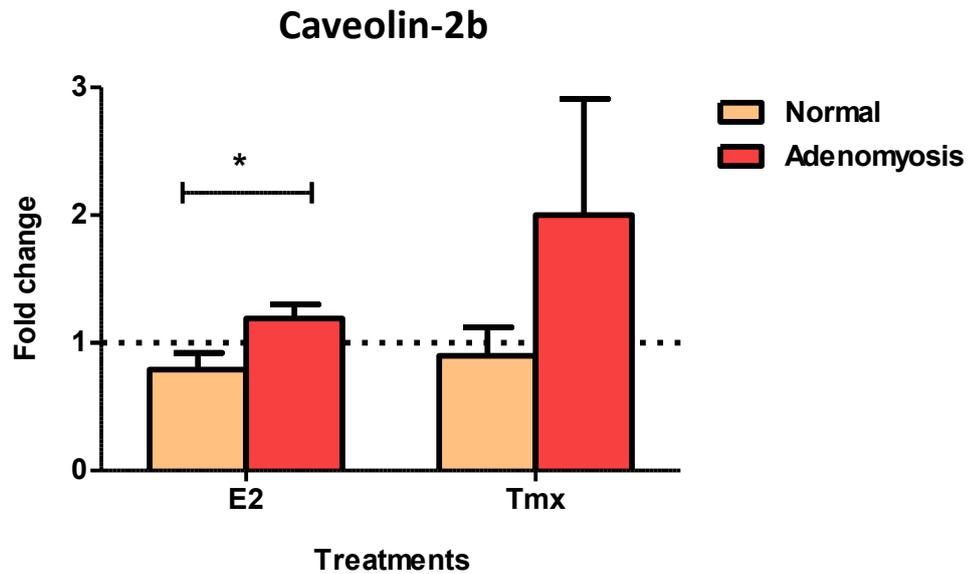
Figure 5.10: Caveolin-2b transcript levels in primary myometrial cells derived from normal and adenomyotic uteri and treated with either 10^{-6}M E2 or 10^{-6}M TMX for 48hr. Data are presented as the mean ± SEM; Caveolin-2b transcript levels in both cell types were compared to Control untreated cultures (Mean: 1.00). One-way ANOVA with Bonferroni's Multiple Comparison *ad hoc* post-test; n=9.

5.6 Discussion

In my immunohistochemistry study, I noted an increased level of caveolin expression in adenomyosis irrespective of menstrual phase, with the expression of both caveolins being lesser in the estrogen dominated proliferative phase when compared to progesterone dominated secretory phase. In cultures of primary myometrial cells derived from normal and adenomyotic uteri, the transcript levels of caveolins 1 and 2, when measured and compared to untreated control, showed that E2 decreases the expression of all caveolin isoforms in the normal myocytes, but has variable effects on the isoform expression of adenomyotic myocytes. By contrast, TMX has variable effects on normal myocytes but consistently up-regulated the expression of all caveolin isoforms in myocyte cultures obtained from adenomyotic tissue. These data suggest a

consistent but opposite effect of E2 and TMX on caveolin expression in normal and adenomyotic myocytes placed in culture. Caveolins are important protein components of caveolae, which are invaginations from the plasma membrane (Couet et al., 2001) and play important roles in intracellular transport (Parton and Simons, 2007), as scaffolding proteins for signal transduction (Patel et al., 2008), and as buffers regulating plasma membrane lipid composition and fatty acid incorporation. Caveolins also act as regulators of cellular proliferation, invasiveness and the metastatic potential of cancer cells (Bagnoli et al., 2000, Bender et al., 2000). The available evidence is in favour of caveolins playing a dual role of promoting the invasiveness of cancer cells to acquire the features of advanced cancer (Williams et al., 2005, Liscovitch, 2005) and also to regulate the function of a specialized cytoskeleton-membrane link that involves integrins, extracellular membrane receptors and initiators of adhesion complex formation (Wary et al., 1996, Upla et al., 2004, Ning et al., 2007).

It is generally thought that E2-induced gene transcription is normally carried out through the actions of the nuclear receptors ER-α and ER-β (Gorski et al., 1984, Welshons et al., 1984). Thus, ERs act as ligand-activated transcriptional factors that enhance the expression of transcripted genes as well as regulate gene transactivation (Truss and Beato, 1993). But there are also some non-genomic actions where E2 activates RNA and protein synthesis through membrane-associated ERs associated with the activation of protein kinase cascades (Losel and Wehling, 2003) that also may indirectly influence gene expression. The caveolae and the associated caveolin proteins integrate and perform these non-genomic actions *via* membrane associated ERs (Kim et al., 1999). Although there is convincing evidence obtained from biochemical and immunofluorescent studies demonstrating the association of ERs with the plasma

membrane (Kiss et al., 2005, Kim et al., 1999), little is known about the mechanism by which ER could be transported to the plasma membrane, but both receptors are found to be originated from the same gene transcript (Norfleet et al., 1999). The data presented in this chapter, indicate the presence of increased level of caveolins in adenomyosis and an up-regulating effect of E2 and TMX on the expression of all but one of the caveolin isoforms. The caveolin 1a isoform expression is in the same decreased direction as occurs in normal myocytes, suggesting a different mode of action for this isoform when compared to the other isoforms. There is not enough information in the literature to argue that caveolins or indeed different isoforms, play a direct causative role in the aetiopathology of adenomyosis, but my observations that higher levels of caveolin immunoreactivity were present in the myometria of the adenomyotic group when compared to that of the normal group, irrespective of menstrual phase, supports the situation of increased estrogenic activity in the cell culture experiments. How this comes about, might be considered through increased activity of membrane bound ERs within caveolae and indirectly assisting the pathogenesis of adenomyosis.

Usually, after an injury or damage to a muscle, the growth and regeneration pattern follows its original embryonic myogenesis (Tajbakhsh, 2003) to some extent and this may occur through the recruitment of resident myogenic stem cells, which are normally present between the myocyte cell membrane and the basal lamina of muscle fibres (Tajbakhsh, 2003). Once muscle injury happens, the satellite cells get activated; undergo several rounds of proliferation, before differentiating to form new fibres or repairing the injured fibres (Schmalbruch and Lewis, 2000). The development, maturation and regeneration of muscle involves the different steps of proliferation, differentiation and morphogenesis that take place under the influence of signals from

the cellular environment and also from paracrine and endocrine actions (Seidl et al., 1998). This process of myogenesis is regulated both positively and negatively by the signals from many growth factors, such as insulin-like growth factor (IGF) and members of the transforming growth factor (TGF)-β family (Deponti et al., 2009), fibroblast (FGF), hepatocyte growth factor (HGF) (Balemans and Van Hul, 2002, Parker et al., 2003) and nerve growth factors (NGF) (Seidl et al., 1998, Erck et al., 1998). HGF is up regulated during muscle regeneration (Volonte et al., 2005), which normally associates with satellite cells after muscle injury (Tatsumi et al., 1998, Anderson, 2000). HGF later stimulates the inactive satellite cells to enter the cell cycle (Tatsumi et al., 1998, Allen et al., 1995) and down regulates the endogenous caveolin-1 in endothelial cells (Bischoff, 1997) to complete muscle repair and regeneration (Volonte et al., 2005).

The over expression of caveolin-1 in these cells negatively affects their ability to differentiate to multinucleated myotubes without promoting cell death (Volonte et al., 2005) resulting in disordered and senescent phenotype (Volonte et al., 2005). In order to restore the pool of satellite cells, only a few of them escape differentiation and undergo self-renewal (Volonte et al., 2005). Muscle injury is not the only stimulus but also stretch, exercise and muscle hypertrophy all act as stimulators for the activation of satellite cells (Schultz and McCormick, 1994, Snow, 1990, Winchester et al., 1991). This is, in turn, supported by the findings from a study on the pregnant rat myometrium, showing gradual and abundant increase in caveolin expression throughout the pregnancy (Turi et al., 2001) in response to the stretching and expansion of the pregnant myometrium. These findings may be relevant to the present study and correlate the possible influence of caveolin in the aetiopathology of adenomyosis.

There is evidence in the literature that over expression of caveolin proteins during muscle regeneration negatively affects their ability to differentiate to multinucleated myotubes (Volonte et al., 2005) resulting in a disordered phenotype (Volonte et al., 2005). During a woman's reproductive life, the uterine junctional zone (EMI) gets disturbed or injured either directly or indirectly by dysfunctional uterine hyper-peristalsis or contractility (Parrott et al., 2001, Kunz et al., 2000), mechanical damage by sharp curettage (Leyendecker et al., 2002), and due to trophoblast invasion in multiparous women (Lee et al., 1984). After such disturbances to the inner myometrium of the junctional zone, it is possible that during the process of tissue recovery, down regulation of caveolin isoform expression may be required to aid proper muscle repair, as has been reported in other parts of the body (Bischoff, 1997). In the above situation within the myometrium, the altered regulation of caveolin might result in the altered myometrial cell phenotype that is more vulnerable to stromal cell invasion from the overlying endometrium.

The other possibility would be disturbance in the architecture of the extracellular matrix making it more vulnerable for cell movement and migration. Extracellular matrix (ECM) remodeling is a dynamic, cell-mediated process that occurs during development and tissue repair (Streuli, 1999). During tissue repair, the precise deposition of ECM molecules such as fibronectin and collagen I, is required to preserve the functional and structural integrity of tissue (R. A. F. Clark, 1988). Fibronectin (FN) also plays a major role in cell adhesion, migration, cytoskeletal organization, apoptosis, tissue remodelling, and morphogenesis (Miyamoto et al., 1998). It is an adhesive extracellular matrix that forms a fibrillar matrix at the cell surface controlling cell morphology, migration, and proliferation (Darribere and Schwarzbauer, 2000). The mechanisms that

control ECM organization and homeostasis are incompletely understood but it has been shown that fibronectin matrix polymerization is essential for the organization, as well as the maintenance of ECM architecture (Sottile and Hocking, 2002). Absence of this polymerization will disturb the ECM architecture because of loss of fibronectin matrix fibrils due to its increased degradation (Sottile and Chandler, 2005). This fibronectin degradation and its turnover are mediated by caveolin-mediated endocytosis (Sottile and Chandler, 2005). Its increased expression in cells increases fibronectin degradation affecting the composition and stability of ECM (Sottile and Chandler, 2005), making the environment more favorable for cell movement and migration.

From the above findings and interpretation, it is reasonable to postulate that the altered regulation of caveolin might result in an altered myometrial cell phenotype that is more vulnerable to stromal cell invasion from the overlying endometrium. Additionally, the differential effect of TMX and E2 on caveolin isoform expression *in vitro* is an interesting and novel finding that supports previous studies and microarray analysis (Mehasseb, 2010), indicating that the caveolins are part the aetiological path that leads towards adenomyosis.

Chapter 6   The Wnt family proteins wnt4, 5a and 7a

6.1 Introduction

The family of Wnt genes are cysteine-rich secreted glycoproteins that normally act through cell surface receptor, called frizzled and lrp (Nusse and Varmus, 1982). Activation of these receptors by wnt proteins and their intracellular signalling pathways play crucial roles in cell proliferation, cell polarity, cell fate determination and overall tissue homeostasis (Logan and Nusse, 2004). Any defect in the wnt signalling pathways often leads to birth defects, cancer and other diseases in the human (Clevers, 2006). The first wnt gene, discovered in 1982 called int-1 and described as a proto-oncogene, became activated when undergoing integration into the mouse mammary tumour virus in mammary tumours (Nusse and Varmus, 1982). The Wnt proteins are thought to elicit their downstream effects through three intracellular signalling pathways:

(1) The Wnt/β-catenin pathway (also known as the canonical pathway), which activates target genes in the nucleus (Huelsken and Behrens, 2002);

(2) The planar cell polarity pathway (non-canonical pathway), which involves jun N-terminal kinase (JNK) and β-catenin involved cytoskeletal rearrangements (Huelsken and Behrens, 2002); and

(3) The Wnt/Ca^{2+} pathway (Huelsken and Behrens, 2002).

The canonical pathway plays a critical role in maintaining various embryonic and adult stem cell functions (Grigoryan et al., 2008) and dysfunction results in pathological conditions such as cancer (Rask et al., 2003, Nishisho et al., 1991, Nakamura et al., 1991). In the planar cell polarity or non-canonical pathway, activation of JNK directs asymmetric cytoskeletal organization and coordinated polarization of cells within the plane of epithelial sheets. In the Wnt/β-catenin signalling pathway, a central role is

played by the ''destruction complex'' consisting of three scaffolding proteins, namely axin 1 and 2 (AXIN1, AXIN2), the adenomatous polyposis coli protein (APC), two kinases - glycogen synthase kinase-3β (GSK3β) and casein-kinase 1a (CK1a), and the central player in all wnt signalling pathways, β-catenin (CTNNB1). In the absence of extracellular wnt ligands, formation of the destruction complex marks β-catenin by Ser-Thr phosphorylation, thus promoting its proteolytic degradation through ubiquitination (Clevers, 2006). In the presence of wnt ligands, formation of the destruction complex is inhibited and β-catenin is able to accumulate in the cytoplasm and eventually translocate to the nucleus, where in association with members of the T-cell factor/Lymphoid enhancing factor (TCF/LEF) family of transcription factors, it activates transcription of a broad spectrum of downstream target genes, such as c-myc, n-myc and c-jun (StanfordEdu, 1997).

This Wnt/β-catenin signalling pathway plays a key role as a regulator of development and disease (Nusse and Varmus, 1982, Clevers, 2006) and its dysfunction or abnormal activation normally results in pathological conditions such as cancer (Rask et al., 2003, Nishisho et al., 1991, Nakamura et al., 1991). In humans, 19 secreted wnt proteins are produced, of which Wnt4, Wnt5a and Wnt7a have been shown to play crucial roles in the epithelial-mesenchymal interactions necessary for the correct patterning of the mammalian female reproductive tract (Mericskay et al., 2004, Miller et al., 1998, Miller and Sassoon, 1998, Franco et al., Franco et al., 2011). Wnt4 knock-out female mice develop normal Wolffian ducts but lack Müllerian ducts (Vainio et al., 1999), whilst wnt5a knockout female mice show defects in the posterior outgrowth of the developing Müllerian ducts and a defect in forming endometrial glands (Mericskay et al., 2004), whilst loss of wnt7a expression leads to incomplete demarcation between the vagina,

uterus and these knockout animals fail to form uterine glands (Miller and Sassoon, 1998). Although several papers in the literature provide information regarding the role of Wnt signalling pathways in maintaining normal endometrial tissue in human, there are only few papers that describe the role of wnt proteins in the myometrium (Jeong et al., 2009, Tanwar et al., 2009). Additionally, microarray analysis of the adenomyotic myometrium indicated that the expression of the wnt5 gene is reduced in both the inner and outer myometrium throughout the menstrual cycle (Mehasseb, 2010).

6.2   Wnt5a Immunohistochemistry

Experiments for Wnt5a, Wnt4 and Wnt7a were performed separately using commercially available antibodies. The amount of each individual immunoreactive protein was measured in the form of a histoscore using ImageScope (as described in Chapter 2, page 29). Wnt5a immunoreactivity was at a moderate intensity and present in both the normal and the adenomyotic tissue (Figures 6.1 and 6.2). Wnt5a staining was present in the cytoplasm and the nucleus of most cells. The expression of wnt5a was predominantly observed in the smooth muscle cells (Figures 6.1 and 6.2), but staining appeared to decrease in the adenomyotic myometrium and the levels appeared to be higher in the secretory phase of the menstrual cycle when compared to estrogen dominated proliferative phase.

Histomorphometric analysis of the immunoreactive staining (Table 6.1 and Figure 6.3) revealed a higher level of wnt5a immunoreactivity present in the secretory phase (2.4 to 2.6-fold higher when compared to proliferative phase) both in the inner and outer myometrium in both normal and adenomyosis, however, only the expression of wnt5a

in the normal myometrium was significantly increased by 2.6-fold in the outer myometrium. When the adenomyotic myometrium was compared to normal myometrium, there was a decrease in wnt5a expression, but only in the proliferative phase adenomyotic inner myometrium (Figure 6.3). The pattern of increased wnt5a expression was noted in the outer myometrium but that increase did not reach statistical significance (Figure 6.3). The level of wnt5a was increased in the secretory phase in adenomyosis biopsies both in inner and outer myometrium but that increase was not statistically significant.
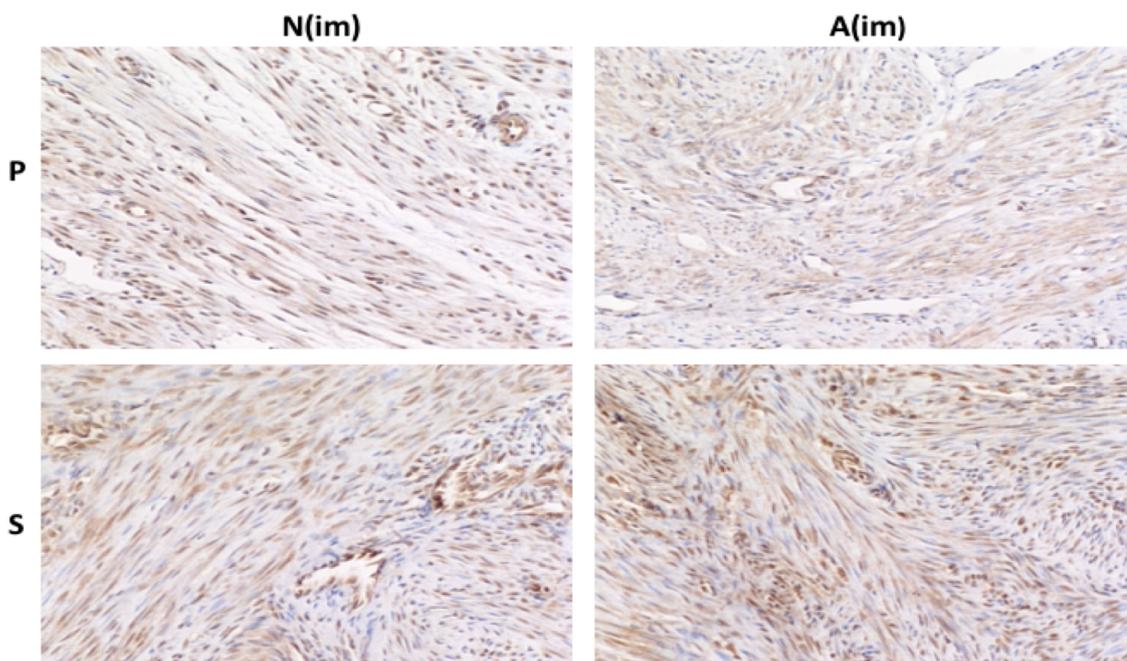
Figure 6.1: IHC showing Wnt5a expression in inner myometrium (im) in Proliferative phase (P) and Secretory phase (N (im): normal myometrium), A (im): adenomyotic myometrium) 20x magnification
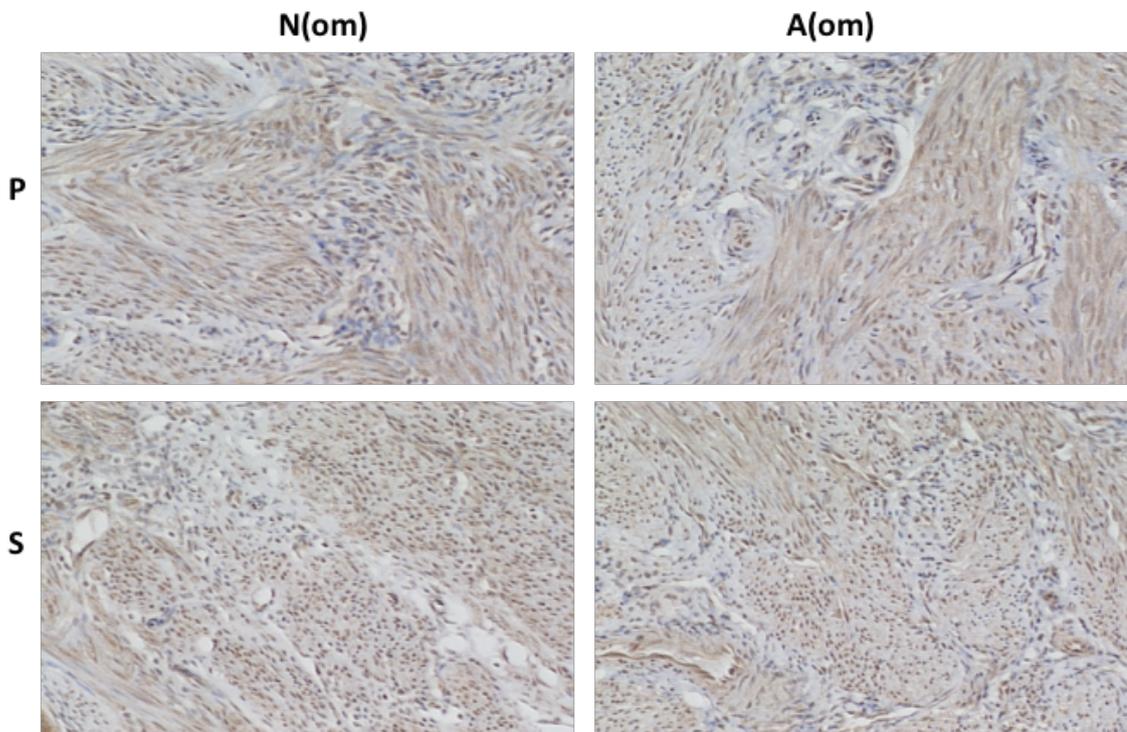
Figure 6.2: IHC images of Wnt5a immunoreactivity in the outer myometrium (om) of proliferative phase (P) and secretory phase (S) normal myometrium (N) and adenomyotic myometrium (A) 20x magnification

Table 6.1: ImageScope histoscore data corrected to amount of Wnt5a/cell for inner (IM) and outer (OM) myometrium for normal (N) and adenomyotic (A) myometrium subdivided into the proliferative (P) and secretory (S) phases of the menstrual cycle. The data are presented as the mean scores for all the six slides (10 fields/slide) examined.

Wnt5a/cell	NP(im)	AP(im)	NS(im)	AS(im)	NP(om)	AP(om)	NS(om)	AS(om)
Mean (n=6)	0.017	0.012	0.041	0.054	0.021	0.023	0.056	0.067
SEM	0.006	0.003	0.012	0.009	0.012	0.009	0.007	0.024
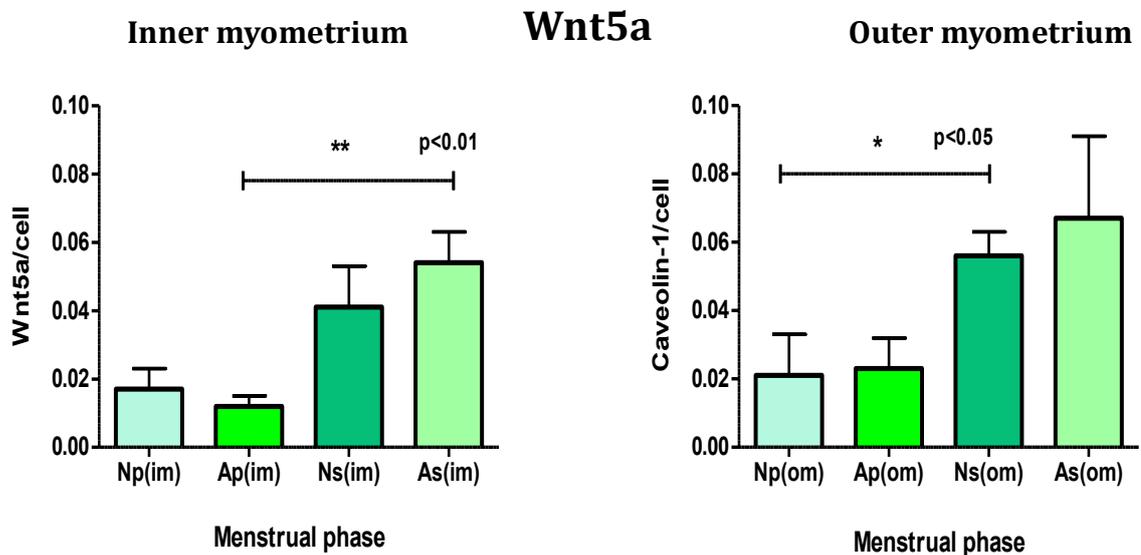
Figure 6.3: Wnt5a/cell in inner (im) & outer myometrium (om). Np: normal proliferative; Ap: adeno proliferative; Ns: normal secretory; As: adeno secretory (Error bar: SEM; One-way ANOVA with Bonferroni's Multiple comparison test, *p<0.05, **p<0.01)

6.3 Wnt5a qRT-PCR Experiment

In cultures of primary myometrial cells derived from normal and adenomyotic uteri treated with either 10^{-6}M E2 or 10^{-6}M TMX for 48 hours, transcript levels of wnt5a when measured and compared to untreated control showed that E2 decreases the expression of wnt5a in normal and adenomyotic myocytes, with variable effects on the expression. Similarly, TMX has the same effects on normal myocytes but up-regulated the expression of wnt5a from myocyte cultures obtained from adenomyotic tissue. These data suggest the opposite effect of E2 and TMX on wnt5a expression in adenomyotic myocytes placed in culture.

Table 6.2: Summary of Wnt5a Q-PCR data (Paffl's method(Pfaffl, 2001) used for PCR calculation)

N=9	Control GAPDH (Ct)	Control Wnt5a (Ct)	Treated GAPDH (Ct)	Treated Wnt5a (Ct)	Fold Change Wnt5a	Fold Change GAPDH	RATIO Wnt5a/GAPDH (Mean)	SEM
Normal								
E2	26.67	28.45	25.79	28.50	1.00	1.89	0.54	0.08
TMX	26.67	28.45	26.43	29.02	0.79	1.53	0.67	0.23
Adenomyosis								
E2	26.33	28.71	26.18	28.97	1.05	1.24	0.78	0.12
TMX	26.33	28.71	26.78	29.02	0.91	0.95	1.19	0.25
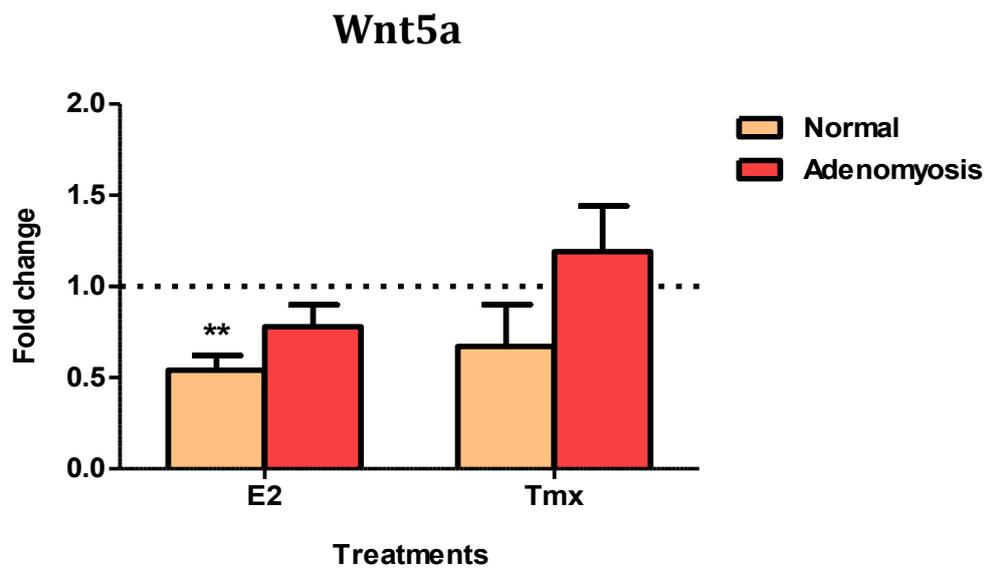
Figure 6.4: Wnt5a transcript levels in primary myometrial cells derived from normal and adenomyotic uteri and treated with either 10^{-6}M E2 or 10^{-6}M TMX for 48hr. Data are presented as the mean ± SEM; **$p<0.01$, Wnt5a transcript levels in both cell types were compared to Control untreated cultures (Mean: 1.00). One-way ANOVA with Bonferroni's Multiple Comparison *ad hoc* post-test; n=9.

6.4   Wnt7a Immunohistochemistry

Wnt7a immunoreactivity was at a moderate intensity when compared to wnt5a and present in both the normal and the adenomyotic tissue (Figures 6.5 and 6.6). Wnt7a staining was present in he cytoplasm and the nucleus of most cells. The expression of wnt7a was predominantly observed in the smooth muscle cells (Figures 6.5 and 6.6) and staining appeared to increase in the adenomyotic myometrium in proliferative phase. The levels were appeared to be lower in the secretory phase of the adenomyotic myometrium when compared to normal.

Histomorphometric analysis of the immunoreactive staining (Table 6.3 and Figure 6.7) revealed higher level of wnt7a immunoreactivity present in the secretory phase (0.5 to 2.0-fold higher when compared to proliferative phase) both in inner and outer myometrium in both normal and adenomyosis. When the adenomyotic myometrium was compared to normal myometrium, there was an increase in wnt7a expression, in the proliferative phase adenomyotic inner and outer myometrium (Figure 6.7). But the pattern of decrease was noted in in the secretory phase adenomyotic inner and outer myometrium (Figure 6.7). The level of wnt7a decrease in secretory phase in adenomyotic inner myometrium was statistically significant.
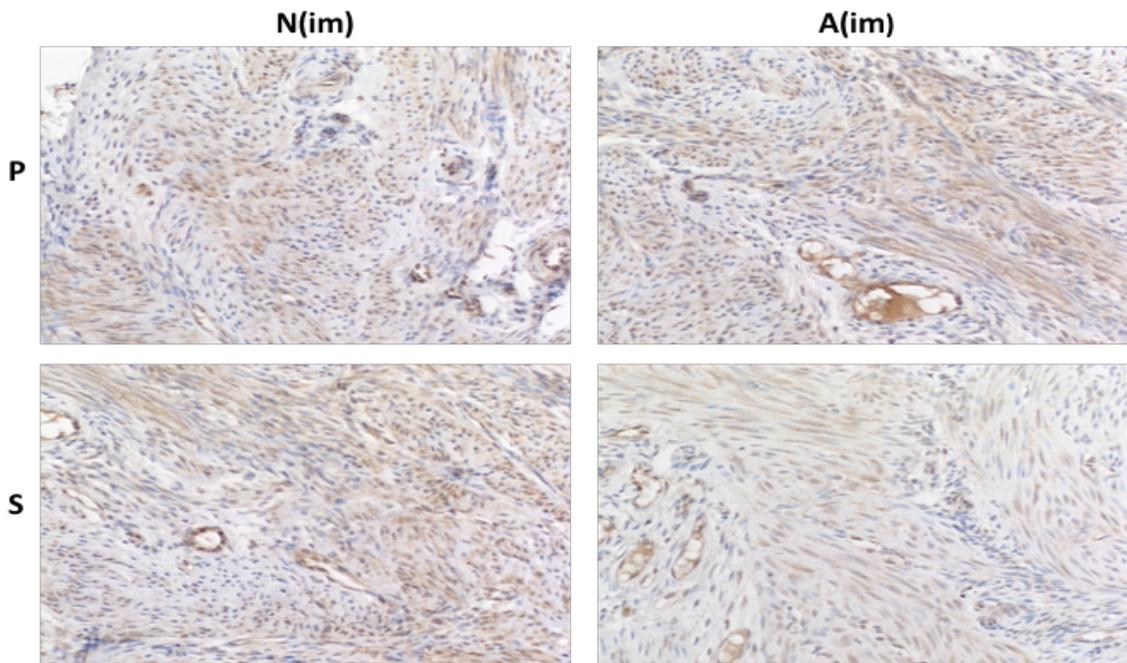
Figure 6.5: IHC showing Wnt5a expression in inner myometrium (im) in Proliferative phase (P) and Secretory phase (N (im): normal myometrium), A (im): adenomyotic myometrium) 20x magnification
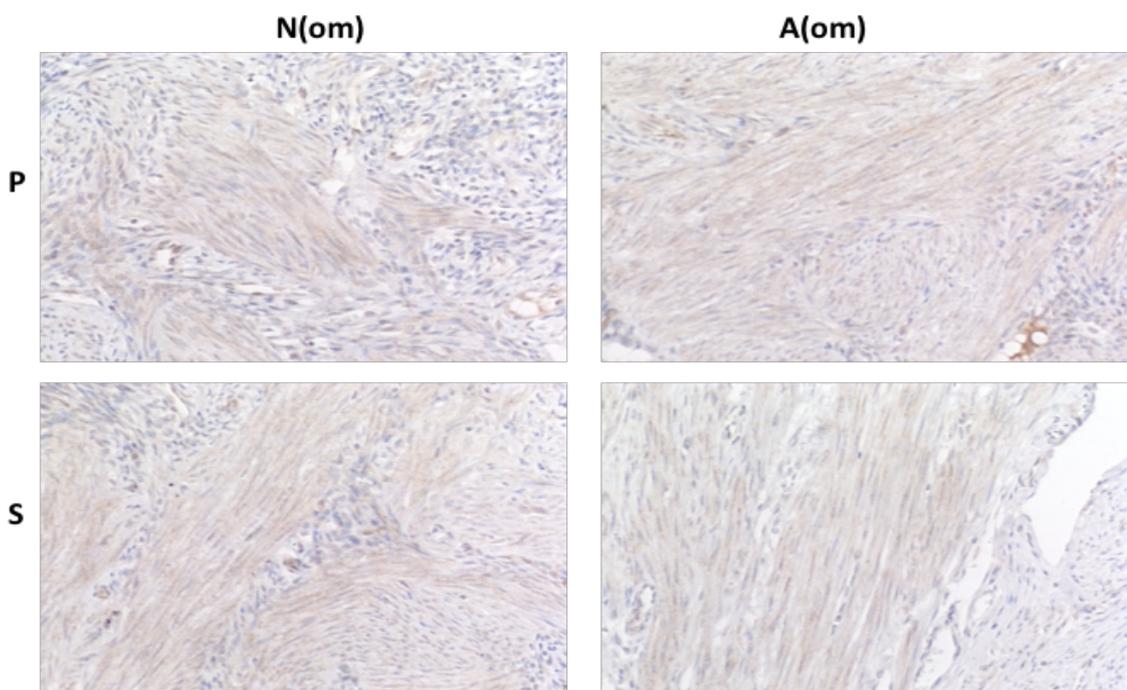
Figure 6.6: IHC images of Wnt5a immunoreactivity in the outer myometrium (om) of proliferative phase (P) and secretory phase (S) normal myometrium (N) and adenomyotic myometrium (A) 20x magnification

Table 6.3: ImageScope histoscore data corrected to amount of Wnt7a/cell for inner (IM) and outer (OM) myometrium for normal (N) and adenomyotic (A) myometrium subdivided into the proliferative (P) and secretory (S) phases of the menstrual cycle. Data are presented as the mean scores for all the six slides (10 fields/slide) examined.

Wnt7a/cell	NP(im)	AP(im)	NS(im)	AS(im)	NP(om)	AP(om)	NS(om)	AS(om)
Mean (n=6)	0.003	0.004	0.006	0.002	0.004	0.005	0.007	0.006
SEM	0.001	0.001	0.001	0.001	0.001	0.001	0.002	0.002
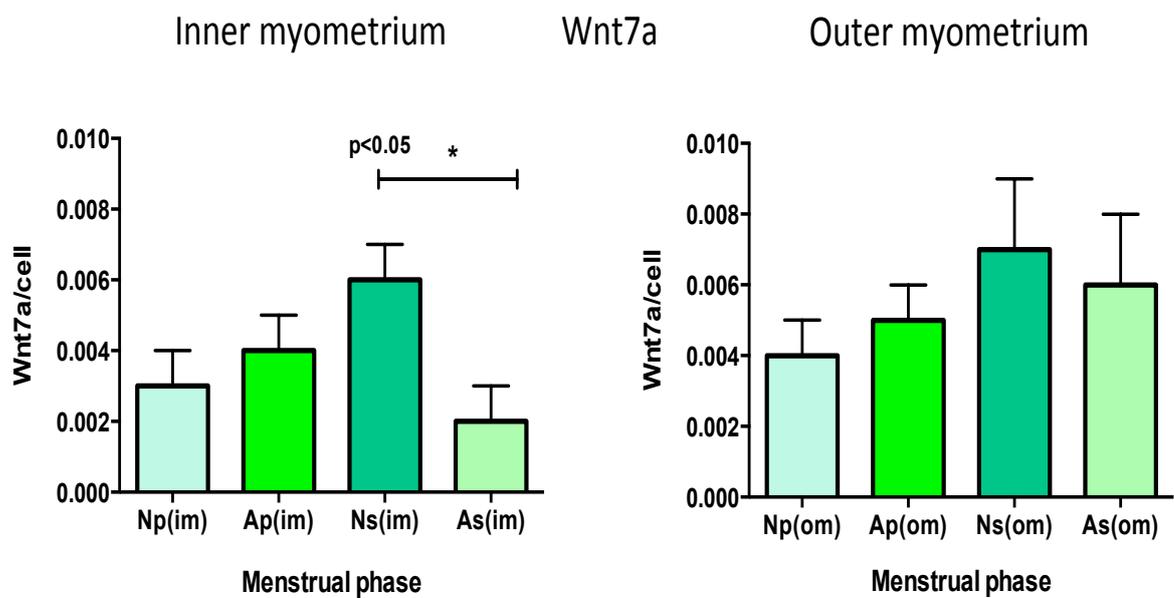
Figure 6.7: Wnt7a/cell in inner (im) & outer myometrium (om). Np: normal proliferative; Ap: adeno proliferative; Ns: normal secretory; As: adeno secretory (Error bar: SEM; One way ANOVA with Bonferroni's Multiple comparison test, *p<0.05)

6.5   Wnt 7a qRT-PCR Experiment

In cultures of primary myometrial cells derived from normal and adenomyotic uteri treated with either 10^{-6}M E2 or 10^{-6}M TMX for 48 hours, transcript levels of wnt7a when measured and compared to untreated control showed that E2 significantly decreases the expression of wnt7a in normal more than that in adenomyotic myocytes (Table 6.4 and Figure 6.8). Similarly, TMX has the same effects on normal myocytes but has variable effect by up-regulating the expression of wnt7a from myocyte cultures obtained from adenomyotic tissue (Table 6.4 and Figure 6.8). These data suggest the opposite effect of E2 and TMX on wnt7a expression in adenomyotic myocytes placed in culture.

Table 6.4: Summary of Wnt5a Q-PCR data (Paffl's method(Pfaffl, 2001) used for PCR calculation)

N=9	Control GAPDH (Ct)	Control Wnt7a (Ct)	Treated GAPDH (Ct)	Treated Wnt7a (Ct)	Fold Change Wnt7a	Fold Change GAPDH	RATIO Wnt7a/GAPDH (Mean)	SEM
Normal								
E2	26.67	23.15	25.79	23.40	1.05	1.89	0.51	0.13
TMX	26.67	23.15	26.43	23.76	0.76	1.53	0.59	0.22
Adenomyosis								
E2	26.33	23.35	26.18	23.33	1.14	1.24	0.93	0.11
TMX	26.33	23.35	26.78	23.63	0.82	0.95	1.50	0.91
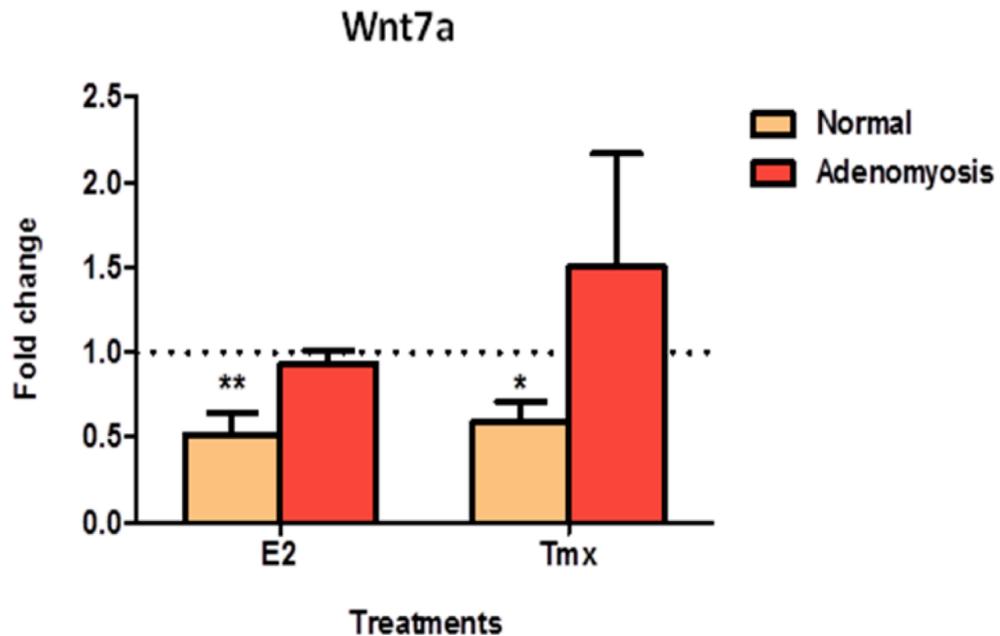
Figure 6.8: Wnt7a transcript levels in primary myometrial cells derived from normal and adenomyotic uteri and treated with either 10^{-6}M E2 or 10^{-6}M TMX for 48hr. Data are presented as the mean ± SEM; *p<0.05, **p<0.01, Wnt7a transcript levels in both cell types were compared to Control untreated cultures (Mean: 1.00). One-way ANOVA with Bonferroni's Multiple Comparison *ad hoc* post-test; n=9.

6.6 Wnt4a Immunohistochemistry

Figure 6.9 shows the wnt4 immunohistochemistry images. For some unknown reason, I got no staining and that the antibodies used were no good for the study. I tried different concentrations to optimise the antibody but all those efforts failed with no staining observed. I am not sure whether the commercial antibodies available at that time were not at the optimum quality required for proper staining (Figure 6.9) or if there was inadequate wnt4 production in the uterus or whether wnt4 produce only transcripts, which I managed to measure in my Q-PCR experiments (as shown below).
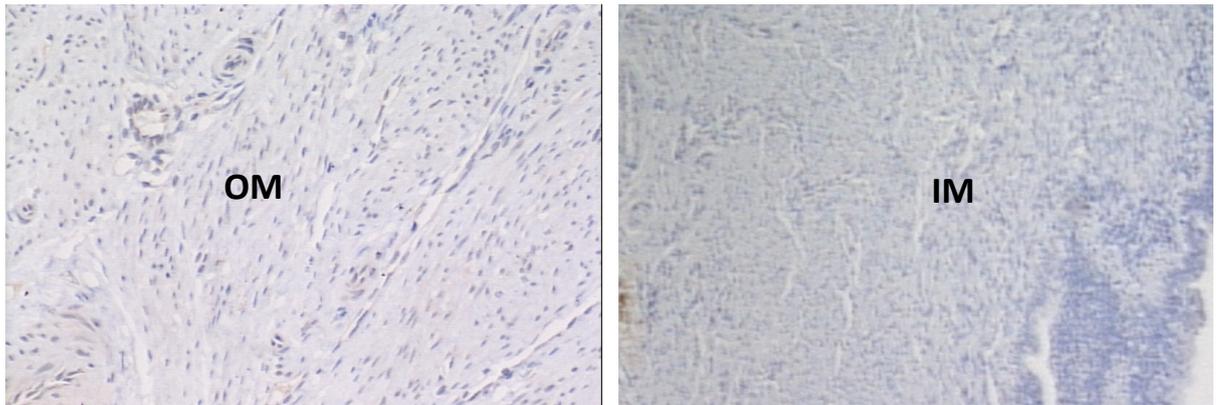
Figure 6.9: images of Wnt4 staining. OM: outer myometrium, IM:inner myometrium. 20x magnification

6.7 Wnt4 qRT-PCR Experiment

In cultures of primary myometrial cells derived from normal and adenomyotic uteri treated with either 10^{-6}M E2 or 10^{-6}M TMX for 48 hours, transcript levels of wnt4 when measured and compared to untreated control showed that E2 significantly decreased expression of wnt4 in normal and adenomyotic myocytes, with a significant effect on the normal myocytes, but not in the adenomyotic myocytes (Table 6.5 and Figure 6.10). Similarly, TMX has the same effect on normal myocytes but showed a variable effect by up-regulating the expression of wnt4 from myocyte cultures obtained from adenomyotic tissue (Table 6.5 and Figure 6.10). These data suggest the opposite effect of E2 and TMX on wnt4 expression in adenomyotic myocytes placed in culture.

Table 6.5: Summary of Wnt4 Q-PCR data (Paffl's method(Pfaffl, 2001) used for PCR calculation)

| N=9	Control GAPDH (Ct)	Control Wnt4 (Ct)	Treated GAPDH (Ct)	Treated Wnt4 (Ct)	Fold Change Wnt4	Fold Change GAPDH	RATIO Wnt4/GABDH (Mean)	SEM
Normal								
E2	26.67	24.35	25.79	24.23	1.18	1.89	0.60	0.08
TMX	26.67	24.35	26.43	24.87	0.88	1.53	0.59	0.02
Adenomyosis								
E2	26.33	24.51	26.18	24.53	1.23	1.24	0.91	0.13
TMX	26.33	24.51	26.78	24.88	0.81	0.95	1.20	0.34
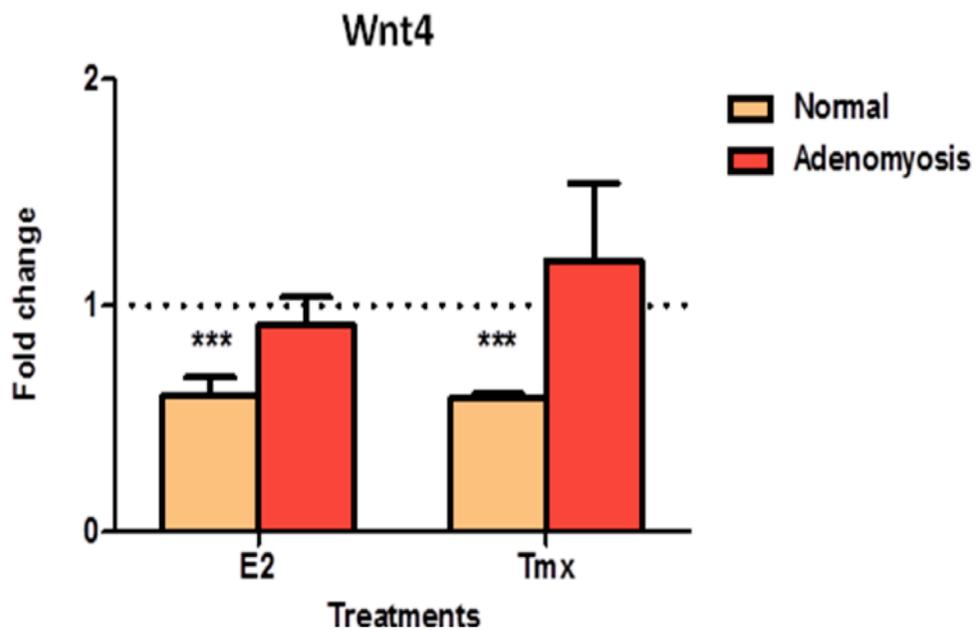
Figure 6.10: Wnt4a transcript levels in primary myometrial cells derived from normal and adenomyotic uteri and treated with either 10^{-6}M E2 or 10^{-6}M TMX for 48hr. Data are presented as the mean ± SEM; ***p<0.001 Wnt4a transcript levels in both cell types were compared to Control untreated cultures (Mean: 1.00). One-way ANOVA with Bonferroni's Multiple Comparison *ad hoc* post-test; n=9.

6.8 Discussion

Immunohistochemical analysis of wnt5a expression indicated that this protein was decreased in the estrogen-dominant proliferative phase when compared to the levels seen in the progesterone-dominated secretory phase in both the inner and outer myometrium and that there was no significant difference between normal and adenomyosis tissues. By contrast, the expression of wnt7a protein was increased in all tissues during the transition to the secretory phase, except for the inner myometrium of the adenomyotic tissue. Because of antibody issues, I could not complete the IHC experiment for Wnt4. Furthermore, after treatment with either E2 or TMX for 48 hours, transcript levels of wnt4, 5a and 7a in cells cultured from normal and adenomyotic myometrial tissue were observed to be significantly down regulated by 10^{-6}M estradiol or10^{-6}M tamoxifen in the normal myometrial cells but up regulated in the adenomyotic myometrial cells. These data suggest that a functional defect in the expression of these 3 wnt proteins may have a role in the pathogenesis of adenomyosis.

Defects in several members of the wnt signalling cascade, i.e. loss of function mutations at the APC gene, inhibits the formation of the destruction complex leading to the accumulation of intracellular and nuclear β-catenin, resulting in constitutive deregulation of target genes (Behrens et al., 1996, Morin et al., 1997, Sparks et al., 1998). In experimental studies, the conditional activation of Wnt/β-catenin in the uterus showed profound effects, inducing endometrial hyperplasia, myometrial hyperplasia, adenomyosis, and mesenchymal tumours similar to leiomyoma and endometrial stromal sarcoma (Jeong et al., 2009, Tanwar et al., 2009). Studies related to endometrial cancer showed intercellular and nuclear accumulation of β-catenin (Saegusa et al., 2001, Scholten et al., 2003) and loss of APC expression (Moreno-Bueno

et al., 2002), explaining the role of wnt signalling in cancer related disorders. Recently, Wang *et al.* (Wang et al., 2011) reported that *in vivo* inactivation of the endogenous mouse APC gene in mesenchymal cells surrounding the Müllerian ducts, results in significant myometrial defects in adult mice, with tissue morphological effects nearing in similarity to that of adenomyosis. These observations further strengthen the arguments for the importance of wnt/β-catenin signalling and members of its cascade in uterine development and tissue homeostasis. β-catenin acts as a dual function protein, both in the β-catenin/E-cadherin complex and as a transcriptional regulator in canonical wnt signalling pathway (Daugherty and Gottardi, 2007).

The structural integrity of many tissues depends on the stability of epithelial cell-cell junctions organized by adhesion proteins and the underlying actin cytoskeleton (Drees et al., 2005). In this context, wnt5a may be important because it is also involved in cell adhesion, motility, and polarity *via* β-catenin/E-cadherin complex (Moon et al., 1993, Pandur et al., 2002). The role of wnt5a as a prognostic marker in various cancers has now been proven (Dejmek et al., 2005, Blanc et al., 2005, Kremenevskaja et al., 2005) and low expression of β-catenin leads to decreased adherence of cells, resulting in increased invasion of cancer cells (Jonsson and Andersson, 2001). This information supports my findings of low expression of wnt5a in the estrogen dominated proliferative phase in adenomyotic myometrium when compared to normal myometrium. Similar observations were noted in lung cancer where down regulation of wnt7a resulted in decreased cadherin-catenin complex, decreased cell adhesion and increased invasion of cancer cells (Ohira et al., 2003). Research also supports the role of wnt proteins on a process known as epithelial-mesenchymal transition (EMT), which is influenced by estrogen in cancers that could also result in the development of

adenomyosis. The process of EMT involves programmed development of biological cells, characterized by loss of cell adhesion, repression of E-cadherin expression and an increase in cell mobility. One of the signals initiating an EMT is the canonical Wnt signalling pathway, which in turn triggers the translocation of β-catenin to the nucleus resulting in the down-regulation of E-cadherin. By inducing EMT, these factors transcriptionally repress epithelial markers such as E-cadherin. My findings of increased wnt7a expression support this argument about the role of wnt7a in adenomyosis through EMT activation. Nonetheless, these phenomena in reproductive biology are poorly understood and require further evaluation.

From the data presented in this chapter, it is reasonable to postulate that during regeneration of the myometrial layer within the EMI, which probably occurs after either disturbance or injury due to dysfunctional uterine hyper-peristalsis or contractility (Parrott et al., 2001, Kunz et al., 2000), mechanical damage by sharp curettage during pregnancy (Leyendecker et al., 2002), and/or because of frequent trophoblast invasion in multiparous women, that the deregulated functioning of wnt/β-catenin signalling pathway results in a weakened myometrial phenotype, making the myocyte layer more prone to invasion by the overlying endometrium. To explore the regulation of APC and β-catenin in adenomyosis, which will help us to learn more about the role of wnt signalling in the human myometrium during the pathogenesis of adenomyosis, further experiments will be required.

Chapter 7   The effect of adenomyosis on *in vitro* stromal cell decidualisation

7.1 Decidualisation

In previous chapters, I focussed on the phenotype of inner myometrium when compared with the outer myometrium, which appears to have a key 'permissive' role in adenomyosis (see Chapter 3), with the suggestion that there is an obvious 'malfunction' in the migratory patterns of adenomyotic stromal cells in the co-culture experiments (see Chapter 3). It has been reported that adenomyosis may be caused by disordered stromal cell differentiation (Parrott et al., 2001). Indeed, some molecular and invasion characteristics of endometrial stromal cells cultured from women with adenomyosis differ from those isolated from unaffected women (Mehasseb et al., 2010b). Furthermore, the expression of both progesterone receptor isoforms (PR-A and PR-B) are lower in adenomyotic endometrial stromal cells, during the secretory phase of the menstrual cycle suggesting a possible difference in stromal cell response to progesterone during the process of implantation (Mehasseb et al., 2011b).

Decidualisation is an important process that results in the remodelling of endometrial stroma, resulting in morphological and biochemical changes in the endometrial environment that aid the smooth implantation of the embryo and appropriate trophoblast invasion (Salamonsen et al., 2003, Jones et al., 2006). However, whether stromal cell differentiation (the decidualisation process) is disordered in adenomyosis has not been directly tested before. In this study, cultured stromal cells obtained from women with or without adenomyosis were examined for the expression of the decidualisation markers, IGFBP-1 and prolactin to see if decidualisation is altered in adenomyosis.

7.2 Methods

Stromal cells were isolated with standard collagenase digestion and cell isolation techniques and grown to confluence. Decidualisation in all cultures was induced by the addition of 1 µM medroxyprogesterone acetate (MPA), 0.5 mM 8-br-cAMP and 10 nM 17β-estradiol (E2) in phenol-red deficient DMEM supplemented with 10% charcoal-stripped serum, with the medium being exchanged every 2 days for 21 days. Cells were photographed at the beginning and end of the experiment. RNA was extracted and subjected to semi-quantitative RT-PCR for the relative levels of the decidualisation markers, IGFBP-1 and prolactin, using the expression of GAPDH as the normalising gene. The primers used are listed in Table 7.1. Experiments with cells not treated with E2, MPA and 8-br-cAMP served as a control. Data were analysed by one-way ANOVA with Tukey's honestly significance difference test.

Table 7.1: Primers used and expected band sizes

Gene	Forward primer	Reverse primer	band size (bp)
IGFBP-1	AGACGACGGAGATAACTGAGGA	GCCCTTGGCTAAACTCTCTACGA	199
Prolactin	GGTGACCCTTCGAGACTGTT	GGAAGAAGTGTGGCAGGTGTT	180
GAPDH	AGAACATCATCCCTGCCTC	GCCAAATTCGTTGTCATACC	346

7.3   Results

Decidualisation was determined by examining the presence of morphological changes in the cells (Figure 7.1). During treatment with E2, MPA and 8-bromo-cAMP, the morphology of cells in culture change markedly by increasing in width (girth). There was also reduction in cell number. By day 21, the cells enlarged substantially and show reduced cell numbers (Figure 7.1, panel B). Similar features are seen in the adenomyotic stromal cell cultures. They did not appear to be any gross morphological differences between the final normal and adenomyotic stromal cells.
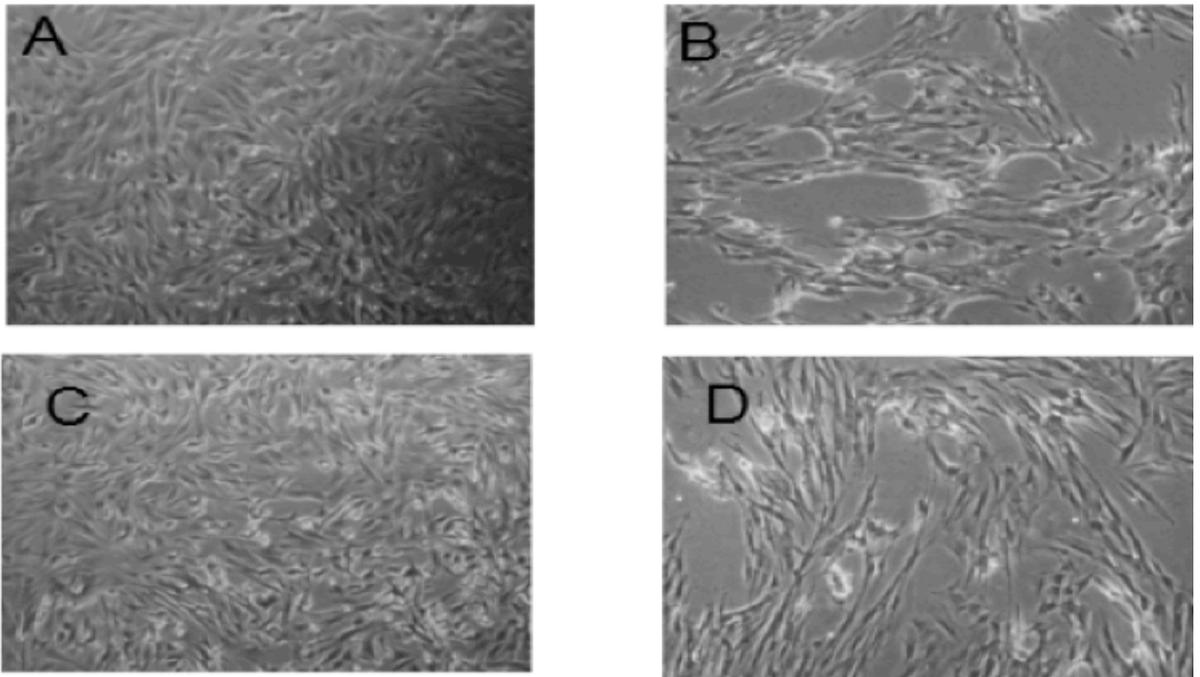
Figure 7.1: Photomicrographs of normal stromal cells before (panel A) and after (panel B) 21 days treatment with 10^{-8}M E2, 0.5mM 8-Br-cAMP and 10^{-6}M MPA. Corresponding images for adenomyotic stromal cells before and after treatment are shown in panels C and D, respectively. Images are representative of 3 experiments performed in triplicate. All images were taken at 200x magnification

7.4   The expression of IGFBP-1

The expression of IGFBP-1 was significantly higher in treatment groups of the both the stromal cells derived from normal endometria (46.35 ± 6.34-fold) and from adenomyotic endometria (49.57 ± 9.46-fold). Furthermore, the magnitude of the increase in IGFBP-1 expression was not significantly different in the two cell types (Figure 7.2 & 7.3).
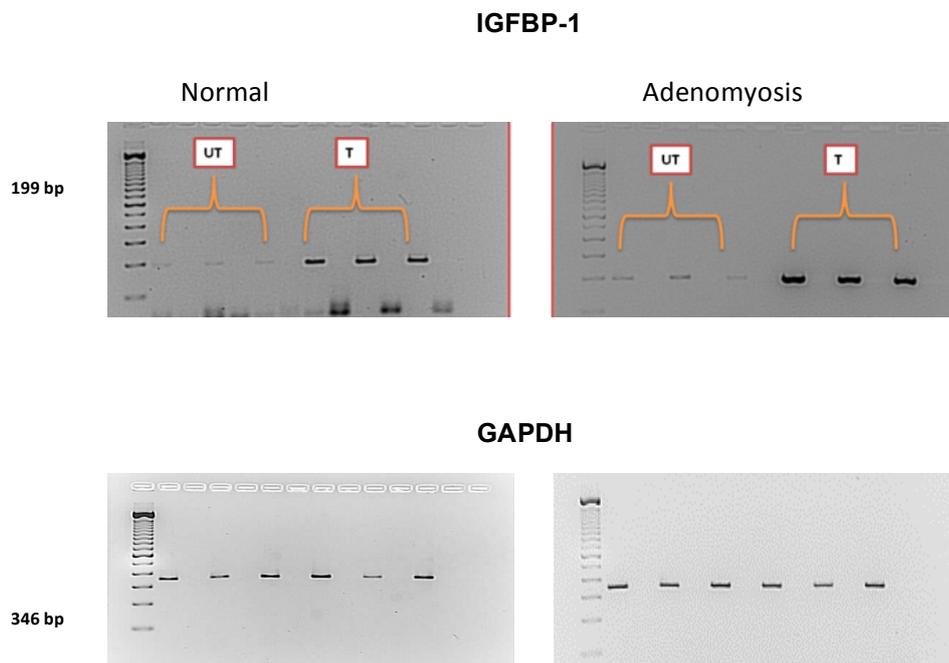
IGFBP-1

GAPDH

Figure 7.2: : EtBr-stained agarose gel images showing the level of IGFBP-1 (upper panels) and GAPDH (lower panels) in stromal cells derived from normal and adenomyotic uteri. Cells are treated (T) or untreated (UT) with 1μM medroxyprogesterone acetate (MPA), 0.5 mM of 8-Br-cAMP and 10⁻⁸ M of 17b-estradiol every 2 days for 21 days. Total cellular RNA was subjected to RT-PCR with IGFBP-1 specific primers. The images are representative of 3 experiments, which were similar in appearance. The lanes with bands present indicate +RT cDNA and the lanes with no visible bands at the expected bp size of 100bp indicate the -RT (no cDNA) control for each sample. The position of the 100bp size ladder is shown on the left hand side of all gels.

7.5   IGFBP-1 RT-PCR

In addition to the morphological changes in the cells in culture (Figure 7.1), the increased level of IGFBP-1 transcripts in the treatment group implies that these cells have undergone decidualisation and that treatment worked successfully. Irrespective of disease, IGFBP-1 levels were significantly increased in each treatment group with the levels being more or less the same in both the normal and adenomyotic groups, supporting the idea that decidualisation occurred in all cultures (Table 7.2 & Figure 7.3).

Table 7.2: RT-PCR data for IGFBP-1 from decidualisation experiments done in triplicates

Sample	IGFBP1 Average	GAPDH Average	Ratio	Normalised Values	Mean	SD
Normal Untreated						
Exp-1	3.70	206.53	0.02	0.55	1.00	0.40
Exp-2	9.14	242.70	0.04	1.15		
Exp-3	8.81	205.24	0.04	1.31		
Normal Treatment						
Exp-1	340.70	255.38	1.33	40.64	46.35	6.34
Exp-2	446.87	255.99	1.75	53.18		
Exp-3	338.53	227.96	1.49	45.24		
Adeno Untreated						
Exp-1	6.98	316.79	0.02	0.67	1.98	1.25
Exp-2	18.41	177.85	0.10	3.15		
Exp-3	9.68	138.91	0.07	2.12		
Adeno Treatment						
Exp-1	468.94	362.55	1.29	39.40	49.57	9.46
Exp-2	426.98	223.82	1.91	58.11		
Exp-3	412.21	245.19	1.68	51.21		
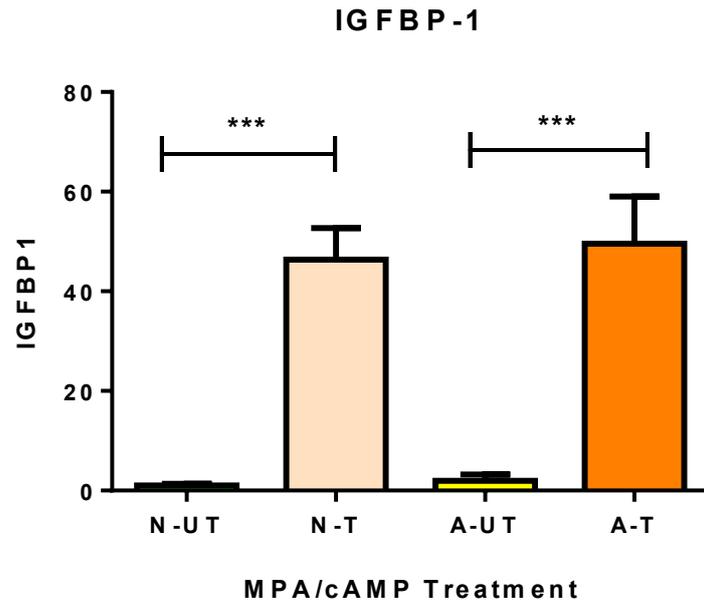
IGFBP-1

Figure 7.3: IGFBP-1 transcript levels in stromal cells derived from normal (N) and adenomyotic (A) uteri subjected to treatment (T) and left in an untreated (UT) condition. (One way ANOVA; p<0.0001; Error bar: SEM)

7.6 The expression of prolactin

The prolactin levels in treated stromal cells were increased in both cells derived from normal and adenomyotic endometria (Figure 7.4). Transcripts for prolactin mRNA was undetectable in the untreated cultures (Figure 7.4). Because a band of the expected size (180bp) was found only in +RT lanes of the treatment group, again indicating successful decidualisation, semi-quantitative analysis of those levels within was not possible (Figure 7.4).

PROLACTIN

GAPDH
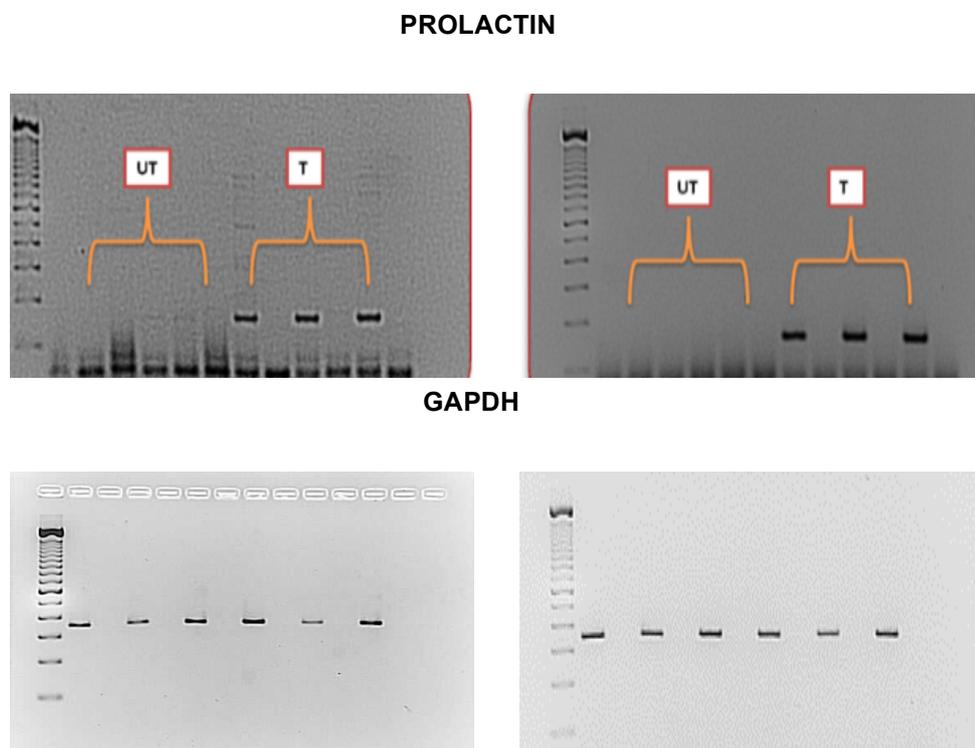
Figure 7.4: Agarose gel image showing the level of Prolactin in stromal cells derived from normal and adenomyotic uteri. Cells were treated or conditions in-group. Cells are treated (T) or untreated (UT) with 1μM medroxyprogesterone acetate (MPA), 0.5 mM of 8-Br-cAMP and 10^{-8} M of 17b-estradiol every 2 days for 21 days Total cellular RNA was subjected to RT-PCR with Prolactin specific primers. The images are representative of 3 experiments that were similar in appearance. The lanes with bands present indicate +RT cDNA and the lanes with no visible bands at the expected bp size of 100bp, indicate the –RT no cDNA control for each sample

7.7   Prolactin RT PCR

In an attempt to determine whether the levels of prolactin expression differed between the normal and adenomyotic cultures, the levels of prolactin in the treatment groups were normalised to GAPDH expression levels and then the ratio between the normal and adenomyotic cultures calculated (Figure 7.5). The data indicated that the level of prolactin in the decidualised adenomyotic stromal cells was 1.34 ± 0.59-fold higher than that of the decidualised normal stromal cell, and that increase was not significantly different (Figure 7.5).

Table 7.3: RT-PCR data for Prolactin from decidualisation experiments done in triplicates

Sample	PROLACTIN average	GABDH Average	Ratio	Normalised Values	Mean	SD
Normal Untreated						
Exp-1	0.00	206.53	0.00	0.00	0.00	0.00
Exp-2	0.00	242.70	0.00	0.00		
Exp-3	0.00	205.24	0.00	0.00		
Normal Treatment						
Exp-1	120.91	255.38	0.47	1.18	1.00	0.15
Exp-2	93.61	255.99	0.37	0.91		
Exp-3	84.15	227.96	0.37	0.92		
Adeno Untreated						
Exp-1	0.00	316.79	0.00	0.00	0.00	0.00
Exp-2	0.00	177.85	0.00	0.00		
Exp-3	0.00	138.91	0.00	0.00		
Adeno Treatment						
Exp-1	97.75	362.55	0.27	0.67	1.34	0.59
Exp-2	138.33	223.82	0.62	1.53		
Exp-3	177.88	245.19	0.73	1.80		
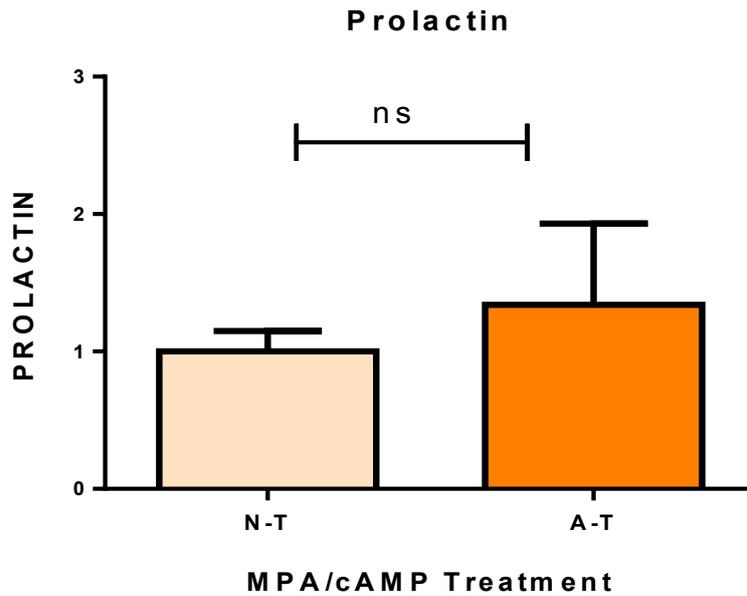
Figure 7.5: Prolactin transcript levels in normal and adenomyosis stromal cells after decidualisation with MPA and cAMP treatment. (ns=Not statistically significant)

7.8 Discussion

The morphological changes in the cultured stromal cells and increased levels of IGFBP-1 and prolactin after treatment indicate that the decidualisation treatment was successful. Though the IGFBP-1 and prolactin levels are slightly higher in adenomyotic group, they were not statistically significant. These observations imply that as a disease, adenomyosis itself has no major impact on the process of decidualisation, although it appears that stromal cells *in vitro* behave differently, suggesting that the process of decidualisation in adenomyosis might produce slightly higher levels of IGFBP-1 and prolactin. What this might mean, is that the adenomyotic stromal cell undergoes premature decidualisation in comparison to its normal counterpart, which may have some impact on implantation, if that occurs *in vivo*.

Decidualisation occurs during most menstrual cycles resulting in regular morphological changes that occur in the endometrial glands and stroma and in the endometrial vasculature in anticipation of an implanting blastocyst and the formation of an embryo towards the end of that cycle (Salamonsen et al., 2003). Any abnormal or deficient decidualisation will result in early pregnancy loss and inadequate trophoblast invasion, or possibly leading to pre-eclampsia in later pregnancy (Brosens et al., 2002). Decidualised stromal cells are functionally different from non-decidualised cells, which can be differentiated by measuring their secreted proteins such as cytokines, growth factor binding proteins, such as IGFBP-1, and prolactin, which all play important roles in embryo implantation and trophoblast invasion (Salamonsen et al., 2003). The decidualisation process starts during the late secretory phase of the menstrual cycle with functional differentiation in endometrial stromal cells and then progresses if conception results in that cycle (Ferenczy and Bergeron, 1991). Decidualisation changes were noted in endometrial stromal cells in *in vitro* studies by treating them with progesterone (Tang and Gurpide, 1993, Frank et al., 1994) or by treating them with combination of 8-bromo-cAMP and MPA (Gellersen and Brosens, 2003). Since the junctional zone is probably affected in adenomyosis, dysfunctional decidualisation may result in impaired placentation during early pregnancy, resulting in miscarriage or preterm labour or fetal growth restriction (Brosens et al., 1972). Uterine peristalsis is thought to play an important role in the early process of reproduction by helping sperm transport towards the oviduct of the ipsilateral dominant follicle (Kunz et al., 1996, Leyendecker et al., 1996). Since adenomyosis was reported to be the result of disordered stromal cell differentiation (Parrott et al., 2001), it is reasonable to assume in such cases that there will be some effect on decidualisation of stromal cells, which could result in disordered blastocyst reception, which is one of the main causes for infertility.

The findings and interpretation from the above experiments suggest that there is no difference in the timing to decidualisation, nor in morphological features, IGFBP-1 or prolactin expression in stromal cells from women with adenomyosis compared to control stromal cells grown in long term culture, suggesting that the origin of the stromal cells has no effect on the behaviour of these cells or that cell response was modified by the culture conditions. This suggests that disordered stromal differentiation is not the main causal event in the pathogenesis of adenomyosis, although the major components of decidualisation were examined, and seemingly less important components were not tested. For example, the protein WFDC1 is a protease produced in the uterus under the decidualisation process. The function of this protein is to aid trophoblast migration during implantation, and leukaemia inhibitory factor-1 (LIF-1) is known to be essential to the implantation process. The uterus produces both of these during the implantation process and as these were not examined in the present study, they could be in the future. The slightly enhanced decidualisation effect with respect to IGFBP-1 and prolactin expression may be an indicator of premature decidualisation, which could affect implantation and thus pregnancy success in women with undiagnosed adenomyosis.

Chapter 8   Discussion

Adenomyosis is a benign disease of the uterus seen most commonly among multiparous women and defined as the presence of ectopic, non-neoplastic endometrial epithelia and stroma within the myometrium, which is surrounded by hypertrophic and hyperplastic myometrial smooth muscle cells (Hever et al., 2006, Bird et al., 1972) and seen most commonly among multiparous women of between 40 to 50 years of age with a wide range of prevalence of between 5-70% (Azziz, 1989). The deep invasion of the myometrium by endometrial tissue is thought to be due to stromal disruption of the endometrial-myometrial interface (EMI) or 'permissiveness' by the inner myometrium. Several theories have been proposed regarding the aetiology of adenomyosis but the most widely accepted current theory is that adenomyosis results from the abnormal down-growth and invagination of endometrium into the myometrium. It is suggested that this may be because of some inherent weakness of the smooth muscle cells close to the EMI (inner myometrium) that causes a change in the myometrial cell in response to that invasion that ultimately results in the formation of focal hypertrophy and hyperplasia surrounding the endometrial cells (Bird et al., 1972). Although the reason for endometrial penetration into the myometrium is not clear, one theory suggest that a breakdown of the myometrial–endometrial border caused by trauma results in reactive hyperplasia of the basalis and its penetration into the myometrium (Emge, 1962, Azziz, 1989).

Recent research from our laboratory has also shown that when the stromal cells of either normal or adenomyotic uteri were placed on top of collagen containing myocytes obtained from uteri with adenomyosis, increased invasiveness of the stromal cells was observed compared to a matrix containing myocytes obtained from normal uteri (Mehasseb et al., 2010b). It has been reported that adenomyosis may be caused by

disordered stromal cell differentiation (Parrott et al., 2001) and there is an obvious 'malfunction' in the migratory patterns of adenomyotic stromal cells in the co-culture experiments (Mehasseb et al., 2010b). Although there were many studies in the literature, which explored the causal relationship of estrogen and tamoxifen with adenomyosis, there were no studies, which actually looked into the effect of steroids on stromal cell invasion into the myometrium and the results from this novel three-dimensional co-culture model has shown that both E2 and TMX significantly increased the migration of both normal and adenomyotic stromal cells. But migration of stromal cells taken from women with adenomyosis was always greater than that of stromal cells obtained from women without adenomyosis suggesting the potentiating effect of estrogen and the observed difference in invasiveness is innate rather than specifically induced or inhibited by steroids. A similar conclusion could be drawn about the effect on myocytes in this culture, suggesting that the role of estrogenic steroids may be to potentiate rather than to induce the disease.

NGF was the first neurotropic factor discovered to play a crucial role in the release of inflammatory factors and aggregation of immunocytes resulting in the production and transmission of pain (Snider, 1994). There is an increased density of nerve fibres in the uteri of adenomyotic women (Zhang et al., 2010), suggesting that NGF might make a major contribution towards the generation of pain in this disease by increasing the density of the nerve fibres in symptomatic women (Watson et al., 2008, Mendell et al., 1999). This is again supported by my finding of increased NGF expression in adenomyosis in both phases of menstrual cycle when compared to that of the normal group. But, this might be due to autoimmune (Ota et al., 1998) and pre-inflammatory changes associated with adenomyosis (Huang et al., Wang et al., 2009), since NGF has

been reported to be commonly involved in such autoimmune and inflammatory diseases, such as allergic diseases and asthma (Bonini et al., 2002, Abram et al., 2009), and intestinal mucosa inflammation (Agro and Stanisz, 1993). Studies in rodents has demonstrated a possible role of neurotrophins, such as nerve growth factor (NGF), which was significantly up-regulated in endometrial luminal epithelium in the CD-1 mouse model of adenomyosis. Thus, neurotrophins may affect myogenic differentiation through paracrine mechanisms. The pattern of nerve growth factor (NGF), brain derived neurotropic factor (BDNF) and neurotrophin receptor (trkB, trkC and p75[NTR]) expression in the human myometrium also points to a possible role.

Caveolins are thought to play important roles in intracellular transport (Parton and Simons, 2007), as scaffolding proteins for signal transduction (Patel et al., 2008), and have a role as regulators of cellular proliferation, invasiveness and the metastatic potential of cancer cells (Bagnoli et al., 2000, Bender et al., 2000). The available evidence is in favour of caveolins which play a dual role by promoting the invasiveness of cancer cells to acquire the features of advanced cancer (Williams et al., 2005, Liscovitch, 2005) and also regulate the function of a specialized cytoskeleton-membrane link that involves integrins, extracellular membrane receptors and initiators of adhesion complex formation (Wary et al., 1996, Upla et al., 2004, Ning et al., 2007). The over expression of caveolin-1 in muscle cells negatively affect their ability to differentiate to multinucleated myotubes without promoting cell death (Volonte et al., 2005) resulting in a disordered and senescent phenotype (Volonte et al., 2005). When there is any insult or injury to muscle, the satellite cells get activated, and then undergo differentiation to restore the integrity of the muscle. In order to restore the pool of satellite cells, few of them escape differentiation and undergo self-renewal (Volonte et

al., 2005). Muscle injury is not the only stimulus but also stretch, exercise and muscle hypertrophy all act as stimulators for the activation of satellite cells (Schultz and McCormick, 1994, Snow, 1990, Winchester et al., 1991). This is, in turn, supported by the findings from a study on pregnant rat myometrium, showing gradual and abundant increase in caveolin expression throughout the pregnancy (Turi et al., 2001) in response to the stretching and expansion of pregnant myometrium.

These findings may be relevant and correlate the possible influence of caveolin in the aetiopathology of adenomyosis during the reproductive period of such women, during which the junctional zone (EMI) gets disturbed or injured either directly or indirectly by dysfunctional uterine hyper-peristalsis or contractility (Parrott et al., 2001, Kunz et al., 2000), mechanical damage by sharp curettage during miscarriage (Leyendecker et al., 2002), uterus with frequent trophoblast invasion as the result of multiparity (Lee et al., 1984). There is evidence in the literature where the over expression of caveolins during muscle regeneration negatively affected their ability to differentiate into multinucleated myotubes (Volonte et al., 2005) resulting in a disordered phenotype (Volonte et al., 2005). In the above situation within myometrium, the altered regulation of caveolin might result in an altered myometrial phenotype that is more vulnerable to stromal cell invasion from the overlying endometrium. Since adenomyosis is not seen in all women of reproductive age, it is reasonable to assume that there might be some other caveolin-mediated or co-ordinated mechanism that might play a significant role in the aetiopathology of adenomyosis.

A previous observation by our research group showed that wnt5a mRNA was consistently down regulated in adenomyosis, both in the secretory and the proliferative phases of the menstrual cycle. Wnt5a is a conserved homologue of Wingless, a key

regulator of *Drosophila melanogaster* embryonic segmentation and patterning (Mericskay et al., 2004). The Wnt gene family proteins are critical regulators of cell polarity, motility, differentiation, apoptosis, and carcinogenesis, with wnt5a being involved in cell adhesion, motility, and polarity *via* β-catenin/E-cadherin complex (Moon et al., 1993, Pandur et al., 2002). The role of wnt5a as prognostic marker in various cancers has now been established (Dejmek et al., 2005, Blanc et al., 2005, Kremenevskaja et al., 2005) and low expression of β-catenin leads to decreased adherence of cells, resulting in increased invasion of cancer cells (Jonsson and Andersson, 2001). The same principle can be applied for the migration of stromal cells into the underlying myometrium causing adenomyosis.

Additionally, experimental studies have demonstrated that conditional activation of Wnt/β-catenin has profound effects in the uterus, inducing endometrial hyperplasia, myometrial hyperplasia, adenomyosis, and mesenchymal tumours similar to leiomyoma and endometrial stromal sarcomas (Jeong et al., 2009, Tanwar et al., 2009) and other findings in the literature support the influence of wnt proteins on epithelial-mesenchymal transition (EMT) influenced by estrogen resulting in the development of adenomyosis (Oh et al., 2013). The process of EMT involves programmed development of biological cells, characterized by loss of cell adhesion, repression of E-cadherin expression and an increase in cell mobility. The canonical wnt signalling pathway initiates EMT, which in turn triggers the translocation of β-catenin to the nucleus, resulting in the down-regulation of E-cadherin. By inducing EMT, these factors transcriptionally repress epithelial markers (such as E-cadherin) affecting the cell-to-cell adhesion. My findings of increased wnt7a expression in adenomyosis support an argument implicating a role for wnt7a in adenomyosis through EMT activation.

Nonetheless, these phenomena are poorly understood in reproductive biology and need to be examined further.

Since adenomyosis was reported to be the result of disordered stromal cell differentiation (Parrott et al., 2001), it is reasonable to assume in such cases that there will be some effect on decidualisation of stromal cells that could result in disordered blastocyst reception, which is one of the main causes for infertility associated with adenomyosis. But the findings and interpretation from the decidualisation experiments suggest that there is no difference in the timing to decidualisation, nor in morphological features, IGFBP-1 or prolactin expression in stromal cells from women with adenomyosis compared to control stromal cells. This suggests that disordered stromal differentiation is not the main causal event in the pathogenesis of adenomyosis. The slightly enhanced decidualisation effect with respect to IGFBP-1 and prolactin expression may be an indicator of premature decidualisation, which could affect implantation and thus pregnancy success in women with undiagnosed adenomyosis.

Conclusions

The results from my experiments and their interpretation support the key hypotheses set at the beginning of this thesis that the primary aetiopathological signal in uterine adenomyosis is an abnormal development or behaviour of the endometrial-myometrial interface (EMI) and that the pathogenesis of adenomyosis may entail steroid-mediated myometrial penetration by the overlying endometrium. The key factor(s) involved are the differential expression of neurotrophins, caveolins and Wnt signalling pathway proteins in the junctional zone myometrium.

Future directions

The data presented in Chapter 3 (myometrial-stromal cell co-culture) suggest that the interaction between stromal cell and myocytes in the uterus is affected by the presence of either estradiol or tamoxifen with that effect being exacerbated by adenomyosis. The findings in Chapters 4, 5 and 6 showed that the differential expression of nerve growth factor, caveolins and Wnt proteins in adenomyosis is also under the influence of estradiol and tamoxifen. There is further scope here to explore the role of these factors in the aetiopathology of adenomyosis by studying the putative role of individual factors in the myometrial cell by using silencing RNA technology and thereby 'knocking out' each factor sequentially. This could be studied in a series of experiments where primary myometrial cells transfected with siRNA (to the nerve growth factor, the individual caveolin and Wnt family proteins), would be immersed in the collagen matrix and overlaid with stromal cells obtained from uteri of women with or without adenomyosis. After culture for 8-9 days in the presence and absence of steroid, the experimental sets would then be examined for evidence of penetration and invasion of the stromal cells. Transfection of the cells would be achieved by transfecting commercially available siRNA against the individual factors using Fugene6, with appropriate non-transfected and scrambled sequence controls. After transfection, the cells can be treated with a stimulating dose of steroid for an appropriate time, and RNA or protein can be prepared. qRT-PCR and western blotting would be used to study the changes in expression profile of the factors most relevant to the hypothesis.

From Chapter 4, I demonstrated that there was a differential expression of nerve growth factor in adenomyosis and that effect was under the influence of estradiol and

tamoxifen. Although it has been suggested that NGF could be considered a regulator of uterine development and has been involved in uterine re-innervations after pregnancy, the precise role of NGF expression in the uterus remains unclear. The effects of NGF in other tissues are mediated by interactions with specific receptors, such as the low affinity p75^{NTR} receptor and the high affinity TrkA, TrkB, TrKC and NT3/NT4 receptors. Recent evidence strongly suggests that NGF and p75^{NTR} might participate in the regulation of tissue morphogenesis, myogenesis and support non-neural cell systems on their way towards terminal differentiation. So further experiments to explore the role of these receptors and their differential expression in adenomyosis under the influence of steroids might be helpful to carry forward the hypothesis that NGF is a key factor in adenomyosis. (Liscovitch, 2005)

The process of EMT involves programmed development of biological cells, characterized by loss of cell adhesion, repression of E-cadherin expression and an increase in cell mobility. One of the signals initiating an EMT is the canonical Wnt signalling pathway. Further experiments to explore the regulation of APC and β-catenin in adenomyosis will help us to learn more about the role of wnt signalling in the human myometrium during the pathogenesis of adenomyosis. The major components of decidualisation were examined in Chapter 7, and seemingly less important components were not tested. For example, the protein WFDC1 is a protease produced in the uterus under the decidualisation process. The function of this protein is to aid trophoblast migration during implantation, and leukaemia inhibitory factor-1 (LIF-1) is known to be essential to the implantation process. The uterus produces both of these during the implantation process and as these were not examined in the present study, they could be in the future

References

ABRAM, M., WEGMANN, M., FOKUHL, V., SONAR, S., LUGER, E. O., KERZEL, S., RADBRUCH, A., RENZ, H. & ZEMLIN, M. 2009. Nerve growth factor and neurotrophin-3 mediate survival of pulmonary plasma cells during the allergic airway inflammation. *J Immunol,* 182**,** 4705-12.

AGRO, A. & STANISZ, A. M. 1993. Inhibition of murine intestinal inflammation by anti-substance P antibody. *Reg Immunol,* 5**,** 120-6.

ALLEN, R. E., SHEEHAN, S. M., TAYLOR, R. G., KENDALL, T. L. & RICE, G. M. 1995. Hepatocyte growth factor activates quiescent skeletal muscle satellite cells in vitro. *J Cell Physiol,* 165**,** 307-12.

ALOE, L. 1988. The effect of nerve growth factor and its antibody on mast cells in vivo. *J Neuroimmunol,* 18**,** 1-12.

ANDERSON, J. E. 2000. A role for nitric oxide in muscle repair: nitric oxide-mediated activation of muscle satellite cells. *Mol Biol Cell,* 11**,** 1859-74.

ARENAS-HERNANDEZ, M. & VEGA-SANCHEZ, R. 2013. Housekeeping gene expression stability in reproductive tissues after mitogen stimulation. *BMC Res Notes,* 6**,** 285.

ARNOLD, J. T., KAUFMAN, D. G., SEPPALA, M. & LESSEY, B. A. 2001. Endometrial stromal cells regulate epithelial cell growth in vitro: a new co-culture model. *Hum Reprod,* 16**,** 836-45.

AZZIZ, R. 1989. Adenomyosis: current perspectives. *Obstet Gynecol Clin North Am,* 16**,** 221-35.

BAGNOLI, M., TOMASSETTI, A., FIGINI, M., FLATI, S., DOLO, V., CANEVARI, S. & MIOTTI, S. 2000. Downmodulation of caveolin-1 expression in human ovarian carcinoma is directly related to alpha-folate receptor overexpression. *Oncogene,* 19**,** 4754-63.

BALEMANS, W. & VAN HUL, W. 2002. Extracellular regulation of BMP signaling in vertebrates: a cocktail of modulators. *Dev Biol,* 250**,** 231-50.

BAZOT, M., CORTEZ, A., DARAI, E., ROUGER, J., CHOPIER, J., ANTOINE, J. M. & UZAN, S. 2001. Ultrasonography compared with magnetic resonance imaging for the diagnosis of adenomyosis: correlation with histopathology. *Hum Reprod,* 16**,** 2427-33.

BEHRENS, J., VON KRIES, J. P., KUHL, M., BRUHN, L., WEDLICH, D., GROSSCHEDL, R. & BIRCHMEIER, W. 1996. Functional interaction of beta-catenin with the transcription factor LEF-1. *Nature,* 382**,** 638-42.

BELLIVEAU, D. J., KRIVKO, I., KOHN, J., LACHANCE, C., POZNIAK, C., RUSAKOV, D., KAPLAN, D. & MILLER, F. D. 1997. NGF and neurotrophin-3 both activate TrkA on sympathetic neurons but differentially regulate survival and neuritogenesis. *J Cell Biol,* 136**,** 375-88.

BENAGIANO, G., HABIBA, M. & BROSENS, I. 2012. The pathophysiology of uterine adenomyosis: an update. *Fertil Steril,* 98**,** 572-9.

BENDER, F. C., REYMOND, M. A., BRON, C. & QUEST, A. F. 2000. Caveolin-1 levels are down-regulated in human colon tumors, and ectopic expression of caveolin-1 in colon carcinoma cell lines reduces cell tumorigenicity. *Cancer Res,* 60**,** 5870-8.

BIELEFELDT, K., OZAKI, N. & GEBHART, G. F. 2003. Role of nerve growth factor in modulation of gastric afferent neurons in the rat. *Am J Physiol Gastrointest Liver Physiol,* 284**,** G499-507.

BIRD, C. C., MCELIN, T. W. & MANALO-ESTRELLA, P. 1972. The elusive adenomyosis of the uterus--revisited. *Am J Obstet Gynecol,* 112**,** 583-93.

BISCHOFF, R. 1997. Chemotaxis of skeletal muscle satellite cells. *Dev Dyn,* 208**,** 505-15.

BISHOP, J. M. 1991. Molecular themes in oncogenesis. *Cell,* 64**,** 235-48.

BLANC, E., ROUX, G. L., BENARD, J. & RAGUENEZ, G. 2005. Low expression of Wnt-5a gene is associated with high-risk neuroblastoma. *Oncogene,* 24**,** 1277-83.

BOHLMAN, M. E., ENSOR, R. E. & SANDERS, R. C. 1987. Sonographic findings in adenomyosis of the uterus. *AJR Am J Roentgenol,* 148**,** 765-6.

BONINI, S., LAMBIASE, A., LAPUCCI, G., PROPERZI, F., BRESCIANI, M., BRACCI LAUDIERO, M. L., MANCINI, M. J., PROCOLI, A., MICERA, A., SACERDOTI, G., LEVI-SCHAFFER, F., RASI, G. & ALOE, L. 2002. Nerve growth factor and asthma. *Allergy,* 57 Suppl 72**,** 13-5.

BROSENS, I. A., ROBERTSON, W. B. & DIXON, H. G. 1972. The role of the spiral arteries in the pathogenesis of preeclampsia. *Obstet Gynecol Annu,* 1**,** 177-91.

BROSENS, J. J., BARKER, F. G. & DE SOUZA, N. M. 1998. Myometrial zonal differentiation and uterine junctional zone hyperplasia in the non-pregnant uterus. *Hum Reprod Update,* 4**,** 496-502.

BROSENS, J. J., DE SOUZA, N. M., BARKER, F. G., PARASCHOS, T. & WINSTON, R. M. 1995. Endovaginal ultrasonography in the diagnosis of adenomyosis uteri: identifying the predictive characteristics. *Br J Obstet Gynaecol,* 102**,** 471-4.

BROSENS, J. J., PIJNENBORG, R. & BROSENS, I. A. 2002. The myometrial junctional zone spiral arteries in normal and abnormal pregnancies: a review of the literature. *Am J Obstet Gynecol,* 187**,** 1416-23.

BROWN, H. K., STOLL, B. S. & NICOSIA, S. V. 1991. Uterine junctional zone: correlation between histologic findings and MR imaging. *Radiology,* 179**,** 409-413.

BULIC, M., KASNAR, V. & DUKOVIC, I. 1986. [Use of ultrasound in the diagnosis of genital endometriosis]. *Jugosl Ginekol Perinatol,* 26**,** 33-4.

BUSTIN, S. A., BEAULIEU, J. F., HUGGETT, J., JAGGI, R., KIBENGE, F. S., OLSVIK, P. A., PENNING, L. C. & TOEGEL, S. 2010. MIQE precis: Practical implementation of minimum standard guidelines for fluorescence-based quantitative real-time PCR experiments. *BMC Mol Biol,* 11**,** 74.

CHEVREL, G., HOHLFELD, R. & SENDTNER, M. 2006. The role of neurotrophins in muscle under physiological and pathological conditions. *Muscle Nerve,* 33**,** 462-76.

CLARK, R.A.C. 1988. Chapter 1. Overview and general considerations of wound repair. Clark, R.A.C. and Henson, P.M. eds. In: *The Molecular and Cellular Biology of Wound Repair*, Plenum Press, New York, USA, pp. 3-34.

CLEVERS, H. 2006. Wnt/beta-catenin signaling in development and disease. *Cell,* 127**,** 469-80.

COHEN, I., BEYTH, Y., SHAPIRA, J., TEPPER, R., FISHMAN, A., CORDOBA, M., BERNHEIM, J., YIGAEL, D. & ALTARAS, M. M. 1997. High frequency of adenomyosis in postmenopausal breast cancer patients treated with tamoxifen. *Gynecol Obstet Invest,* 44**,** 200-5.

COHEN, I., BEYTH, Y., TEPPER, R., FIGER, A., SHAPIRA, J., CORDOBA, M., YIGAEL, D. & ALTARAS, M. M. 1995. Adenomyosis in postmenopausal breast cancer patients treated with tamoxifen: a new entity? *Gynecol Oncol,* 58**,** 86-91.

COHEN, M. & BISCHOF, P. 2009. Coculture of decidua and trophoblast to study proliferation and invasion. *Methods Mol Biol,* 550**,** 63-72.

COUET, J., BELANGER, M. M., ROUSSEL, E. & DROLET, M. C. 2001. Cell biology of caveolae and caveolin. *Adv Drug Deliv Rev,* 49**,** 223-35.

DARRIBERE, T. & SCHWARZBAUER, J. E. 2000. Fibronectin matrix composition and organization can regulate cell migration during amphibian development. *Mech Dev,* 92**,** 239-50.

DAS, K., LEWIS, R. Y., SCHERER, P. E. & LISANTI, M. P. 1999. The membrane-spanning domains of caveolins-1 and -2 mediate the formation of caveolin hetero-oligomers. Implications for the assembly of caveolae membranes in vivo. *J Biol Chem,* 274**,** 18721-8.

DAUGHERTY, R. L. & GOTTARDI, C. J. 2007. Phospho-regulation of Beta-catenin adhesion and signaling functions. *Physiology (Bethesda),* 22**,** 303-9.

DEJMEK, J., DEJMEK, A., SAFHOLM, A., SJOLANDER, A. & ANDERSSON, T. 2005. Wnt-5a protein expression in primary dukes B colon cancers identifies a subgroup of patients with good prognosis. *Cancer Res,* 65**,** 9142-6.

DEJMEK, J., SAFHOLM, A., KAMP NIELSEN, C., ANDERSSON, T. & LEANDERSSON, K. 2006. Wnt-5a/Ca2+-induced NFAT activity is counteracted by Wnt-5a/Yes-Cdc42-casein kinase 1alpha signaling in human mammary epithelial cells. *Mol Cell Biol,* 26**,** 6024-36.

DEPONTI, D., BUONO, R., CATANZARO, G., DE PALMA, C., LONGHI, R., MENEVERI, R., BRESOLIN, N., BASSI, M. T., COSSU, G., CLEMENTI, E. & BRUNELLI, S. 2009. The low-affinity receptor for neurotrophins p75NTR plays a key role for satellite cell function in muscle repair acting via RhoA. *Mol Biol Cell,* 20**,** 3620-7.

DISSEN, G. A., HILL, D. F., COSTA, M. E., MA, Y. J. & OJEDA, S. R. 1991. Nerve growth factor receptors in the peripubertal rat ovary. *Mol Endocrinol,* 5**,** 1642-50.

DREES, F., POKUTTA, S., YAMADA, S., NELSON, W. J. & WEIS, W. I. 2005. Alpha-catenin is a molecular switch that binds E-cadherin-beta-catenin and regulates actin-filament assembly. *Cell,* 123**,** 903-15.

EMGE, L. A. 1962. The elusive adenomyosis of the uterus. Its historical past and its present state of recognition. *Am J Obstet Gynecol,* 83**,** 1541-63.

ERCK, C., MEISINGER, C., GROTHE, C. & SEIDL, K. 1998. Regulation of nerve growth factor and its low-affinity receptor (p75NTR) during myogenic differentiation. *J Cell Physiol,* 176**,** 22-31.

ERNFORS, P., WETMORE, C., ERIKSDOTTER-NILSSON, M., BYGDEMAN, M., STROMBERG, I., OLSON, L. & PERSSON, H. 1991. The nerve growth factor receptor gene is expressed in both neuronal and non-neuronal tissues in the human fetus. *Int J Dev Neurosci,* 9**,** 57-66.

EVANS, S., MOALEM-TAYLOR, G. & TRACEY, D. J. 2007. Pain and endometriosis. *Pain,* 132 Suppl 1**,** S22-5.

EZAKI, K., MOTOYAMA, H. & SASAKI, H. 2001. Immunohistologic localization of estrone sulfatase in uterine endometrium and adenomyosis. *Obstet Gynecol,* 98**,** 815-9.

FERENCZY, A. 1998. Pathophysiology of adenomyosis. *Hum Reprod Update,* 4**,** 312-22.

FERENCZY, A. & BERGERON, C. 1991. Histology of the human endometrium: from birth to senescence. *Ann N Y Acad Sci,* 622**,** 6-27.

FRANCO, H. L., DAI, D., LEE, K. Y., RUBEL, C. A., ROOP, D., BOERBOOM, D., JEONG, J. W., LYDON, J. P., BAGCHI, I. C., BAGCHI, M. K. & DEMAYO, F. J. WNT4 is a key regulator of normal postnatal uterine development and progesterone signaling during embryo implantation and decidualization in the mouse. *FASEB J,* 25**,** 1176-87.

FRANCO, H. L., DAI, D., LEE, K. Y., RUBEL, C. A., ROOP, D., BOERBOOM, D., JEONG, J. W., LYDON, J. P., BAGCHI, I. C., BAGCHI, M. K. & DEMAYO, F. J. 2011. WNT4 is a key regulator of normal postnatal uterine development and progesterone signaling during embryo implantation and decidualization in the mouse. *FASEB J,* 25**,** 1176-87.

FRANK, G. R., BRAR, A. K., CEDARS, M. I. & HANDWERGER, S. 1994. Prostaglandin E2 enhances human endometrial stromal cell differentiation. *Endocrinology,* 134**,** 258-63.

FRIXEN, U. H., BEHRENS, J., SACHS, M., EBERLE, G., VOSS, B., WARDA, A., LOCHNER, D. & BIRCHMEIER, W. 1991. E-cadherin-mediated cell-cell adhesion prevents invasiveness of human carcinoma cells. *J Cell Biol,* 113**,** 173-85.

FUKAMATSU, Y., TSUKAHARA, Y. & FUKUTA, T. 1984. A clinicopathologic study on adenomyosis uteri. *Nippon Sanka Fujinka Gakkai Zasshi,* 36**,** 431-6.

GELLERSEN, B. & BROSENS, J. 2003. Cyclic AMP and progesterone receptor cross-talk in human endometrium: a decidualizing affair. *J Endocrinol,* 178**,** 357-72.

GOLDBERGER, M. A., MARSHAK, R. H. & HERMEL, M. 1949. Roentgen diagnosis of adenomyosis uteri. *Am J Obstet Gynecol,* 57**,** 563-8.

GORSKI, J., WELSHONS, W. & SAKAI, D. 1984. Remodeling the estrogen receptor model. *Mol Cell Endocrinol,* 36**,** 11-5.

GREAVES, P. & WHITE, I. N. 2006. Experimental adenomyosis. *Best Pract Res Clin Obstet Gynaecol,* 20**,** 503-10.

GRIGORYAN, T., WEND, P., KLAUS, A. & BIRCHMEIER, W. 2008. Deciphering the function of canonical Wnt signals in development and disease: conditional loss- and gain-of-function mutations of beta-catenin in mice. *Genes Dev,* 22**,** 2308-41.

GUMBINER, B. M. 1996. Cell adhesion: the molecular basis of tissue architecture and morphogenesis. *Cell,* 84**,** 345-57.

HAASE, E. B., BUCHMAN, J., TIETZ, A. E. & SCHRAMM, L. P. 1997. Pregnancy-induced uterine neuronal degeneration in the rat. *Cell Tissue Res,* 288**,** 293-306.

HALL, J. B., YOUNG, R. H. & NELSON, J. H., JR. 1984. The prognostic significance of adenomyosis in endometrial carcinoma. *Gynecol Oncol,* 17**,** 32-40.

HAUTH, E. A., JAEGER, H. J., LIBERA, H., LANGE, S. & FORSTING, M. 2007. MR imaging of the uterus and cervix in healthy women: determination of normal values. *Eur Radiol,* 17**,** 734-42.

HEVER, A., ROTH, R. B., HEVEZI, P. A., LEE, J., WILLHITE, D., WHITE, E. C., MARIN, E. M., HERRERA, R., ACOSTA, H. M., ACOSTA, A. J. & ZLOTNIK, A. 2006. Molecular characterization of human adenomyosis. *Mol Hum Reprod,* 12**,** 737-48.

HUANG, H. Y., YU, H. T., CHAN, S. H., LEE, C. L., WANG, H. S. & SOONG, Y. K. Eutopic endometrial interleukin-18 system mRNA and protein expression at the level of endometrial-myometrial interface in adenomyosis patients. *Fertil Steril,* 94**,** 33-9.

HUANG, H. Y., YU, H. T., CHAN, S. H., LEE, C. L., WANG, H. S. & SOONG, Y. K. 2010. Eutopic endometrial interleukin-18 system mRNA and protein expression at the level of endometrial-myometrial interface in adenomyosis patients. *Fertil Steril,* 94**,** 33-9.

HUARD, J., VERREAULT, S., ROY, R., TREMBLAY, M. & TREMBLAY, J. P. 1994. High efficiency of muscle regeneration after human myoblast clone transplantation in SCID mice. *J Clin Invest,* 93**,** 586-99.

HUELSKEN, J. & BEHRENS, J. 2002. The Wnt signalling pathway. *J Cell Sci,* 115**,** 3977-8.

IP, F. C., CHEUNG, J. & IP, N. Y. 2001. The expression profiles of neurotrophins and their receptors in rat and chicken tissues during development. *Neurosci Lett,* 301**,** 107-10.

IZUMI, T., SHIBATA, Y. & YAMAMOTO, T. 1988. Striped structures on the cytoplasmic surface membranes of the endothelial vesicles of the rat aorta revealed by quick-freeze, deep-etching replicas. *Anat Rec,* 220**,** 225-32.

JEONG, J. W., LEE, H. S., FRANCO, H. L., BROADDUS, R. R., TAKETO, M. M., TSAI, S. Y., LYDON, J. P. & DEMAYO, F. J. 2009. beta-catenin mediates glandular formation and dysregulation of beta-catenin induces hyperplasia formation in the murine uterus. *Oncogene,* 28**,** 31-40.

JONES, J. L., ROYALL, J. E., CRITCHLEY, D. R. & WALKER, R. A. 1997. Modulation of myoepithelial-associated alpha6beta4 integrin in a breast cancer cell line alters invasive potential. *Exp Cell Res,* 235**,** 325-33.

JONES, J. L., SHAW, J. A., PRINGLE, J. H. & WALKER, R. A. 2003. Primary breast myoepithelial cells exert an invasion-suppressor effect on breast cancer cells via paracrine down-regulation of MMP expression in fibroblasts and tumour cells. *J Pathol,* 201**,** 562-72.

JONES, R. L., FINDLAY, J. K. & SALAMONSEN, L. A. 2006. The role of activins during decidualisation of human endometrium. *Aust N Z J Obstet Gynaecol,* 46**,** 245-9.

JONSSON, M. & ANDERSSON, T. 2001. Repression of Wnt-5a impairs DDR1 phosphorylation and modifies adhesion and migration of mammary cells. *J Cell Sci,* 114**,** 2043-53.

KADISH, I. & VAN GROEN, T. 2002. Low levels of estrogen significantly diminish axonal sprouting after entorhinal cortex lesions in the mouse. *J Neurosci,* 22**,** 4095-102.

KILKKU, P., ERKKOLA, R. & GRONROOS, M. 1984. Non-specificity of symptoms related to adenomyosis. A prospective comparative survey. *Acta Obstet Gynecol Scand,* 63**,** 229-31.

KIM, H. P., LEE, J. Y., JEONG, J. K., BAE, S. W., LEE, H. K. & JO, I. 1999. Nongenomic stimulation of nitric oxide release by estrogen is mediated by estrogen receptor alpha localized in caveolae. *Biochem Biophys Res Commun,* 263**,** 257-62.

KING, K. L. & CIDLOWSKI, J. A. 1998. Cell cycle regulation and apoptosis. *Annu Rev Physiol,* 60**,** 601-17.

KISS, A. L., TURI, A., MULLNER, N., KOVACS, E., BOTOS, E. & GREGER, A. 2005. Oestrogen-mediated tyrosine phosphorylation of caveolin-1 and its effect on the oestrogen receptor localisation: an in vivo study. *Mol Cell Endocrinol,* 245**,** 128-37.

KITAWAKI, J. 2006. Adenomyosis: the pathophysiology of an oestrogen-dependent disease. *Best Pract Res Clin Obstet Gynaecol,* 20**,** 493-502.

KREMENEVSKAJA, N., VON WASIELEWSKI, R., RAO, A. S., SCHOFL, C., ANDERSSON, T. & BRABANT, G. 2005. Wnt-5a has tumor suppressor activity in thyroid carcinoma. *Oncogene,* 24**,** 2144-54.

KUNZ, G., BEIL, D., DEININGER, H., WILDT, L. & LEYENDECKER, G. 1996. The dynamics of rapid sperm transport through the female genital tract: evidence from vaginal sonography of uterine peristalsis and hysterosalpingoscintigraphy. *Hum Reprod,* 11**,** 627-32.

KUNZ, G., BEIL, D., HUPPERT, P. & LEYENDECKER, G. 2000. Structural abnormalities of the uterine wall in women with endometriosis and infertility

visualized by vaginal sonography and magnetic resonance imaging. *Hum Reprod,* 15**,** 76-82.

KUST, B. M., COPRAY, J. C., BROUWER, N., TROOST, D. & BODDEKE, H. W. 2002. Elevated levels of neurotrophins in human biceps brachii tissue of amyotrophic lateral sclerosis. *Exp Neurol,* 177**,** 419-27.

LEE, J. K., GERSELL, D. J., BALFE, D. M., WORTHINGTON, J. L., PICUS, D. & GAPP, G. 1985. The uterus: in vitro MR-anatomic correlation of normal and abnormal specimens. *Radiology,* 157**,** 175-9.

LEE, N. C., DICKER, R. C., RUBIN, G. L. & ORY, H. W. 1984. Confirmation of the preoperative diagnoses for hysterectomy. *Am J Obstet Gynecol,* 150**,** 283-7.

LEVGUR, M., ABADI, M. A. & TUCKER, A. 2000. Adenomyosis: symptoms, histology, and pregnancy terminations. *Obstet Gynecol,* 95**,** 688-91.

LEVI-MONTALCINI, R. 1987. The nerve growth factor 35 years later. *Science,* 237**,** 1154-62.

LEWIN, G. R., RUEFF, A. & MENDELL, L. M. 1994. Peripheral and central mechanisms of NGF-induced hyperalgesia. *Eur J Neurosci,* 6**,** 1903-12.

LEYENDECKER, G., HERBERTZ, M., KUNZ, G. & MALL, G. 2002. Endometriosis results from the dislocation of basal endometrium. *Hum Reprod,* 17**,** 2725-36.

LEYENDECKER, G., KUNZ, G., WILDT, L., BEIL, D. & DEININGER, H. 1996. Uterine hyperperistalsis and dysperistalsis as dysfunctions of the mechanism of rapid sperm transport in patients with endometriosis and infertility. *Hum Reprod,* 11**,** 1542-51.

LI Y, Z. S., XIAN X, ZOU S 2010. Adenomyosis uterine innervation in mice correlates to nerve growth factor expression, inflammation, and vascularization. *Neural Regen Res,* 5**,** 15-20.

LISANTI, M. P., SCHERER, P. E., VIDUGIRIENE, J., TANG, Z., HERMANOWSKI-VOSATKA, A., TU, Y. H., COOK, R. F. & SARGIACOMO, M. 1994. Characterization of caveolin-rich membrane domains isolated from an endothelial-rich source: implications for human disease. *J Cell Biol,* 126**,** 111-26.

LISCOVITCH, M., E. BURGERMEISTER, N. JAIN, D. RAVID, M. SHATZ, L.TENCER, 2005. Caveolin and cancer: a complex relationship. *M.P.Mattson (Ed.), Membrane Microdomain Signaling: Lipid Rafts in Biology and Medicine***,** pp. 161–190.

LOGAN, C. Y. & NUSSE, R. 2004. The Wnt signaling pathway in development and disease. *Annu Rev Cell Dev Biol,* 20**,** 781-810.

LOSEL, R. & WEHLING, M. 2003. Nongenomic actions of steroid hormones. *Nat Rev Mol Cell Biol,* 4**,** 46-56.

LU, Z., GHOSH, S., WANG, Z. & HUNTER, T. 2003. Downregulation of caveolin-1 function by EGF leads to the loss of E-cadherin, increased transcriptional activity of beta-catenin, and enhanced tumor cell invasion. *Cancer Cell,* 4**,** 499-515.

LYONS, E. A., GRATTON, D. & HARRINGTON, C. 1992. Transvaginal sonography of normal pelvic anatomy. *Radiol Clin North Am,* 30**,** 663-75.

MAMET, J., BARON, A., LAZDUNSKI, M. & VOILLEY, N. 2002. Proinflammatory mediators, stimulators of sensory neuron excitability via the expression of acid-sensing ion channels. *J Neurosci,* 22**,** 10662-70.

MARWAN HABIBA, G. B. 2016. Uterine Adenomyosis. *Book,* Chapter 3 The Pathophysiology of Adenomyosis**,** 46-47.

MCCAUSLAND, A. M. 1992. Hysteroscopic myometrial biopsy: its use in diagnosing adenomyosis and its clinical application. *Am J Obstet Gynecol,* 166**,** 1619-26; discussion 1626-8.

MCEWEN, B. 2002. Estrogen actions throughout the brain. *Recent Prog Horm Res,* 57**,** 357-84.

MEHASSEB, M. 2010. Pathogenesis of Uterine adenomyosis. *PHD Thesis, Univerisity of Leicester*.

MEHASSEB, M. K., BELL, S. C., BROWN, L., PRINGLE, J. H. & HABIBA, M. 2011a. Phenotypic characterisation of the inner and outer myometrium in normal and adenomyotic uteri. *Gynecol Obstet Invest,* 71**,** 217-24.

MEHASSEB, M. K., BELL, S. C. & HABIBA, M. A. 2009. The effects of tamoxifen and estradiol on myometrial differentiation and organization during early uterine development in the CD1 mouse. *Reproduction,* 138**,** 341-50.

MEHASSEB, M. K., BELL, S. C. & HABIBA, M. A. 2010a. Neonatal administration of tamoxifen causes disruption of myometrial development but not adenomyosis in the C57/BL6J mouse. *Reproduction,* 139**,** 1067-75.

MEHASSEB, M. K., PANCHAL, R., TAYLOR, A. H., BROWN, L., BELL, S. C. & HABIBA, M. 2011b. Estrogen and progesterone receptor isoform distribution through the menstrual cycle in uteri with and without adenomyosis. *Fertil Steril,* 95**,** 2228-35, 2235 e1.

MEHASSEB, M. K., TAYLOR, A. H., PRINGLE, J. H., BELL, S. C. & HABIBA, M. 2010b. Enhanced invasion of stromal cells from adenomyosis in a three-dimensional coculture model is augmented by the presence of myocytes from affected uteri. *Fertil Steril,* 94**,** 2547-51.

MENDELL, L. M., ALBERS, K. M. & DAVIS, B. M. 1999. Neurotrophins, nociceptors, and pain. *Microsc Res Tech,* 45**,** 252-61.

MENETREY, J., KASEMKIJWATTANA, C., DAY, C. S., BOSCH, P., VOGT, M., FU, F. H., MORELAND, M. S. & HUARD, J. 2000. Growth factors improve muscle healing in vivo. *J Bone Joint Surg Br,* 82**,** 131-7.

MERICSKAY, M., KITAJEWSKI, J. & SASSOON, D. 2004. Wnt5a is required for proper epithelial-mesenchymal interactions in the uterus. *Development,* 131**,** 2061-72.

MILLER, C., PAVLOVA, A. & SASSOON, D. A. 1998. Differential expression patterns of Wnt genes in the murine female reproductive tract during development and the estrous cycle. *Mech Dev,* 76**,** 91-9.

MILLER, C. & SASSOON, D. A. 1998. Wnt-7a maintains appropriate uterine patterning during the development of the mouse female reproductive tract. *Development,* 125**,** 3201-11.

MIYAMOTO, S., KATZ, B. Z., LAFRENIE, R. M. & YAMADA, K. M. 1998. Fibronectin and integrins in cell adhesion, signaling, and morphogenesis. *Ann N Y Acad Sci,* 857**,** 119-29.

MOON, R. T., CAMPBELL, R. M., CHRISTIAN, J. L., MCGREW, L. L., SHIH, J. & FRASER, S. 1993. Xwnt-5A: a maternal Wnt that affects morphogenetic movements after overexpression in embryos of Xenopus laevis. *Development,* 119**,** 97-111.

MORENO-BUENO, G., HARDISSON, D., SANCHEZ, C., SARRIO, D., CASSIA, R., GARCIA-ROSTAN, G., PRAT, J., GUO, M., HERMAN, J. G., MATIAS-GUIU, X., ESTELLER, M. & PALACIOS, J. 2002. Abnormalities of the APC/beta-catenin pathway in endometrial cancer. *Oncogene,* 21**,** 7981-90.

MORIN, P. J., SPARKS, A. B., KORINEK, V., BARKER, N., CLEVERS, H., VOGELSTEIN, B. & KINZLER, K. W. 1997. Activation of beta-catenin-Tcf signaling in colon cancer by mutations in beta-catenin or APC. *Science,* 275**,** 1787-90.

MUNDY, D. I., MACHLEIDT, T., YING, Y. S., ANDERSON, R. G. & BLOOM, G. S. 2002. Dual control of caveolar membrane traffic by microtubules and the actin cytoskeleton. *J Cell Sci,* 115**,** 4327-39.

NAKAMURA, Y., NISHISHO, I., KINZLER, K. W., VOGELSTEIN, B., MIYOSHI, Y., MIKI, Y., ANDO, H., HORII, A. & NAGASE, H. 1991. Mutations of the adenomatous polyposis coli gene in familial polyposis coli patients and sporadic colorectal tumors. *Princess Takamatsu Symp,* 22**,** 285-92.

NING, Y., BURANDA, T. & HUDSON, L. G. 2007. Activated epidermal growth factor receptor induces integrin alpha2 internalization via caveolae/raft-dependent endocytic pathway. *J Biol Chem,* 282**,** 6380-7.

NISHIDA, M. 1991. Relationship between the onset of dysmenorrhea and histologic findings in adenomyosis. *Am J Obstet Gynecol,* 165**,** 229-31.

NISHISHO, I., NAKAMURA, Y., MIYOSHI, Y., MIKI, Y., ANDO, H., HORII, A., KOYAMA, K., UTSUNOMIYA, J., BABA, S. & HEDGE, P. 1991. Mutations of chromosome 5q21 genes in FAP and colorectal cancer patients. *Science,* 253**,** 665-9.

NORFLEET, A. M., THOMAS, M. L., GAMETCHU, B. & WATSON, C. S. 1999. Estrogen receptor-alpha detected on the plasma membrane of aldehyde-fixed GH3/B6/F10 rat pituitary tumor cells by enzyme-linked immunocytochemistry. *Endocrinology,* 140**,** 3805-14.

NOYES, R. W., HERTIG, A. T. & ROCK, J. 1975. Dating the endometrial biopsy. *Am J Obstet Gynecol,* 122**,** 262-3.

NUSSE, R. & VARMUS, H. E. 1982. Many tumors induced by the mouse mammary tumor virus contain a provirus integrated in the same region of the host genome. *Cell,* 31**,** 99-109.

OH, S. J., SHIN, J. H., KIM, T. H., LEE, H. S., YOO, J. Y., AHN, J. Y., BROADDUS, R. R., TAKETO, M. M., LYDON, J. P., LEACH, R. E., LESSEY, B. A., FAZLEABAS, A. T., LIM, J. M. & JEONG, J. W. 2013. beta-Catenin activation contributes to the pathogenesis of adenomyosis through epithelial-mesenchymal transition. *J Pathol,* 231**,** 210-22.

OHIRA, T., GEMMILL, R. M., FERGUSON, K., KUSY, S., ROCHE, J., BRAMBILLA, E., ZENG, C., BARON, A., BEMIS, L., ERICKSON, P., WILDER, E., RUSTGI, A., KITAJEWSKI, J., GABRIELSON, E., BREMNES, R., FRANKLIN, W. & DRABKIN, H. A. 2003. WNT7a induces E-cadherin in lung cancer cells. *Proc Natl Acad Sci U S A,* 100**,** 10429-34.

ORTEGREN, U., ABOULAICH, N., OST, A. & STRALFORS, P. 2007. A new role for caveolae as metabolic platforms. *Trends Endocrinol Metab,* 18**,** 344-9.

OTA, H., IGARASHI, S., HATAZAWA, J. & TANAKA, T. 1998. Is adenomyosis an immune disease? *Hum Reprod Update,* 4**,** 360-7.

PANDUR, P., MAURUS, D. & KUHL, M. 2002. Increasingly complex: new players enter the Wnt signaling network. *Bioessays,* 24**,** 881-4.

PARKER, M. H., SEALE, P. & RUDNICKI, M. A. 2003. Looking back to the embryo: defining transcriptional networks in adult myogenesis. *Nat Rev Genet,* 4**,** 497-507.

PARROTT, E., BUTTERWORTH, M., GREEN, A., WHITE, I. N. & GREAVES, P. 2001. Adenomyosis--a result of disordered stromal differentiation. *Am J Pathol,* 159**,** 623-30.

PARTON, R. G. & SIMONS, K. 2007. The multiple faces of caveolae. *Nat Rev Mol Cell Biol,* 8**,** 185-94.

PATEL, H. H., MURRAY, F. & INSEL, P. A. 2008. Caveolae as organizers of pharmacologically relevant signal transduction molecules. *Annu Rev Pharmacol Toxicol,* 48**,** 359-91.

PERL, A. K., WILGENBUS, P., DAHL, U., SEMB, H. & CHRISTOFORI, G. 1998. A causal role for E-cadherin in the transition from adenoma to carcinoma. *Nature,* 392**,** 190-3.

PERSSON, H., AYER-LE LIEVRE, C., SODER, O., VILLAR, M. J., METSIS, M., OLSON, L., RITZEN, M. & HOKFELT, T. 1990. Expression of beta-nerve growth factor receptor mRNA in Sertoli cells downregulated by testosterone. *Science,* 247**,** 704-7.

PFAFFL, M. W. 2001. A new mathematical model for relative quantification in real-time RT-PCR. *Nucleic Acids Res,* 29**,** e45.

RASK, K., NILSSON, A., BRANNSTROM, M., CARLSSON, P., HELLBERG, P., JANSON, P. O., HEDIN, L. & SUNDFELDT, K. 2003. Wnt-signalling pathway in ovarian epithelial tumours: increased expression of beta-catenin and GSK3beta. *Br J Cancer,* 89**,** 1298-304.

RAZANI, B., WOODMAN, S. E. & LISANTI, M. P. 2002. Caveolae: from cell biology to animal physiology. *Pharmacol Rev,* 54**,** 431-67.

RENDE, M., BRIZI, E., CONNER, J., TREVES, S., CENSIER, K., PROVENZANO, C., TAGLIALATELA, G., SANNA, P. P. & DONATO, R. 2000. Nerve growth factor (NGF) influences differentiation and proliferation of myogenic cells in vitro via TrKA. *Int J Dev Neurosci,* 18**,** 869-85.

RUSSO, M. A., ODORISIO, T., FRADEANI, A., RIENZI, L., DE FELICI, M., CATTANEO, A. & SIRACUSA, G. 1994. Low-affinity nerve growth factor receptor is expressed during testicular morphogenesis and in germ cells at specific stages of spermatogenesis. *Mol Reprod Dev,* 37**,** 157-66.

SAEGUSA, M., HASHIMURA, M., YOSHIDA, T. & OKAYASU, I. 2001. beta-Catenin mutations and aberrant nuclear expression during endometrial tumorigenesis. *Br J Cancer,* 84**,** 209-17.

SALAMONSEN, L. A., DIMITRIADIS, E., JONES, R. L. & NIE, G. 2003. Complex regulation of decidualization: a role for cytokines and proteases--a review. *Placenta,* 24 Suppl A**,** S76-85.

SAMMOUR, A., PIRWANY, I., USUBUTUN, A., ARSENEAU, J. & TULANDI, T. 2002. Correlations between extent and spread of adenomyosis and clinical symptoms. *Gynecol Obstet Invest,* 54**,** 213-6.

SCHERER, P. E., OKAMOTO, T., CHUN, M., NISHIMOTO, I., LODISH, H. F. & LISANTI, M. P. 1996. Identification, sequence, and expression of caveolin-2 defines a caveolin gene family. *Proc Natl Acad Sci U S A,* 93**,** 131-5.

SCHERER, P. E., TANG, Z., CHUN, M., SARGIACOMO, M., LODISH, H. F. & LISANTI, M. P. 1995. Caveolin isoforms differ in their N-terminal protein sequence and subcellular distribution. Identification and epitope mapping of an isoform-specific monoclonal antibody probe. *J Biol Chem,* 270**,** 16395-401.

SCHMALBRUCH, H. & LEWIS, D. M. 2000. Dynamics of nuclei of muscle fibers and connective tissue cells in normal and denervated rat muscles. *Muscle Nerve,* 23**,** 617-26.

SCHOLTEN, A. N., CREUTZBERG, C. L., VAN DEN BROEK, L. J., NOORDIJK, E. M. & SMIT, V. T. 2003. Nuclear beta-catenin is a molecular feature of type I endometrial carcinoma. *J Pathol,* 201**,** 460-5.

SCHULTZ, E. & MCCORMICK, K. M. 1994. Skeletal muscle satellite cells. *Rev Physiol Biochem Pharmacol,* 123**,** 213-57.

SEIDL, K., ERCK, C. & BUCHBERGER, A. 1998. Evidence for the participation of nerve growth factor and its low-affinity receptor (p75NTR) in the regulation of the myogenic program. *J Cell Physiol,* 176**,** 10-21.

SHIMIZU, H., JULIUS, M. A., GIARRE, M., ZHENG, Z., BROWN, A. M. & KITAJEWSKI, J. 1997. Transformation by Wnt family proteins correlates with regulation of beta-catenin. *Cell Growth Differ,* 8**,** 1349-58.

SNIDER, W. D. 1994. Functions of the neurotrophins during nervous system development: what the knockouts are teaching us. *Cell,* 77**,** 627-38.

SNOW, M. H. 1990. Satellite cell response in rat soleus muscle undergoing hypertrophy due to surgical ablation of synergists. *Anat Rec,* 227**,** 437-46.

SOTTILE, J. & CHANDLER, J. 2005. Fibronectin matrix turnover occurs through a caveolin-1-dependent process. *Mol Biol Cell,* 16**,** 757-68.

SOTTILE, J. & HOCKING, D. C. 2002. Fibronectin polymerization regulates the composition and stability of extracellular matrix fibrils and cell-matrix adhesions. *Mol Biol Cell,* 13**,** 3546-59.

SPARKS, A. B., MORIN, P. J., VOGELSTEIN, B. & KINZLER, K. W. 1998. Mutational analysis of the APC/beta-catenin/Tcf pathway in colorectal cancer. *Cancer Res,* 58**,** 1130-4.

STANFORDEDU 1997. Wnt Target Genes. *Wnt Home page:* http://web.stanford.edu/~rnusse/pathways/targets.html.

STREULI, C. 1999. Extracellular matrix remodelling and cellular differentiation. *Curr Opin Cell Biol,* 11**,** 634-40.

TAJBAKHSH, S. 2003. Stem cells to tissue: molecular, cellular and anatomical heterogeneity in skeletal muscle. *Curr Opin Genet Dev,* 13**,** 413-22.

TAMAYA, T., MOTOYAMA, T., OHONO, Y., IDE, N., TSURUSAKI, T. & OKADA, H. 1979. Steroid receptor levels and histology of endometriosis and adenomyosis. *Fertil Steril,* 31**,** 396-400.

TANG, B. & GURPIDE, E. 1993. Direct effect of gonadotropins on decidualization of human endometrial stroma cells. *J Steroid Biochem Mol Biol,* 47**,** 115-21.

TANG, Z., SCHERER, P. E., OKAMOTO, T., SONG, K., CHU, C., KOHTZ, D. S., NISHIMOTO, I., LODISH, H. F. & LISANTI, M. P. 1996. Molecular cloning of caveolin-3, a novel member of the caveolin gene family expressed predominantly in muscle. *J Biol Chem,* 271**,** 2255-61.

TANWAR, P. S., LEE, H. J., ZHANG, L., ZUKERBERG, L. R., TAKETO, M. M., RUEDA, B. R. & TEIXEIRA, J. M. 2009. Constitutive activation of Beta-catenin in uterine stroma and smooth muscle leads to the development of mesenchymal tumors in mice. *Biol Reprod,* 81**,** 545-52.

TATSUMI, R., ANDERSON, J. E., NEVORET, C. J., HALEVY, O. & ALLEN, R. E. 1998. HGF/SF is present in normal adult skeletal muscle and is capable of activating satellite cells. *Dev Biol,* 194**,** 114-28.

TOKUSHIGE, N., MARKHAM, R., RUSSELL, P. & FRASER, I. S. 2006. High density of small nerve fibres in the functional layer of the endometrium in women with endometriosis. *Hum Reprod,* 21**,** 782-7.

TOTI, P., VILLANOVA, M., VATTI, R., SCHUERFELD, K., STUMPO, M., BARBAGLI, L., MALANDRINI, A. & COSTANTINI, M. 2003. Nerve growth factor expression in human dystrophic muscles. *Muscle Nerve,* 27**,** 370-3.

TRUSS, M. & BEATO, M. 1993. Steroid hormone receptors: interaction with deoxyribonucleic acid and transcription factors. *Endocr Rev,* 14**,** 459-79.

TURI, A., KISS, A. L. & MULLNER, N. 2001. Estrogen downregulates the number of caveolae and the level of caveolin in uterine smooth muscle. *Cell Biol Int,* 25**,** 785-94.

UEYAMA, T., HAMADA, M., HANO, T., NISHIO, I., MASUYAMA, Y. & FURUKAWA, S. 1993. Production of nerve growth factor by cultured vascular smooth muscle cells from spontaneously hypertensive and Wistar-Kyoto rats. *J Hypertens,* 11**,** 1061-5.

UPLA, P., MARJOMAKI, V., KANKAANPAA, P., IVASKA, J., HYYPIA, T., VAN DER GOOT, F. G. & HEINO, J. 2004. Clustering induces a lateral redistribution of alpha 2 beta 1 integrin from membrane rafts to caveolae and subsequent protein kinase C-dependent internalization. *Mol Biol Cell,* 15**,** 625-36.

URABE, M., YAMAMOTO, T., KITAWAKI, J., HONJO, H. & OKADA, H. 1989. Estrogen biosynthesis in human uterine adenomyosis. *Acta Endocrinol (Copenh),* 121**,** 259-64.

VAINIO, S., HEIKKILA, M., KISPERT, A., CHIN, N. & MCMAHON, A. P. 1999. Female development in mammals is regulated by Wnt-4 signalling. *Nature,* 397**,** 405-9.

VAROL, F. G., DUCHEMIN, A. M., NEFF, N. H. & HADJICONSTANTINOU, M. 2000. Nerve growth factor (NGF) and NGF mRNA change in rat uterus during pregnancy. *Neurosci Lett,* 294**,** 58-62.

VLEMINCKX, K., VAKAET, L., JR., MAREEL, M., FIERS, W. & VAN ROY, F. 1991. Genetic manipulation of E-cadherin expression by epithelial tumor cells reveals an invasion suppressor role. *Cell,* 66**,** 107-19.

VOGELSTEIN, B., FEARON, E. R., HAMILTON, S. R., KERN, S. E., PREISINGER, A. C., LEPPERT, M., NAKAMURA, Y., WHITE, R., SMITS, A. M. & BOS, J. L. 1988. Genetic alterations during colorectal-tumor development. *N Engl J Med,* 319**,** 525-32.

VOLONTE, D., LIU, Y. & GALBIATI, F. 2005. The modulation of caveolin-1 expression controls satellite cell activation during muscle repair. *FASEB J,* 19**,** 237-9.

VON WOLFF, M., THALER, C. J., STROWITZKI, T., BROOME, J., STOLZ, W. & TABIBZADEH, S. 2000. Regulated expression of cytokines in human endometrium throughout the menstrual cycle: dysregulation in habitual abortion. *Mol Hum Reprod,* 6**,** 627-34.

WANG, F., LI, H., YANG, Z., DU, X., CUI, M. & WEN, Z. 2009. Expression of interleukin-10 in patients with adenomyosis. *Fertil Steril,* 91**,** 1681-5.

WANG, Y., JIA, Y., FRANKEN, P., SMITS, R., EWING, P. C., LYDON, J. P., DEMAYO, F. J., BURGER, C. W., ANTON GROOTEGOED, J., FODDE, R. & BLOK, L. J. 2011. Loss of APC function in mesenchymal cells surrounding the Mullerian duct leads to myometrial defects in adult mice. *Mol Cell Endocrinol,* 341**,** 48-54.

WARY, K. K., MAINIERO, F., ISAKOFF, S. J., MARCANTONIO, E. E. & GIANCOTTI, F. G. 1996. The adaptor protein Shc couples a class of integrins to the control of cell cycle progression. *Cell,* 87**,** 733-43.

WATSON, J. J., ALLEN, S. J. & DAWBARN, D. 2008. Targeting nerve growth factor in pain: what is the therapeutic potential? *BioDrugs,* 22**,** 349-59.

WELSHONS, W. V., LIEBERMAN, M. E. & GORSKI, J. 1984. Nuclear localization of unoccupied oestrogen receptors. *Nature,* 307**,** 747-9.

WHEELER, E. F. & BOTHWELL, M. 1992. Spatiotemporal patterns of expression of NGF and the low-affinity NGF receptor in rat embryos suggest functional roles in tissue morphogenesis and myogenesis. *J Neurosci,* 12**,** 930-45.

WILLIAMS, T. M., HASSAN, G. S., LI, J., COHEN, A. W., MEDINA, F., FRANK, P. G., PESTELL, R. G., DI VIZIO, D., LODA, M. & LISANTI, M. P. 2005. Caveolin-1 promotes tumor progression in an autochthonous mouse model of prostate cancer: genetic ablation of Cav-1 delays advanced prostate tumor development in tramp mice. *J Biol Chem,* 280**,** 25134-45.

WINCHESTER, P. K., DAVIS, M. E., ALWAY, S. E. & GONYEA, W. J. 1991. Satellite cell activation in the stretch-enlarged anterior latissimus dorsi muscle of the adult quail. *Am J Physiol,* 260**,** C206-12.

WODARZ, A. & NUSSE, R. 1998. Mechanisms of Wnt signaling in development. *Annu Rev Cell Dev Biol,* 14**,** 59-88.

WOLF, D. M. & SPATARO, R. F. 1988. The current state of hysterosalpingography. *Radiographics,* 8**,** 1041-58.

YAMADA, E. 1955. The fine structure of the gall bladder of the mouse. *J. Biophys. Biochem. Cytol.,* 1**,** 445–458.

YAMAMOTO, T., NOGUCHI, T., TAMURA, T., KITAWAKI, J. & OKADA, H. 1993. Evidence for estrogen synthesis in adenomyotic tissues. *Am J Obstet Gynecol,* 169**,** 734-8.

ZHANG, X., LU, B., HUANG, X., XU, H., ZHOU, C. & LIN, J. Innervation of endometrium and myometrium in women with painful adenomyosis and uterine fibroids. *Fertil Steril,* 94**,** 730-7.

ZHANG, X., LU, B., HUANG, X., XU, H., ZHOU, C. & LIN, J. 2010. Innervation of endometrium and myometrium in women with painful adenomyosis and uterine fibroids. *Fertil Steril,* 94**,** 730-7.

Publications & Presentations from the project

Publications

'Estradiol and tamoxifen enhance invasion of endometrial stromal cells in a three-dimensional coculture model of adenomyosis'

- Fertility and Sterility, 2014 Jan; 101(1): 288-93.

Presentations

1. 'The Effect of Tamoxifen and Estradiol on Stromal Cell Migration through a 3-D Co-culture Model of Adenomyosis'

   - Poster presentation at the World Congresses on Endometriosis, September 2011, Montpellier, France.

2. **'**Neurotrophin Signalling in Adenomyosis: the Effect of Estradiol and Tamoxifen'

   - Poster presentation at the World Congresses on Endometriosis, September 2011,
     Montpellier, France.

3. 'Differential regulation of the neurotrophins, NGF and BDNF, and their receptors in the myometrium of women affected by adenomyosis'

   - Poster presentation at the British Endocrine Society Meeting, April 2011 at Birmingham, United Kingdom.

4. 'The Neurotrophin System in the Human Adenomyotic Myometrium'

   - Poster presentation at the Annual Academic Meeting of the Royal College of Obstetricians & Gynaecologists (Blair Bell Meeting), RCOG, London, UK. December 2008

Appendix 1

Training & Courses attended

The details of the research training I have undertaken during the past 12 months are as follows:

1. Laboratory safety — 02/10/2009
2. Demonstrating & teaching skills — 07/10/2009
3. Planning & managing your doctorate — 16/10/2009
4. Critical appraisal & study skills — 02/11/2009
5. Creativity and problem-solving workshop — 03/11/2009
6. Advanced database searching: use of ENDNOTE — 16/11/2009
7. Protein sequencing & proteomics: science and services — 17/11/2009
8. Research governance & ethical approval procedures — 18/11/2009
9. General Presentation Skills — 19/01/2010
10. Off to Conference? Posters and How to Prepare Them — 02/02/2010
11. Experimental Design and Statistics — 03/02/2010
12. Improving PowerPoint Presentations — 04/02/2010
13. Writing Up Your Research for Publication — 11/03/2010
14. Use of MS-Word for long documents — 23/03/2010
15. Preparing for APG assessment — 13/05/2010

Appendix 2

Leicestershire, Northamptonshire & Rutland Research Ethics Committee 1

<div align="right">

1 Standard Court
Park Row
Nottingham
NG1 6GN

Telephone: 0115 8839428
Facsimile: 0115 9123300

</div>

14 October 2009

Mr Marwan Habiba
Senior Lecturer/Honarary Consultant Obstetrician & Gynaecologist
University of Leicester and UHL-NHS Trust
University of Leicester
Reproductive Sciences Section
Leicester
LE2 7LX

Dear Mr Habiba

Study Title:	**Study of the endometrial-myometrial interaction in the aetiology of uterine adenomyosis**
REC reference number:	**09/H0406/99**
Protocol number:	**2.0**

Thank you for your letter of 07 October 2009, responding to the Committee's request for further information on the above research and submitting revised documentation.

The further information has been considered on behalf of the Committee by the Chair.

Confirmation of ethical opinion

On behalf of the Committee, I am pleased to confirm a favourable ethical opinion for the above research on the basis described in the application form, protocol and supporting documentation as revised, subject to the conditions specified below.

Ethical review of research sites

The favourable opinion applies to all NHS sites taking part in the study, subject to management permission being obtained from the NHS/HSC R&D office prior to the start of the study (see "Conditions of the favourable opinion" below).

Conditions of the favourable opinion

The favourable opinion is subject to the following conditions being met prior to the start of the study.

<u>Management permission or approval must be obtained from each host organisation prior to the start of the study at the site concerned.</u>

It is the responsibility of the sponsor to ensure that all the conditions are complied with before the start of the study or its initiation at a particular site (as applicable).

Approved documents

The final list of documents reviewed and approved by the Committee is as follows:

Document	Version	Date
Covering Letter	2.0	09 August 2009
REC application	27657/56987/1/517	18 August 2009
Protocol	2.0	09 July 2009
Investigator CV	Chief Investigator	12 August 2009
Investigator CV	Student	12 August 2009
Referees or other scientific critique report		16 February 2009
Information and consent sheet	2.1	October 2009
Response to Request for Further Information		07 October 2009

Statement of compliance

The Committee is constituted in accordance with the Governance Arrangements for Research Ethics Committees (July 2001) and complies fully with the Standard Operating Procedures for Research Ethics Committees in the UK.

After ethical review

Now that you have completed the application process please visit the National Research Ethics Service website > After Review

You are invited to give your view of the service that you have received from the National Research Ethics Service and the application procedure. If you wish to make your views known please use the feedback form available on the website.

The attached document *"After ethical review – guidance for researchers"* gives detailed guidance on reporting requirements for studies with a favourable opinion, including:

- • Notifying substantial amendments
- • Adding new sites and investigators
- • Progress and safety reports
- • Notifying the end of the study

The NRES website also provides guidance on these topics, which is updated in the light of changes in reporting requirements or procedures.

We would also like to inform you that we consult regularly with stakeholders to improve our service. If you would like to join our Reference Group please email referencegroup@nres.npsa.nhs.uk.

09/H0406/99	**Please quote this number on all correspondence**

Yours sincerely

Dr Carl Edwards / Miss Jeannie D McKie
Chair / Committee Coordinator

Email: jeannie.mckie@nottspct.nhs.uk

Enclosures:	"After ethical review – guidance for researchers" *SL- AR2 for other studies*
Copy to:	*Sponsor / R&D office for NHS care organisation at lead site - UHL*

Appendix 3

Patient Information Leaflet & Consent form

> *Patient name, address, DOB* (or ID label)

REPRODUCTIVE TISSUE RESOURCE- INFORMATION AND CONSENT SHEET

Name of Principal Investigator: <u>Mr. Marwan Habiba</u>

Illnesses related to the womb are very common but it is often difficult to obtain samples of basically healthy tissues from the womb. So, we are aiming to create a store of samples from ladies who are having their womb removed for benign problems (e.g. heavy periods/prolapsed/benign cysts) so that we can compare things we find with other illnesses

Your womb would normally be thrown away and what we are asking is that scientists be able to anonymously collect and store a sample of this for use in this research. The tissue will in no way be traceable to an individual and the tests done on them will not affect any medical care provision in the future.

Thank you for considering the use of this tissue for medical research, if you agree to participate you should keep a copy of this sheet to take away with you for future reference.

1. I confirm that I have read and understood this sheet dated July 2009, version 2.1 for the ☐
    reproductive research resource and have had the opportunity to ask questions.

2. I agree to donate womb tissue anonymously and allow its use in medical research by Leicester ☐
    University and other research partners.

3. I understand that my donation is voluntary and that I am free to withdraw at any time, without ☐
    giving any reason, without medical care or any legal rights being affected, but that anonymised
    samples cannot be retrieved from the resource.

4. *I understand that the tissue is a gift and that I will not benefit from any intellectual property that may result from the use of the tissue.* ☐

5. *I understand that individuals may look at relevant sections of my medical notes and data collected during the study, from regulatory authorities or from the NHS Trust, where it is relevant to my taking part in this research. I give permission for these individuals to have access to my records.*

☐

Enquiries about the resource can be made to: Mr. Marwan Habiba, Department of Cancer Studies and Molecular Medicine, Robert Kilpatrick Clinical Sciences Building, Leicester Royal Infirmary, LE2 7XL. Phone: 0116 252 3170 Email: mah6@le.ac.uk

_____   _____   _____

Name of patient/parent/guardian   Date   Signature

_____   _____
                                         _____

Name of Person taking consent   Date   Signature

1 for patient; 1 to be kept with hospital notes